Enhancing the Potency and Water Solubility of the Sesquiterpene Lactone Parthenolide

A Thesis
SUBMITTED TO THE FACULTY OF
UNIVERSITY OF MINNESOTA
BY

Timothy Edward Andrews

IN PARTIAL FULFILLMENT OF THE REQUIREMENTS
FOR THE DEGREE OF
MASTER OF SCIENCE

Dr. Daniel A. Harki, Advisor

March, 2013

Acknowledgements

First and foremost I'd like to thank my advisor Dr. Daniel A Harki for absolutely everything he has done for me. I would not be half the scientist that I am today without him.

Additionally, I'd like to thank the entirety of the Harki lab. You are an amazing group of people and help foster an environment for not only scientific discussion but also camaraderie. I will truly miss seeing you guys every day and I wish you all the best.

I'd also like to extend my thanks to the Department of Medicinal Chemistry for taking me on and believing in me and my potential.

Finally, I'd like to thank my friends and family for their never ending support. I wouldn't be where I am without you.

Dedication

To Myron Eugene Andrews,

who inspired me to become a chemist.

May you rest in peace.

Table of Contents

List of Figures

List of Schemes

List of Tables

Preface

Please Note the following:

Chapter 1. This chapter is a review article co-authored with Dan Wang and Dr. Daniel A. Harki. *Drug Delivery and Translational Research.* **2013**, *3*, 121-141 DOI: 10.1007/s13346-012-0075-1

Chapter 2: Biological testing of parthenolide analogues was assisted by the following Harki lab members: Joe Hexum, Dan Wang, Fred Meece, Margaret Olson, Matt Bockman, Erick Carlson, and Ezra Menon. Rearranged parthenolide analogues **9**, **10** and **14** were synthesized and characterized by Dan Wang. Crystal structure of **PTL** analogue **4** was solved by Vic Young (UMN Department of Chemistry) from a crystal grown by Fred Meece

Chapter 1. Cell surface markers of cancer stem cells: diagnostic macromolecules and targets for drug delivery

1.1 Introduction

Cancer stem cells (CSCs), also known as tumor-propagating cells or tumor-initiating cells, are subpopulations of undifferentiated, highly tumorigenic cells found within bulk tumors. CSCs have the ability to self-renew, differentiate, and generate a phenotype-identical copy of the tumor from which they were isolated upon implantation in a recipient animal (Fig. 1). Accordingly, CSCs reside at the apex of the tumor cell hierarchy and can differentiate into all of the cell types that comprise the host tumor.[1-8] CSC theory directly challenges the traditional stochastic model of cancer cell growth that predicts that all cells from a tumor have tumorigenic potential.[9]

The development of suitable technologies to isolate CSCs from tumors (e.g., monoclonal antibodies of unique CSC surface macromolecules coupled with fluorescence-activated cell sorting (FACS) techniques) and appropriate animal models for xenotransplantation assays of isolated cell populations (e.g., non-obese diabetic, severe combined immuno-deficient (NOD/SCID) mice) have facilitated the identification of CSC populations from a variety of blood and solid tumors. [3] These technological advancements were prerequisite to the discovery of CSCs in acute myelogenous leukemia (AML), which is arguably the prototypical human cancer bearing an established CSC hierarchy. Seminal work by John Dick and colleagues provided the first critical evidence for CSCs by isolating (with FACS) the $CD34^{+}/CD38^{-}$ fraction of human donor AML cells and engrafting those cells into severe combined

immunodeficient (SCID) mice.[9,10] Engrafted cells were able to proliferate and differentiate, resulting in identical disease to that of the donor. Isolation of the AML CSC population ($CD34^+/CD38^-$) from the recipient mouse, followed by serial transplantation into a secondary recipient mouse yielded the same disease, thereby demonstrating the self-renewal properties of the initially engrafted $CD34^+/CD38^-$ AML cell fraction. This pioneering study provided insight into the long-standing observation that AML cells have only limited proliferative capacity by supporting the hypothesis that a rare leukemic clone must maintain the AML population.[11-13] Additionally, this work provided crucial evidence for the hierarchical model of tumor heterogeneity by demonstrating that some populations of leukemic cells ($CD34^+/CD38^-$) exhibited CSC activity, whereas other leukemic cell populations (e.g., $CD34^+/CD38^+$ and $CD34^-$) did not.[10] The feature that only a sub-population of cells from a tumor can facilitate tumorigenesis is a tenant of the hierarchical model of tumor cell growth.[3,10] AML CSCs exclusively give rise to clinical AML.[9,10]

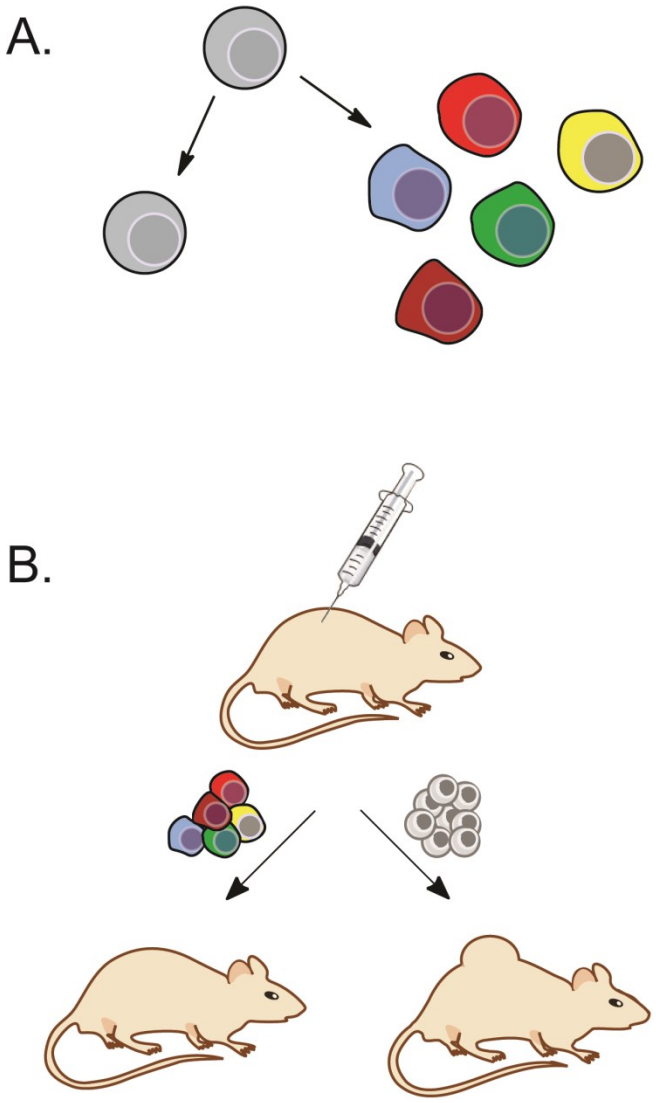

Fig. 1.1 Depiction of the properties that are characteristic of cancer stem cells (CSCs). **A.** CSCs (shown in gray) can self-renew and undergo multi-lineage differentiation (cells in color). **B.** Tumorigenicity. CSCs are more tumorigenic than differentiated bulk tumor cells.

Cancer therapies that are resisted by the CSC population are predicted to fail by the CSC model.[6,7] Although outside the focus of this review, the drug resistance properties of CSCs may result due to increased cell quiescence,[14,15] expression of anti-apoptotic proteins,[16] and upregulation of ABC multidrug resistance transporter proteins.[16,17] The CSC hypothesis is also supported by clinical data. In the case of AML, approximately 44,000 new cases of AML are diagnosed annually in the United States, and 5-year survival rates are only 24%.[18] Front-line small molecule treatments for AML include nucleoside analogues (e.g., cytarabine) and anthracyclines (e.g., idarubicin, daunorubicin), which are designed to induce apoptosis in rapidly dividing cancer cells.[19,20] AML CSCs, which are largely quiescent, are typically resistant to standard chemotherapeutic agents. Furthermore, recent data have demonstrated that cytarabine actually facilitates AML CSC entry into G0/G1 phase, thereby promoting cell cycle quiescence and providing a mechanism that allows AML CSCs to survive chemotherapy.[21] Consequently, viable strategies to eradicate CSC populations are clearly needed if curative cancer therapies are to be developed. A realized example of this concern has been documented with patients receiving the targeted bcr-abl tyrosine kinase antagonist imatinib (Gleevec®) for chronic myelogenous leukemia (CML). Although imatinib effectively converts CML into a chronically managed disease,[22,23] a patient withdrawing from imatinib treatment will ultimately exhibit disease relapse because imatinib does not eliminate CML CSCs.[24,25]

Elucidation of the molecular differences between differentiated cancer cells with high proliferation rates and nondifferentiated CSCs that are mostly quiescent is an

intense area of ongoing research.[3,26-28] Equally important is the need to characterize those chemical features that confer cancerous versus non-cancerous stem cells (e.g., the differences in biochemistry between a leukemic stem cell and a normal hematopoietic stem cell).[3] A variety of cytosolic and cell surface macromolecules have been characterized as diagnostic markers for the identification of CSCs from differentiated cancer cells, normal stem cells, or other cells from tissue. Many of these markers are utilized in combination for characterization of the CSC population (e.g., $CD34^{+}$/ $CD38^{-}$ for AML CSCs described above).[10] However, for isolation and drug targeting of CSCs, surface markers have proven to be more useful.[29-32] Cell surface macromolecules are readily captured by magnetic micro-bead isolation techniques and are easily detected by flow cytometry, and the unique ligands presented on the cell surface offer receptors for targeted drug delivery.[33] In this chapter, we have consolidated the known CSC cell surface markers that have been described for various blood and solid tumors into one document. Since intracellular markers for CSCs have been described and reviewed elsewhere,[30,34] we have focused this review only on well-characterized cell surface markers due to their ability to serve as mediators for drug delivery into CSCs. In addition to compiling CSC surface markers, we review the unique chemical and structural features of the most well-known CSC surface markers and report recent efforts to deliver therapeutic agents into CSCs mediated by CSC specific cell surface macromolecules. Compendium of cell surface markers for identification of cancer stem cells summarized herein is the current knowledge of CSC markers from the following human cancers: leukemias (**Table 1.1-1.3**), breast (**Table 1.4**), colorectal (**Table 1.5**),

liver (**Table 1.6**), pancreatic (**Table 1.7**), prostate (**Table 1.8**), melanoma (**Table 1.9**), brain (**Table 1.10**), bladder (**Table 1.11**), lung (**Table 1.12**), and ovarian carcinomas (**Table 1.13**). Recent efforts to deliver therapeutic molecules to CSCs are described in **Table 1.14**. **Table 1.15** provides a compendium of the other commonly used names of the CSC markers discussed in the following sections.

1.2 Cancer Stem Cells Found in Liquid Tumors

1.2.1 Leukemia

Leukemia is a family of diseases, comprised of blood, bone marrow, or lymphoid system cancers that are characterized by abnormal increases in white blood cell count.[35] In 2011, more than 44,000 children and adults in the United States were expected to develop some form of leukemia, and approximately 22,000 deaths were projected.[18,36,37] In 1994, Dick and coworkers first characterized the acute myelogenous leukemia stem cell population utilizing the $CD34^+/CD38^-$ cell surface marker combination.[10] This landmark discovery catalyzed the search for CSC populations from related blood as well as solid tumors. The repertoire of CSC markers in leukemia is complicated and variable depending on leukemia subtype and stage of disease.[38]

1.2.1.1 Acute myelogenous leukemia (AML)

As has been introduced above, $CD34^+/CD38-$ (**Table 1.1**) is the earliest documented stem cell marker combination in cancer and is still widely used to identify leukemic CSCs. In a seminal study, Dick and coworkers demonstrated that a small

subpopulation of AML cells with the $CD34^+/CD38^-$ cell surface phenotype was capable of producing a large number of colony-forming progenitors when engrafted to SCID mice. On the other hand, $CD34^+/CD38^+$ and $CD34^-$ cell fractions did not exhibit these properties.[10] Later studies from the same group provided evidence that $CD34^+/CD38^-$ was a common immune phenotype for leukemic CSCs in multiple AML subtypes and also demonstrated their self-renewal potential.[9]

Additional studies have further refined and developed the cell surface phenotypes of AML. The Suthland group has shown that, in both in vitro and in vivo models, $CD34^+/CD90^-$ (Thy-1), $CD34^+/CD71^-$/HLA-DR^-, and $CD34^+/CD117^-$ (c-kit) are unique cell surface marker phenotypes of AML CSCs.[39-41] In 2000, the Jordan group indicated that $CD34^+/CD38^-/CD123^+$ (interleukin-3 receptor α chain) is a specific cell surface phenotype for human AML stem cells.[42] Additionally, CD123 expression has also been reported on CSCs in CML, myelodysplastic syndrome, and systemic mastocytosis,[43] suggesting that CD123 might be a broadly applicable cell surface marker for the development of targeted therapies against CSCs across multiple leukemias. CD33 is another important surface marker for characterizing AML CSCs. CD33 has long been known for its extensive expression on leukemic blasts,[44] but only recently has it been reported as a marker for AML CSCs. Hauswirth et al. have shown that addition of $CD33^+$ to phenotype $CD34^+/CD38^-/CD123^+$ yields a robust marker combination for AML CSCs that is unique to cancerous stem cells.[45] Additionally, Florian et al. demonstrated that $CD34^+/CD38^-/CD45^+/CD123^+$ was a general marker phenotype for AML CSCs and that additional markers, such as $CD13^+$, $CD71^-$, $CD33^+$, $CD117^+$,

$CD133^+$, and $HLADR^-$, were observed in variable combinations with the $CD34^+/CD38^-/CD45^+/CD123^+$ phenotype.[43] $CD34^+/CD38^-/CD123^+$ CSC populations have also been noted for their upregulation of drug efflux pumps. Compared with bulk (differentiated) tumor cells, the upregulation of multidrug-resistance related protein 1, breast cancer resistance protein, and lung resistance protein have been observed in AML CSC populations.[46] C-type lectin-like molecule-1 (CLL-1), which is a transmembrane protein with a heavily N-glycosylated extracellular domain, has been found to be exclusively expressed on AML CSCs in 92% of all studied AML cases. Isolation and transplantation of $CD34^+/CD38^-/CLL\text{-}1^+$ cells generated AML blasts in NOD/SCID mice.[47] Another important marker of AML CSCs is CD96, which belongs to the immunoglobulin superfamily. Recent studies have demonstrated that CD96 protein might be selectively overexpressed as a $CD34^+/CD38^-/CD90^-/Lin-/CD96^+$ phenotype on AML CSCs as compared with the basal expression level of CD96 on normal HSCs.[48] The elevated expression of several isoforms of adhesion molecule CD44 has been identified in the interaction between hematopoietic progenitor cells and the surrounding stromal cells (i.e., CSC niche) in primary human AML samples.[49] CD44 has been previously exploited in targeted drug delivery to AML CSCs [20] (see section "The chemical biology and drug targeting of cell surface markers on cancer stem cells"; Table 1.14). The Ishikawa group has reported the identification of CD25 and CD32 in conjunction with $CD34^+/CD38^-$ as potential CSC markers for AML. In their study, they found that both $CD34^+/CD38^-/CD25^+$ and $CD34^+/CD38^-/CD32^+$ leukemia cells are enriched in quiescent, chemotherapeutic drug-resistant CSCs, are capable of initiating

AMLs in vivo, and are expressed at a very limited level in normal HSCs.[50] Majeti et al. also reported CD47 as a new potential target for CSC therapy of AML. $CD34^+/CD38^-/CD90^-/Lin^-/CD47^+$ expression was observed only in AML CSCs when compared with their HSC counterparts.[51] See Table 1.1 for a listing of AML CSC surface markers.

Table 1.1. Previously reported CSC markers for acute myelogenous leukemia (AML).

Cancer Type	Marker(s)	Reference
Acute Myelogenous Leukemia (AML)	$CD34^+/CD38^-$	10
	$CD34^+/CD90^-$	39
	$CD34^+/CD71^-/HLA^-DR^-$	40
	$CD34^+/CD117^-$	41
	$CD34^+/CD38^-/CD123^+$	42,46
	$CD34^+/CD38^-/CD45^+/CD123^+$	43
	$CD34^+/CD38^-/CD123^+/CD33^+$	45
	$CD34^+/CD38^-/CLL^-1^+$	47
	$CD34^+/CD38^-/CD90^-/Lin^-/CD96^+$	48
	$CD44^+$	49
	$CD34^+/CD38^-/CD25^+$	50
	$CD34^+/CD38^-/CD32^+$	50
	$CD34^+/CD38^-/CD90^-/Lin^-/CD47^+$	51

1.2.1.2 Acute lymphoblastic leukemia

Acute lymphoblastic leukemia (ALL) is the most common childhood cancer and is characterized by clonal proliferation of lymphoblasts.[18] ALL CSCs present the same $CD34^+/CD38^-$ cell surface marker phenotype as AML CSCs; however, the $CD34^+/CD38^-/CD33^-/CD19^-$ phenotype has been characterized as a more robust marker to define ALL CSCs.[52] A population of ALL CSCs that are committed to lymphoid

differentiation has been shown to express the Philadelphia chromosome ($CD34^+/CD38^-/Ph^+$).[53] The Philadelphia chromosome contains a chromosomal translocation between the break point cluster region (bcr) and the gene encoding c-Abl (abl), which encodes for the bcr-abl tyrosine kinase.[54] The presence of the Philadelphia chromosome in ALL indicates an overall poor prognosis.[55] Subsequent studies have shown that, in $CD34^+/CD38^-$ bone marrow cells, a predominant and aberrant $CD34^+/CD38^-/ CD19^+$ cell population that is not present in healthy individuals carries the Philadelphia chromosome, while the $CD19^-$ cell population in this compartment does not.[56] These results indicate that the $CD34^+/CD38^-/CD19^+$ phenotype marrow compartment in childhood ALL is another potential marker of ALL CSCs,[56] which is contradictory to previous findings.[52] However, it has been suggested that $CD19^+$ might not be a broadly applicable AML CSC marker.[56] ALL can be classified as T lineage (T-ALL) or B lineage (B-ALL).[57] Cox et al. have demonstrated that ALL cells capable of long-term proliferation and differentiation into pre-B-ALL in vitro (suspension culture assay) and in vivo (NOD/SCID transplant model) were derived from only $CD34^+/CD10^-$ or $CD34^+/CD19^-$ sub-fractions, indicating that the target cells for transformation in pre-B-ALL have a more immature phenotype than the bulk ALL population.[58] The same group also discovered that $CD34^+/CD4^-$ or $CD34^+/CD7^-$ sub-fractions of childhood T-ALL cells were highly proliferative and capable of NOD/SCID engraftment.[59] More recently, Cox et al. reported that in childhood ALLs, the small subpopulation of $CD133^+/CD19^-$ cells were capable of initiating and maintaining long-term in vitro cultures of B-ALLs and engrafting serially into NOD/SCID recipient mice.[60] In a recent

study from the Morimoto group, the stem cell characteristics of $CD9^+$ cell populations in B-ALL were demonstrated both in vitro and in transplantation experiments, suggesting that CD9 is a useful positive-selection marker for the identification of CSCs in B-ALL. Their study also showed that, in some cases, $CD9^+$ in ALL CSCs was a more reliable CSC marker than $CD34^+$.[61] The same group also reported the importance of CD90 (Thy-1) and CD110 (c-Mpl) as positive-selection markers for T-ALL CSCs. In both *in vitro* and *in vivo* assays, their results suggested that small subpopulations of $CD90^+/CD110^+$ cells isolated from either childhood or adult ALL specimens retained the ability to self-renew, proliferate, and differentiate [62]. See Table 1.2 for a listing of ALL CSC surface markers.

Table 1.2. Previously reported CSC markers for acute lymphocytic leukemia (ALL).

Cancer Type	Marker(s)	Reference
Acute Lymphocytic Leukemia (ALL)	$CD34^+/CD38^-/CD33^-/CD19^-$	52
	$CD34^+/CD38^-/Ph^+$	53
	$CD34^+/CD38^-/CD19^+$	56
	$CD34^+/CD10^-$	58
	$CD34^+/CD19^-$	58
	$CD34^+/CD4^-$	59
	$CD34^+/CD7^-$	59
	$CD133^+/CD19^-$	60
	$CD9^+$	61
	$CD90^+/CD110^+$	62

1.2.1.3 Chronic myelogenous leukemia (CML)

CML is often characterized by the overproduction of mature myeloid cells. As with ALL, CML is most closely associated with the bcr-abl chromosomal translocation, which is present in pluripotent stem cells.[38] CML CSCs are also characterized by the $CD34^+/Ph^+$ cell phenotype (Table 1) and are phenotypically similar to normal HSCs.[63] In addition to its role as an AML CSC marker, $CD123^+$ has also been characterized as a surface marker for CML CSCs (phenotype $CD34^+/CD38^-/CD123^+$). Queries for the presence of other markers in CML cells bearing the $CD34^+/ CD38^-/CD123^+$ phenotype revealed variable positivity for CD13, CD33, CD44, and CD117 molecules;[43] however, the presence of CD117 on the surface of CML CSCs conflicts with previous reports.[41] See Table 1.3 for a listing of CML CSC surface markers

Table 1.3. Previously reported CSC markers for chronic myelogenous leukemia (ALL).

Cancer Type	Marker(s)	Reference
Chronic Myelogenous	$CD34^+/CD38^-/CD123^+$	[43]
Leukemia (CML)	$CD34^+/Ph^+$	[63]

1.3 Cancer Stem Cells Found in Solid Tumors

1.3.1 Breast cancer

Breast cancer accounts for the deaths of more than 40,000 women each year in the United States. Although the 5-year survival rate for breast cancer patients has dramatically increased over the past few decades, tumor relapse and metastasis is still a significant problem in breast cancer therapy.[18,64] The evasion of breast CSCs during therapy is a significant contributor to disease relapse.[65]

Al-Hajj et al. were the first to identify breast CSCs from whole cell population of breast cancer specimens using the cell surface marker profile $CD44^{+}/CD24^{-/low}/Lin^{-}$ (Table 2), which was the seminal report of CSCs identified from a solid tumor.[66] The marker profiles $CD44^{+}/CD24^{-/low}/Lin^{-}$ has been correlated with high resistance to traditional cancer therapies,[67] poor prognosis,[68] and enhanced invasive properties.[69] Notably, lineage (Lin) markers are a standard combination of monoclonal antibodies including CD2, CD3, CD4, CD5, CD8, NK1.1, B220, TER-119, and Gr-1 in mice and CD3, CD14, CD16, CD19, CD20, and CD56 in humans.[70] Addition of epithelial cell adhesion molecule (EpCAM), yielding marker combination $CD44^{+}/CD24^{-/low}/EpCAM^{high}$, was later found to be a more robust surface marker combination for the isolation of human breast CSCs.[66] The multiplexing of cytoplasmic enzyme ALDH1, membrane protein CD44, and cytokeratin has been employed to identify putative breast CSCs and indicate poor prognosis, which is independent of tumor size, nodal status, ER-, PR-, and HER2-status, and histological grade.[71]

Another important cell surface marker of human breast CSCs is Thy1 (CD90). In an MMTV-Wnt-1 breast cancer mouse model, cancer cells with the phenotype $THY1^{+}/CD24^{+}$ (1–4% of tumor cell population) were identified to be highly tumorigenic in comparison to non-$THY1^{+}/CD24^{+}$ populations and displayed properties of CSCs.[72] The observation of $CD24^{+}$ phenotype in combination with Thy1 is contradictory to previous reports that found breast CSCs to have a $CD44^{+}/CD24^{-/low}/Lin^{-}$ phenotype.[66] The expression of cell surface marker CD133 is also reported to be of significance and prognostic value for identifying CSCs in breast tumors, especially when combined with

$CD44^+$.[73-75] CD173 (H2) and CD174 (Lewis Y) are cell surface carbohydrate antigens that are expressed to varying extents on different human carcinomas. Co-expression of CD173 and CD174 with CD44 is another cell surface marker combination proposed to identify breast CSCs.[76] Similar to CD173 and CD174, CD176 is also a cell surface carbohydrate antigen that has been reported to be co-expressed with CD44 and CD133 in breast carcinoma.[77] Another study has shown that in BRCA1 (breast cancer-associated gene 1)-mutant breast cancer cell lines, a small subpopulation of cancer cells expressing $CD24^+/CD29^+$ (β integrin) or $CD24^+/CD49f^+$ (α6 integrin) surface markers exhibited enhanced proliferation and colony forming ability in vitro and increased tumor generating ability in vivo. In addition, purified $CD24^+/CD29^+$ cells exhibit self-renewal capability, and as low as 500 cells could reconstitute the heterogeneity of the parent cancer cells in vivo, which is strongly indicative of a CSC population.[78] Shipistin et al. confirmed that CD201, which is also known as protein C receptor (PROCR), was expressed on 100% of $CD44^+$ breast cancer cells and was used as a cell surface marker to isolate CSCs from primary invasive breast cancer tumors.[79] In addition, high PROCR expression was also reported to associate with poor prognosis in clinical patients.[79] See Table 1.4 for a listing of breast CSC surface markers.

Table 1.4. Previously reported CSC markers for breast cancer.

Solid Tumor Type	Marker(s)	Reference
Breast	$CD44^+/CD24^{-/low}/Lin^-$	66,69
	$CD44^+/CD24^{-/low}/EpCAM^{high}$	66
	$ALDH1^+/CD44^+/cytokeratin^+$	71
	$CD90^+/CD24^+$	72
	$CD133^+/CD44^+$	73-75
	$CD173^+/CD174^+/CD44^+$	76
	$CD176^+/CD44^+$	77
	$CD176^+/CD133^+$	77
	$CD24^+/CD29^+$	78
	$CD24^+/CD49f^+$	78
	$CD44^+/CD201\ (PROCR)^+$	79

1.3.2 Colorectal cancer

Dalerba et al. have isolated colorectal CSCs from specimens using cell surface markers CD44 and EpCAM.[80] When purified $CD44^+/EpCAM^{high}$ epithelial cells (Table 2) were injected into immunodeficient mice, the engrafted tumors yielded the differentiated phenotype profile as well as the morphologic heterogeneity of the parent lesions from which the $CD44^+/EpCAM^{high}$ epithelial cells were isolated. Furthermore, the authors also reported $CD166^+$ as a co-marker that could be used for validation of colorectal CSCs in both xenografts and primary tumors, and the $CD44^+/EpCAM^{high}/CD166^+$ phenotype was consistent with poor prognosis.[80] However, the CD44/EpCAM marker phenotypes were not the first reported colorectal CSCs. Prior studies had first indicated that CD133 was a potential cell surface CSC marker in primary human colorectal cancer,[81,82] but more recent findings by Shmelkov et al. have shown that both $CD133^+$ and $CD133^-$ populations are tumorigenic and contain tumor-

initiating cells.[83] In order to explain this discrepancy, Du et al. have suggested that, unlike CD44, a surface protein that is of functional importance for the survival of CSCs, CD133 has not been found to have any essential functions associated with the growth and survival of colorectal CSCs.[84] Although $CD44^+/EpCAM^{high}/CD166^+$ is a relatively more reliable marker for colorectal CSCs than $CD133^+$, some exceptions have also been documented. Lugli et al. reported that the loss of this combined marker ($CD44^+/EpCAM^{high}/CD166^+$) was rather linked to an aggressive tumor phenotype.[85,86] Studies have also shown that CD49f, which has been reported as a CSC marker in breast cancer,[78] is expressed on colon cancer cells, and that even higher levels of CD49f expression are observed with $CD44^+$ cells, a known marker of colorectal CSCs.[80] Additionally, $CD133^+/CD24^+$ has been identified as a colorectal CSC marker.[87] See Table 1.5 for a listing of colorectal CSC surface markers.

Table 1.5. Previously reported CSC markers for colorectal cancer.

Solid Tumor Type	Marker(s)	Reference
Colorectal	$CD44^+/EpCAM^{high}$	80
	$CD44^+/EpCAM^{high}/CD166^+$	80
	$CD44^+/CD49f^+$	80
	$CD133^+$	81,82
	$CD44^+$	88
	$CD133^+/CD24^+$	87

1.3.3 Liver cancer

The incidence of hepatocellular carcinoma (HCC) cases has risen by 3% every year since 1992, and the 5-year survival rate ranges from 14% to 26% depending on the

stage of diagnosis.[18] In spite of the intensive research efforts devoted to the discovery of new HCC drugs, tumor relapse is still observed in the majority of cases.[89] The recent identification of liver CSCs has yielded new targets for HCC drug discovery efforts, which, if successful, may help to address the problem of disease relapse.

The $CD133^+$ phenotype was the first reported putative HCC CSC population.[90] In this report by Ma et al. $CD133^+$ HCC cells exhibited greater colony-forming capacities and higher proliferation rates than CD133− HCC cells, as well as the ability to generate new tumors in both in vitro and in vivo models. Additionally, in $CD133^+$ tumor cells, the expression level of stemness genes such as those involved in Wnt/β-catenin, Notch, and Hedgehog/SMO signaling were largely upregulated, indicating those $CD133^+$ tumor cells were putative HCC CSCs. The $CD133^+$ population was further characterized for other common CSC markers and CD34 and CD44 were found to be upregulated when compared with the $CD133^-$ population.[90] Another well-established cell surface marker of HCC stem cell is $CD44^+$. Within the HCC $CD133^+$ population, $CD44^+$ cells were found to be more tumorigenic than $CD44^-$ cells in NOD/SCID mouse model. Recent studies also revealed that the blocking of CD44 function by treatment with a CD44 specific monoclonal antibody might be a potential strategy to eradicate liver CSCs[91] (see section "The chemical biology and drug targeting of cell surface markers on cancer stem cells"). Moreover, the cell surface carbohydrate antigen CD176 was found to co-express with CD44 at a high rate on the surface of HCC stem cells in both cancer cell lines and surgical specimens of malignant tumors.[77] Besides CD133 and CD44, EpCAM was identified as an early biomarker of HCC CSCs.[92,93] The sorted

$EpCAM^+$ subpopulation of HCC cells yielded more colonies in clonogenicity assays than the sorted $EpCAM^-$ cells from the same cell line. Further in vivo evaluation in mouse models indicated that as little as 100 $EpCAM^+$ HCC cells were needed to generate a new tumor, and $EpCAM^+$ cells retained the ability to differentiate into both $EpCAM^+$ and $EpCAM^-$ cells, while $EpCAM^-$ cells always sustained their phenotype during cell propagation.[92] Additionally, CD133 expression was observed in both $EpCAM^+$ and $EpCAM^-$ populations, indicating that EpCAM functions as a better indicator of the CSC population.[93] Recently, CD13 (alanine aminopeptidase), which is a membrane-bound enzyme, has been identified as a marker for semiquiescent CSCs and a potential therapeutic target for liver cancers. $CD13^+/CD133^+$ and $CD13^+/CD90^-$ populations were observed to be extremely tumorigenic, requiring only 100 cells for tumor formation upon transplantation.[94] In a xenograft mouse model, CD13 inhibition, which was achieved with either a CD13 neutralizing antibody or by the CD13 inhibitor Ubenimex, repressed tumor-initiating and self-renewing capability of the majority of CSCs[94] (see section "The chemical biology and drug targeting of cell surface markers on cancer stem cells"). CD90 (Thy-1) has also been identified as a CSC marker in HCC cell lines.[95] In comparison to $CD90^-$ cells, $CD90^+$ cells sorted from HCC cells lines were found to exhibit strong tumorigenic capacity, and the subpopulation of cells with $CD90^+/CD45^-$ phenotype could generate tumor nodules in an immunodeficient mouse model.[95] OV6, which is a marker of hepatic progenitor (oval) cells, has been shown to be another CSC marker in HCC cells. $OV6^+$ HCC cells are capable of generating new tumors in vivo and show substantial resistance to standard chemotherapeutic drugs

compared with $OV6^-$ HCC cells. Furthermore, the inhibition of the Wnt/β-catenin signaling pathway, which is known to be important for the survival of CSCs,[96] decreases the population of $OV6^+$ cells. The $OV6^+$ cell population also gained higher proliferation potential after β-catenin activation.[97] See Table 1.6 for a listing of liver CSC surface markers.

Table 1.6. Previously reported CSC markers for liver cancer.

Solid Tumor Type	Marker(s)	Reference
Liver	$CD176^+/CD44^+$	77
	$CD133^+$	90
	$CD133^+/CD44^+$	91
	$EpCAM^+$	92,93
	$CD13^+/CD133^+$	94
	$CD13^+/CD90^-$	94
	$CD90^+/CD45^-$	95
	$OV6^+$	97

1.3.4 Pancreatic cancer

Pancreatic cancer is one of the deadliest forms of human cancers. Currently, there are no known methods of early detection, and the average 5-year survival rate is 6%.[18] The mortality rate of this disease approaches 100% because of its characteristically high resistance to radiation and chemotherapy, and the tendency of early systemic dissemination.[98] In spite of the significant advances in cancer biology over the past decade, the efficacy of drugs to treat pancreatic cancer has not substantially improved.[99] Targeting the pancreatic CSC population could allow development of more efficacious therapies to combat this lethal disease.

A pancreatic CSC population was identified only recently.[99] A small population (0.2–0.8%) of highly tumorigenic pancreatic cancer cells with the $CD44^+/CD24^+/EpCAM^{high}$ phenotype (Table 2) from primary human pancreatic adenocarcinomas was xenografted into immunocompromised mice. In comparison with non-tumorigenic cells, the $CD44^+/CD24^+/EpCAM^{high}$ pancreatic cancer cells exhibited a 100-fold increase in tumorigenic potential, and as few as 100 such cells could reconstitute tumors that were indistinguishable by histology from the original ones.[99] In related studies, Hermann et al. demonstrated that $CD133^+$ expression on the surface of pancreatic cancer cells was consistent with increased tumorigenicity and high resistance to standard chemotherapy. In addition, they further revealed that a unique small population of CSCs bearing the $CD133^+/ CXCR4^+$ phenotype determined the metastatic potential of the tumor. Although $CD133^+/CXCR4^+$ cells and $CD133^+/ CXCR4^-$ cells showed similar tumorigenicity when xenografted into nude mice, only the $CD133^+/CXCR4^-$ cells eliminated tumor metastasis.[100] See Table 1.7 for a listing of pancreatic CSC surface markers.

Table 1.7. Previously reported CSC markers for pancreatic cancer.

Solid Tumor Type	Marker(s)	Reference
Pancreatic	$CD44^+/CD24^+/EpCAM^+$	99
	$CD133^+$	100
	$CD133^+/CXCR4^+$	100

1.3.5 Melanoma

Approximately 70,000 new cases of human melanoma and 9,000 melanoma-related deaths were expected in the United States in 2011.[18] Although melanoma is not a leading cause of cancer-related mortality, it is one of few cancer types associated with both annual increases in incidence and death rate.[101] Human malignant melanoma cells are highly aggressive and drug resistant and contain cell populations with enhanced tumorigenicity.[102] The discovery of putative CSCs in melanoma cell lines was first reported in 2005,[102] preceding their subsequent isolation and characterization from cell lines and surgical specimens.[103] Nestin (Table 2), which is an intermediate filament protein, was first described as a potential stem cell marker in melanoma cell lines.[104] Nestin expression was associated with aggressive behavior of the malignant tumors and was found to be upregulated during the development of invasive melanoma from banal nevi (a benign chronic lesion of the skin).[104] Co-expression of nestin with CD133 has been described in context with stem cell populations in circulating melanoma cells, which are closely related to their metastatic potentials.[105] Monzani et al. first utilized CD133 as a cell surface marker to separate melanoma stem cells. Their data showed that in contrast to $CD133^-$ cells, $CD133^+$ melanoma cells were highly tumorigenic and able to generate a Mart-1 (a typical melocytic marker) positive tumor when implanted into NOD/SCID mice. In the same study, they also revealed that melanoma cells expressing both CD133 and ABCG2 (ATP-binding cassette sub-family G member 2) were able to self-renew and differentiate into astrocytes and mesenchymal lineages under specific conditions, demonstrating the utility of ABCG2 as a CSC marker.[103] Schatton et al.

identified a small subpopulation of melanoma cells that were enriched for human malignant melanoma-initiating cells, which were defined by the expression of P-glycoprotein ABCB5, a well-known chemoresistance mediator. $ABCB5^+$ melanoma cells were found to be highly aggressive, possess greater tumorigenic capacity than $ABCB5^-$ cells, and could re-establish clinical tumor heterogeneity. ABCB5 has also been studied as a target of anticancer therapy[106,107] (see section "The chemical biology and drug targeting of cell surface markers on cancer stem cells). See Table 1.8 for a listing of melanoma CSC surface markers.

Table 1.8. Previously reported CSC markers for skin cancer.

Solid Tumor Type	Marker(s)	Reference
Skin	$CD133^+$	103
	$CD133^+/ABCG^-2^+$	103
	$Nestin^+/CD133^+$	105
	$ABCB5^+$	107

1.3.6 Brain cancer

Malignant brain tumors are among the deadliest human cancers. Glioblastoma (GBM) multiforme is the most common primary brain tumor in adults with 12,000 deaths in the United States annually.[108] In children, glioblastoma multiforme occurs less frequently, accounting for 7–9% of all intracranial tumors, yet the median survival after diagnosis is 50 weeks.[109] Currently, there is a scarcity of effective treatments for brain cancers, which is attributable to the sensitive environment of the disease and the inability of many drugs to permeabilize the blood–brain barrier. Unfortunately, most

drugs that can access brain malignancies are inefficient at eradicating the tumor cells and frequently leave behind a side population of radio- and chemoresistant cells. The existence of this side population provides a mechanism for disease relapse,[33] and recent studies strongly suggest that brain tumors have an established CSC hierarchy.[110,111] Drug targeting of brain CSCs may yield better therapy outcomes.

In 2003, Singh et al. first identified CD133 as a CSC marker (Table 2) in glioblastomas and medulloblastomas.[112] Studies of human medulloblastoma specimens from children have also revealed a $CD133^+$ subpopulation of cells that is positive for nestin.[113] Sorted $CD133^+$ populations of childhood medulloblastoma specimens have demonstrated the stem cell characteristics of self-renewal and differentiation, and subjection of these cells to differentiation conditions resulted in the loss of the $CD133^+$ marker.[112] The tumorigenicity of $CD133^+$ human donor medulloblastoma and glioblastoma cancer cells were evaluated in NOD/SCID mice, and as few as 100 cells were required for the development of new tumors of the same phenotype.[113]

Another glioblastoma CSC marker that has been identified is integrin A2B5, a polysialo ganglioside. Tchoghandjian et al. used A2B5 to characterize CSC populations in glioblastoma samples using magnetic micro-beads and FACS. In addition, the authors sorted the cells for a secondary known CSC marker, CD133. $A2B5^+$ populations expressed characteristic features of CSCs regardless of CD133 expression, and both $A2B5^+/CD133^+$ and $A2B5^+/CD133^-$ populations were highly tumorigenic, requiring only 1,000 cells for development of a new tumor of the same phenotype. However, only the $A2B5^+/CD133^-$ population of cells was found to be invasive within the brain.[114]

Studies by Ogden et al. have suggested that only the A2B5$^+$ phenotype is characteristic of glioblastoma CSCs, and CD133 positivity is not indicative of a CSC population.[115] In support of the evidence that CD133$^+$ cells are putative CSCs, studies by Wang et al. found that CD133$^+$ glioblastomas were aggressive tumors and were typified by the onset of angiogenesis, shorter survival times, and metastatic potential. However, the CD133$^-$ populations were also shown to be capable of differentiating into CD133$^+$ cells, which suggests that CD133$^-$ are stem cell-like.[116] Although characterization of universal diagnostic markers for CSCs is the ultimate goal for the development of targeted therapies, these contradictory results with CD133 clearly illustrate that patients can express different surface markers for the same disease and/or that multiple CSC populations can be present in glioblastoma specimens.

L1CAM, a transmembrane adhesion protein found in CD133$^+$ glioma cell populations, was identified as a brain CSC marker in 2008.[117] D456MG pediatric glioblastoma xenografts and primary human samples were utilized to study the role of L1CAM.[118] Neurosphere formation, a cellular morphology consistent with a stem cell-like state, was quantified as a measure of the self-renewal properties of the CSC population. Targeting L1CAM with shRNA decreased the ability of the CD133$^+$ cells to form neurospheres, indicating that the L1CAM$^+$/CD133$^+$ population was the in vitro CSC population. In vivo studies conducted in nude mice also showed that knockdown of L1CAM with shRNA resulted in a reduction in tumor size and increased survival.[117]

Stage-specific embryonic antigen-1 (SSEA-1), or CD15, has also been identified as a potential marker of GBM CSCs.[119] Utilizing primary human samples, SSEA-1$^+$

cells were isolated and characterized for self-renewal, differentiation, and tumorigenicity. The presence of $CD133^+$ was also investigated in the $SSEA\text{-}1^+$ populations in early studies; however, $SSEA\text{-}1^+/CD133^+$ and $SSEA\text{-}1^+/CD133^-$ were both shown to have CSC characteristics. Sorting of primary human GBM specimens for only SSEA-1 expression and xenograftment of isolated cells into NOD/SCID mice revealed that $SSEA\text{-}1^+$ cells exhibited at least 100-fold greater tumorigenic potential than $SSEA\text{-}1^-$ GBM cells. Therefore, $SSEA\text{-}1^+$ can be used to identify CSC populations in GBM.[119] SSEA-1 has also been identified as a medulloblastoma CSC marker.[120] See Table 1.9 for a listing of brain CSC surface markers.

Table 1.9. Previously reported CSC markers for brain cancer.

Solid Tumor Type	Marker(s)	Reference
Brain	$CD133^+$	112
	$CD133^+/Nestin^+$	113
	$CD133^+/A2B5^+$ and $CD133^-/A2B5^+$	114
	$A2B5^+$	115
	$CD133^+/L1CAM^+$	117
	$SSEA^-1^+$	119

1.3.7 Lung cancer

Lung cancer is the most common, yet preventable, cancer related death worldwide, resulting in more mortalities than colon, breast, and prostate cancers combined. The 5-year survival rate for small cell lung carcinoma is 6% while nonsmall cell carcinoma is 17%.[18] Current lung cancer therapies are usually transient and fail to completely eradiate the tumor, causing resistance. One potential hypothesis for drug

resistance to chemotherapy is the presence of drug refractory lung CSC populations in the tumor masses.[121] Eramo et al. identified $CD133^+$ CSC subpopulations (Table 2) in small cell and non-small cell lung cancer from primary human donors. CD133 expression was observed on the surface of 0.32–22% of lung cancer cells by flow cytometry analyses, which varied depending on different disease stages of the sample. In vivo analysis showed that tumor formation required only 1,000 cells to be implanted into SCID mice, while differentiated cell populations injected at 50,000 cells per animal failed to produce tumors.[122] CD176 has also been identified as a potential marker for lung CSC populations and has been observed in combination with CD133 and CD44 cell surface markers. $CD176^+/CD133^+$ and $CD176^+/CD44^+$ phenotypes were observed after sorting cells for CD176 expression, and $CD176^+$ cell populations were found to exhibit features of CSCs, such as tumorigenicity. These results imply that $CD176^+$ may be used as a potential lung CSC marker.[77] See Table 1.10 for a listing of lung CSC surface markers.

Table 1.10. Previously reported CSC markers for lung cancer.

Solid Tumor Type	Marker(s)	Reference
Lung	$CD176^+/CD44^+$	77
	$CD176^+/CD133^+$	77
	$CD133^+$	122

1.3.8 Bladder cancer

Bladder transitional cell carcinoma (BTCC) is the second most prevalent cancer of the urinary tract.[123] Five-year survival rates for BTCC vary by stage of development,

ranging from 6% to 97%.[18] Traditional therapy consists of surgery, radiation, and chemotherapy,[124] but if disease becomes invasive, then treatment outcomes are typically poor due to metastasis.[125] The development of diagnostic markers and new therapies for BTCC is currently needed.

Yang and Chang have identified a subpopulation of BTCC samples from primary human donors that display a $CD44^+/EMA^-$ (epithelial membrane antigen) phenotype (specifically the isoform CD44v6; Table 2). $CD44^+/EMA^-$ populations were shown to overexpress Bmi-1 and EZH2, which are proteins that play a role in self-renewal of normal bladder stem cells. $CD44^+/EMA^-$ cells also were able to form colonies and proliferate in vitro, which are characteristic features of CSCs.[126]

Chan et al. have also postulated that BTCC CSCs can be characterized by the cell surface phenotype $Lin^-/CD44^+$/cytokeratin $(CK)5^+/CK20^-$. Tumors from primary human donors were sorted for $CD44^+$ and $CD44^-$ cells and then transplanted into immunocompromised mice ($RAG2^-/\gamma c^-$). The $CD44^+$ cells were found to be more tumorigenic, requiring only 100–1,000 cells to form tumors, while the $CD44^-$ population required 200,000–500,000 cells to elicit tumors in mice. Immunofluorescence analysis of $CD44^+$ xenografts showed co-expression of CK5 and lack of expression of CK20 (phenotype $Lin^-/CD44^+/CK5^+/ CK20^-$), and this marker phenotype was deemed to be the BTCC CSC population. The authors also queried for other common CSC cell surface markers and discovered that CD47 is highly expressed on $CD44^+$ cells. CD47 inhibits phagocytosis by macrophages, allowing for pathogenesis of the bladder cancer.[125]

Hoechst 33342 dye is a widely used indicator of side populations with potential CSC characteristics.[127] ATPbinding cassette (ABC) and multidrug resistance efflux pumps are responsible for the elimination of Hoechst 33342 dye, as well as cytotoxic drugs, from cells. This process is detectable by FACS and allows for the identification and isolation of subpopulations of cells displaying these characteristics that are common of CSCs.[127,128] ABC-G2 transporters were detected in the BTCC cell line T24. ABC-$G2^+$ and ABC-$G2^-$ cells were cultured in vitro, and their growth characteristics were evaluated. ABC-$G2^+$ cells demonstrated consistent proliferation, whereas the ABC-$G2^-$ did not. Side populations of ABC-$G2^+$ also were able to differentiate into ABC-$G2^-$ cells, which further supports the hypothesis that ABC-$G2^+$ is a marker of BTCC CSCs.[127] See Table 1.11 for a listing of bladder CSC surface markers.

Table 1.11. Previously reported CSC markers for bladder cancer.

Solid Tumor Type	Marker(s)	Reference
Bladder	$Lin^-/CD44^+/CK5^+/CK20^-$	[125]
	$CD47^+/CD44^+$	[125]
	$CD44v6^+/EMA^-$	[126]
	ABC^-G2^+	[127]

1.3.9 Prostate cancer

Prostate cancer is the most commonly diagnosed malignancy and second leading cause of death in men in the United States.[18] More than 80% of men will develop prostate cancer in their lifetime, and most diseases will not be diagnosed.[129] Prostate cancer is routinely treated by hormone ablation therapy, but this therapy regimen fails

when the disease progresses to a hormone-refractory state.[130] Currently, cytotoxic small molecules are the only therapeutic regimen able to improve outcomes for patients with hormone-refractory prostate cancers.[131] Identification of CSC surface markers could provide a foundation for the development of next-generation drugs that target prostate CSCs.[130]

The first CSC surface marker identified for prostate cancer was CD44 (Table 2). In 1997, Liu et al. reported their observation that $CD44^+$ prostate cancer cells were negative for prostate-specific antigen (PSA) and prostate acid phosphatase secretion, which are proteins that are produced during cancer cell differentiation. On the other hand, when $CD44^+$ prostate cancer cells were co-cultured with stromal cells, the secretion of PSA was detected, indicating that the interaction between stromal cells and $CD44^+$ prostate cancer cells stimulated the differentiation ability of the latter, since PSA production was not detected when either stromal cells or $CD44^+$ prostate cancer cells when cultured alone.[88] Collins et al. demonstrated that prostate CSCs could be identified from human specimens with a $CD44^+/\alpha2\beta1^{high}/ CD133^+$ phenotype, and this population comprised 0.1– 0.3% of the total amount of cells in the tumor. In a colony-forming assay, the $CD44^+/\alpha2\beta1^{high}/CD133^+$ population yielded 3.7-fold greater number of colonies compared with the total cell population and more than 30-fold greater number of colonies compared with $CD44^+/\alpha2\beta1^{hi}/CD133^-$ or $CD44^+/\alpha2\beta1^{low}$ cells, which suggests the $CD44^+/\alpha2\beta1^{high}/CD133^+$ phenotype has the ability to self-renew.[28] Patrawala et al. performed in vivo studies in NOD/SCID mice utilizing prostate cancer cell lines that were enriched for the $CD44^+/\alpha2\beta1^{high}$ combination phenotype.[132,133] They

found that the $CD44^{+}/\alpha2\beta1^{high}$ population had greater tumorigenicity than other populations isolated ($CD44^{+}/\alpha2\beta1^{low}$, $CD44^{-}/\alpha2\beta1^{high}$, $CD44^{-}/\alpha2\beta1^{low}$), further supporting the evidence that the $CD44^{+}/\alpha2\beta1^{high}$ phenotype is the CSC population.[133]

Mulholland et al. later confirmed that the $Lin^{-}/Sca\text{-}1^{+}/CD49f^{high}$ subpopulation of prostate cancer cells were CSCs in a murine prostate $PTEN^{-}$ model (PTEN is a tumor suppressor gene in the protein kinase B pathway).[130] The loss of PTEN activity is strongly associated with the initiation and metastasis of prostate cancer.[134] Tissue samples were taken from murine PTEN mutant prostate tumor grafts on SCID mice after 6–8 weeks, digested into single-cell suspensions, and sorted by FACS. Through a systematic study of various potential surface markers, Sca-1 and CD49f were identified as surface markers of prostate CSCs. Sorted cells ($Lin^{-}/Sca\text{-}1^{+}/CD49f^{high}$ and $Lin^{-}/Sca\text{-}1^{+}/CD49f^{low}$) were then injected into SCID mice and only $Lin^{-}/Sca\text{-}1^{+}/CD49f^{high}$ cells induced tumor growth.[130] See Table 1.12 for a listing of prostate CSC surface markers.

Table 1.12. Previously reported CSC markers for prostate cancer.

Solid Tumor Type	Marker(s)	Reference
Prostate	$CD44^{+}/\alpha_2\beta_1^{high}/CD133^{+}$	[28]
	$Lin^{-}/Sca\text{-}1^{+}/CD49f^{high}$	[130]
	$CD44^{+}/\alpha_2\beta_1^{high}$	[133]

1.3.10 Ovarian cancer

The most lethal disease of the female reproductive tract is ovarian cancer.[135] High mortality rates occur due to the difficulty in diagnosing early stage ovarian cancer as well as the high prevalence of drug-refractory relapse after initial treatment, which is

likely a result of CSC subpopulations that survive therapy.[136] Ovarian cancer 5-year survival rates vary depending on the stage of development of the tumor. Early stage diagnosis, when the disease has yet to metastasize, has a 5-year survival rate of 73%, while late-stage ovarian cancer diagnosis results in a 28% survival rate.[18]

Zhang et al. first identified CD44 as a potential ovarian CSC surface marker in 2008. Analysis of human ovarian specimens revealed a small population (0.14–0.2%) of $CD44^+/CD117^+$ cells (Table 2) that were highly tumorigenic and demonstrated self-renewal by spheroid formation. Tumorigenicity was measured by engraftment of $CD44^+/CD117^+$ and $CD44^-/CD117^-$ subpopulations into nude mice. The $CD44^+/CD117^+$ subpopulation was able to repopulate the tumor following injection of only 100 cells, whereas the isolated $CD44^-/CD117^-$ phenotype required 500,000 cells for tumor development after 3 months.[135]

Ferrandina et al. identified $CD133^+$ subpopulations as ovarian CSCs in primary human samples. The $CD133^+$ subpopulation was 4.7-fold more active in a colony-forming assay, which demonstrated replicative capacity.[137] Work by Curley et al. verified the presence of a $CD133^+$ subpopulation with tumor-initiating properties and found that 0.2– 12.5% of the tumors expressed this phenotype.[138]

$CD24^+$ has also been characterized as a potential surface marker of human ovarian CSCs. Two weeks after the plating of isolated $CD24^+$ ovarian cancer cells, analysis of the cell population revealed both $CD24^+$ and $CD24^-$ phenotypes, which suggests that $CD24^+$ cells are CSCs due to their ability to self-renew and differentiate. Conversely, the same experiment performed with $CD24^-$ cells failed to yield $CD24^+$

cells after the same amount of time in culture. Additional in vivo studies demonstrated that only 5,000 $CD24^+$ cells were needed for tumor formation after injection into nude mice, whereas $CD24^-$ cells injected at the same concentration were unable to generate tumors.[139] Therefore, $CD24^+$ cells are more tumorigenic than $CD24^-$ cells.

To add to the growing number of ovarian CSC markers, Wei et al. isolated a triple surface marker phenotype, $CD44^+/CD24^+/EpCAM^+$, which best characterized the most proliferative cell subpopulation when compared with all other marker combinations. Cells lines OVCAR-5, SKOV-3, and IGROV-1, as well as primary human donor samples were used for experiments. Colony-formation assays were performed on $CD44^+/CD24^+/EpCAM^+$ sorted cells to measure proliferation rates and to characterize self-renewal properties. In vivo studies were performed comparing $CD44^+/CD24^+/EpCAM^+$ and $CD44^-/CD24^-/EpCAM^-$ phenotypes by injection into NOD/SCID mice. These studies demonstrated that as few as 100 $CD44^+/CD24^+/EpCAM^+$ cells injected in NOD/SCID mice were capable of tumor formation, and $CD44^+/CD24^+/EpCAM^+$ cells grew tumors faster and more aggressively than the $CD44^-/CD24^-/EpCAM^-$ population.[140] Consequently, the $CD44^+/CD24^+/EpCAM^+$ phenotype was deemed to be more tumorigenic and likely a CSC population. See Table 1.13 for a listing of ovarian CSC surface markers.

Table 1.13. Previously reported CSC markers for ovarian cancer.

Solid Tumor Type	Marker(s)	Reference
Ovarian	$CD44^+/CD117^+$	[135]
	$CD133^+$	[137,138]
	$CD24^+$	[139]
	$CD44^+/CD24^+/EpCAM^+$	[140]

1.4 The chemical biology and drug targeting of cell surface markers on cancer stem cells

The repertoires of cell surface macromolecules found on CSCs are widely used as markers for characterizing CSC populations (described previously). In addition to these diagnostic applications, the unique molecules that are presented on the surfaces of CSCs are valuable targets for drug delivery. However, many of the surface markers that are presented on CSCs are known to also be expressed at varying levels on the surfaces of normal, non-cancerous cells. Some of the reported CSC surface markers, in addition, have not been rigorously queried for expression across panels of non-cancerous tissue. Therefore, cell surface markers that are selected for targeted drug delivery applications must be evaluated for cancer cell selectivity during development studies to probe for off-target effects.[8] In the following section we review, where known, several of the established chemical and structural features that are characteristic of the most common CSC surface molecules, as well as previous efforts to deliver therapeutic agents to CSCs by targeting their unique cell surface markers. We recognize that an equally exciting area of intense investigation involves the identification of small molecules that possess CSC inhibitory properties, such as the recent reports of the anti-CSC activities of the

natural products parthenolide and salinomycin.[19,141] However, we have focused here on those therapeutic molecules that target CSC surface markers as part of their mechanism of inhibition.

1.4.1 CD133

CD133 is a five-transmembrane protein consisting of 865 amino acid residues. It consists of two extracellular glycosylated loops and two cytoplasmic loops, bringing the final molecular weight of CD133 to 120 kDa.[142] Under bioenergetic stresses, such as hypoxic conditions, CD133 expression is upregulated significantly.[143] No ligands or signaling mechanisms have been defined for CD133. Although the biological functions of CD133 have not been fully elucidated, the localization of CD133 to protrusions in the plasma membrane suggests a possible role in membrane organization.[143] The rationale for this hypothesis is the observation that CD133 is commonly located on cell membrane protrusions, such as microvilli-like structures on epithelial cells, which are important for increasing the surface area and the reabsorption characteristics of those cells.[144,145] In addition to its presence on CSCs from multiple diseases (*vide supra*), CD133 is commonly found as a marker of somatic stem cells, ranging from hematopoietic, neural, prostate, kidney, liver, and pancreas.[146]

Table 1.14: Targeting of CSC populations by antibodies and small molecules.

Antibody/Agents	Description	Cancer Indication	Reference
Clone7	Monoclonal antibody against CD133	Brain	[147]
CD133 targeted carbon nanotubes	Single walled carbon nanotubes functionalized with anti-CD133 monoclonal antibodies	Brain	[36]
CD133 targeted lipid nanocapsules	Lipid nanocapsules functionalized with anti-CD133 monoclonal antibodies	Colorectal	[148]
Catumaxomab	Monoclonal trifunctional antibody against EpCAM, CD3 and APCs	Malignant ascites, ovarian and gastric	[149]
MT110	Monoclonal single chain bispecific antibody against EpCAM and CD3	Colorectal, lung, gastric	[150]
Edrecolomab	Monoclonal antibody against EpCAM	Colorectal	[151]
Adecatumumab (MT201)	Monoclonal antibody against EpCAM	Breast, colorectal, prostate	[152]
H90	Monoclonal antibody against CD44	Acute myelogenous leukemia	[20]
P245	Monoclonal antibody against CD44	Breast	[153]
Gemtuzumab ozogamicin (GO)	Small molecule-anti-CD33 antibody conjugate	Acute myelogenous leukemia	[154,155]
3C2-1D12	Monoclonal antibody against ABCB5	Melanoma	[156]
Ubenimex	Dipeptide small molecule inhibitor of CD13	Liver	[94]
7G3	Monoclonal antibody against CD123	Acute myelogenous leukemia	[157]
Clone B6H12.2	Monoclonal antibody against CD47	Acute myelogenous leukemia	[51]

CD133 is one of the most prominent CSC surface markers. Although a multitude of monoclonal antibodies against CD133 have been previously described, most commercially available CD133 antibodies have limited applicability because they only recognize glycosylated $CD133^+$ epitopes.[158] Consequently, the majority of CD133

antibodies fail to identify the entire $CD133^+$ population. Nonetheless, a repertoire of CD133-recognizing antibodies is available for various uses.

Clone7 is an anti-human $CD133^+$ monoclonal antibody that recognizes glycosylated, as well as non-glycosylated, epitopes of CD133. Clone7 allows for multiple experiments with CD133 to be performed regardless of post-translational glycosylation status. Clone7 can be utilized in Western blotting, immunofluorescence, flow cytometry, and immunohistochemistry applications.[147]

Single-walled carbon nanotubes functionalized with anti-CD133 antibodies to actively target $CD133^+$ have been developed by Wang et al. Selective uptake of the nanotubes was observed only in the $CD133^+$ population, and phototherapy eradication of the $CD133^+$ cells bearing the nanotubes was achieved by absorption of 808-nm near IR light.[159] This study has yielded a potential photothermal approach to selectively target $CD133^+$ glioblastoma cells.

Lipid nanocapsules functionalized with anti-CD133 antibodies have been shown to target $CD133^+$ CSCs, in recent work by Bourseau-Guilmain et al. Selective uptake by the $CD133^+$ population was observed by fluorescence of Nile red, which was loaded into the lipid nanocapsules. Loading of hydrophobic drugs into the lipophilic cores of the nanocapsules are now being tested for the direct therapeutic targeting of $CD133^+$ tumors with the goal of diminished side effects.[148]

1.4.2 Epithelial cell adhesion molecules

EpCAM is a single transmembrane domain glycoprotein that plays a major role in cell-to-cell adhesion, both constructive and disruptive.[160] EpCAM is specifically expressed on epithelial cancers such as breast, colorectal, pancreatic, liver and ovarian tumors and can interfere with cell-to-cell adhesion in various ways. One interference method is the disruption of the bonding of α-cadherin and F-actin, which translates into a loss of E-cadherin-mediated cell-to-cell adhesion.[161] Alternatively, EpCAM was originally observed to prevent cell scattering due to cellular adhesion characteristics.[162] Because of this dual role in adhesion of cells, EpCAM expression is both tumor-promoting as well as tumorsuppressive. The role EpCAM takes within a tumor is dependent on the tumor type.[160]

Catumaxomab (Removab®, developed by Fresenium Biotech GmbH and Trion Phama) is a rat–mouse hybrid monoclonal and tri-functional antibody against EpCAM, CD3 antigen in T cells, and antigen-presenting cells (APC; such as microphages, natural killer cells, and dendritic cells).[163,164] Its capability of binding three different types of cells comes from its unique structure: it is a heterozygous antibody with one chain of mouse anti-EpCAM antibody and one chain of rat anti-CD3 antibody. The heavy-chain Fc region of both chains can bind to the Fc receptors on APCs. Catumaxomab is more than 1,000-fold more potent than a monospecific anti-EpCAM antibody in killing cancer cells.[163,164] Catumaxomab does not require the utilization of any additional reagent(s) to stimulate the immune response. The different specificities of the antigen binding sites of the two antibody chains enable simultaneous recognition of both tumor cells (especially

CSCs) and T cells, and the functionalized heavy chain Fc domain is able to recruit and stimulate APC, resulting in the initiation of complex immune reactions. In a pivotal phase II/III clinical study, Catumaxomab treatment lead to activation of peritoneal T cells and a completion elimination of $CD133^+/EpCAM^+$ cells from the peritoneal fluid of malignant ascites patients.[165,166] Catumaxomab was approved in the European Union in 2009 and is undergoing phase III clinical trials in the United States for the treatment of malignant ascites, ovarian cancer, and gastric cancer.[149] In addition to Catumaxomab, there are other bi-functional or trifunctional EpCAM-targeting antibodies undergoing preclinical studies or clinical trials.

MT110 (developed by Micromet GmbH) belongs to a class of single-chain antibodies called bispecific T cell engager or BiTE. MT110 was constructed by coupling the antigen binding domains of α-CD3 and α-EpCAM monoclonal antibodies, yielding a hybrid antibody with specificity for both EpCAM and CD3.[167] A BiTE antibody enables the generation of a cytolytic synapse between a cytotoxic T cell and a target cell that binds to the BiTE antibody.[168] In the case of MT110, the target cell is a tumor cell that expresses the EpCAM cell surface marker. The formation of the cytolytic synapse induces T cells for redirected lysis of the $EpCAM^+$ target cell at pico- to femtomolar concentrations.[167] MT110 has been shown to have high antitumor activity in various animal models[167,169] and is capable of completely eliminating colorectal CSCs in cell culture and in animal models.[170] MT110 is currently in phase I clinical trials in the United States for lung and gastrointestinal cancers.[150]

Edrecolomab (Mab17-1A, Panorex®, developed by Cancer and Leukemia Group B) was one of the first monoclonal antibodies administered to humans for cancer therapy. Edrecolomab is a low-affinity murine IgG2a monoclonal antibody that targets the cell-surface glycoprotein EpCAM. Because of the extensive basal level expression of EpCAM molecules on normal epithelial cells,[171] the toxicity of EpCAM-targeting antibodies was viewed as a potential obstacle for the development of this class of therapies.[172] Since the expression level of EpCAM on the surface of CSCs is much higher than it is on the surface of normal epithelial cells, the designed low-affinity edrecolomab decreases the possibility of off target effects while maintaining efficacy for targeting CSCs, which makes edrecolomab a well-tolerated drug with a relatively wide therapeutic window.[172] Edrecolomab, which is thought to eliminate tumor cells by antibody-dependent cell-mediated cytotoxicity (ADCC) and/or complement-dependent cytotoxicity (CDC),[152,173] underwent phase II–III clinical trials in the United States as a potential postoperative adjuvant treatment of stage II colon cancer. However, the clinical trial was terminated in 2005 because of lack of improvement of overall or disease-free survival.[151]

Adecatumumab (MT201, developed by Micromet GmbH) is a fully humanized, recombinant IgG1 monoclonal antibody that specifically binds to EpCAM with low affinity. It was designed to retain the safety profile, yet improve the antitumor potency of edrecolomab. MT201 exhibited EpCAM-specific CDC with potency similar to that of edrecolomab, but the efficacy of ADCC induction of MT201 was two-fold greater than that of edrecolomab.[152] It also has been reported that the combination of adecatumumab

and docetaxel is safe and efficacious in heavily pretreated advanced-stage breast cancer patients.[174] MT201 is now in phase II clinical trials in the United States for the treatment of prostate, colorectal, and metastatic breast cancers.[152]

1.4.3 CD44

The lymphocyte adhesion receptor CD44, first described in 1983,[175] is a transmembrane glycoprotein that binds hyaluronate (HA).[176] CD44 was first cloned in 1989,[177] and the binding domain was crystallized in 2004 (PDB 1POZ).[178] CD44 is involved in many important cellular processes, including cell growth, survival, differentiation, and apoptosis.[179-181] CD44 plays a crucial role in cancer migration and matrix adhesion in response to the cellular microenvironment, and high CD44 levels are associated with increasing cellular aggregation and tumor metastatic potential.[176] The importance of CD44 in cancer cells, especially in CSCs, is closely related to its unique structure and function. The extracellular domain of CD44, which is a globular structure, contains two domains: a link domain and a HA binding domain.[176,182] Binding sites for microenvironment proteins, such as laminin, collagen, and fibronectin,[183,184] receptors such as E- and L-selectin,[185] and other glycosaminoglycans have also been characterized.[186] The transmembrane region of CD44 contains a glycolipid-enriched microdomain (GEM), which is responsible for the oligomerization of CD44s.[187] The crosslinking and GEM association of CD44s, which is often induced by the binding of HA or other ligands, leads to a conformational change of the molecule and is important in CD44-mediated signal transduction.[188] The main function of the cytoplasmic domain

of CD44 is to recognize its partner molecules ankyrin, ezrin, radixin, and moesin (ERM). ERM proteins are cytoskeleton proteins that regulate cell migration, cell shape, and protein resorting in the plasma membrane.[189] The unique structure of CD44 molecules indicates that they are functionally important to CSCs. CD44 regulates cancer cell adhesion and homing,[26] cell extravasation and migration,[190] the crosstalk between stem cells and their niche,[191] epithelial mesenchymal transition,[192] and the repression of cell apoptosis.[193] Each of these functions contributes to the observation that CD44 is one of the most prevalent surface markers in CSCs.[194] CD44 is a cell surface marker extensively expressed on the surface of a large range of CSCs including AML, bladder, breast, colorectal, liver, ovarian, pancreatic, and prostate cancers (Tables 1 and 2).

H90 is an anti-CD44 monoclonal antibody that was first reported by John Dick and colleagues in 2006 as a therapeutic approach to treat AML.[20] Currently, the majority of leukemia chemotherapeutics are antiproliferative drugs that target rapidly cycling leukemic cells. However, disease relapse is observed in more than 70% of adult patients, indicating that quiescent AML CSCs have not been effectively removed.[195] AML CSCs are more difficult to target than highly proliferative and differentiated leukemic cells due to their quiescent nature. However, the survival and self-renewal of AML CSCs requires attachment to extracellular niche proteins.[196] Thus, targeting the interaction between niche proteins and AML CSCs, which is mediated by the cell surface marker CD44, may provide a mechanism to eradicate AML CSCs.[197] In vivo administration of H90 to NOD/SCID mice transplanted with human AML showed a significant decrease in leukemia repopulation.[20]

P245 is another CD44-specific monoclonal antibody with a design and targeting rationale similar to H90. Administration of P245 to human breast cancer xenografts markedly decreased the growth of tumor cells and effectively prevented tumor relapse after chemotherapy-induced remission. P245 is now under preclinical study for the treatment of breast cancer.[153] Both of the above CD44-specific antibodies also have the effect of inducing differentiation in CSCs.[26]

1.4.4 CD33

CD33 is a myeloid cell surface antigen that is expressed on leukemic blasts from 85% - 90% of AML patients,[44] and the combination phenotype $CD34^{+}/CD38^{-}/CD123^{+}/CD33^{+}$ is uniquely expressed on the surface of AML CSCs.[45] CD33 is a single transmembrane protein that is activated by phosphorylation.[198] CD33 functions as a putative adhesion molecule of monocytic and myeloid lineage cells and modulates sialic acid-dependent binding and cell differentiation.[44] In immune responses, CD33 acts as an inhibitory receptor of ligand binding induced tyrosine phosphorylation by recruiting cellular phosphatases to its SH2 domain and blocking signal transduction through hydrolysis of the phosphates of signaling molecules.[199,200] CD33 also induces apoptosis in acute myeloid leukemia through mechanisms that are not fully characterized.[201]

Gemtuzumab ozogamicin (Mylotarg®, developed by Wyeth and Pfizer) is a small-molecule–anti-CD33 monoclonal antibody conjugate. The small-molecule component of this drug is N-acetyl γ-calicheamicin dimethyl hydrazide, a stable

enediyne antitumor antibiotic that was identified from a screen of potent DNA alkylators.[202] The antibody component is a humanized IgG4 anti-CD33 antibody (hP67.6) that is conjugated to calicheamicin by an acidlabile hydrazone linker. Studies have shown that the antibody–drug conjugate exhibits good potency, as well as selectivity, which is attributed to its property of only releasing the DNA alkylator in the acidic environment of cellular lysosomes (i.e., it is stable in blood).[154,155] The antibody component of gemtuzumab ozogamicin (GO) is largely non-toxic and functions to facilitate the uptake of calicheamicin into $CD33^+$ AML cells. Once released, calicheamicin undergoes rearrangement to form a diradical metabolite that is capable of binding DNA and initiating single- and double-stranded DNA breaks, which results in cell cycle arrest or apoptosis.[203] GO was marketed as an AML therapeutic from 2000 to 2010 but was voluntary withdrawn from the market in June 2010 when postclinical trials showed an increasing number of deaths and a lack of benefit compared with other conventional cancer therapies.[204] Currently, the combination of GO and other chemotherapeutics are under various stages of clinical investigations.[205]

1.4.5 CD34

HSC antigen CD34 is a single transmembrane glycoprotein and belongs to the CD34 family of proteins.[206] CD34 was first identified as a surface marker of immature lymphohematopoietic progenitor cells in 1984.[207] Four years later, Berenson et al. reported that, following the transplantation of $CD34^+$ human marrow cells, hematopoietic systems were able to reconstitute in lethally irradiated baboons.[208] CD34

has been widely used as a surface marker for the identification of non-cancerous hematopoietic stem cells for over three decades[209] and, more recently, has been identified as a CSC marker for multiple diseases (vide supra). Besides hematopoietic and leukemic stem and progenitor cells, CD34 is also widely expressed on the surface of vascular endothelial cells and mast cells.[209] In spite of the functional importance of CD34, the crystal structure of this protein remains unsolved. As a result, the structure and function of CD34 is not as well studied as CD44. The extracellular domain of CD34 contains a serine-, threonine- and proline-rich domain that is extensively glycosylated and sialylated.[210,211] Moreover, a juxtamembrane stalk region, a cysteine-bonded globular domain, and a putative N-glycosylation site were also identified in the extracellular section of CD34.[206] The most well-known intercellular binding partner of CD34 is L-selectin, which is a cellular adhesion molecule expressed on the surface of leukocytes.[212] Other potential ligands of CD34 are also under exploration. In addition, each CD34 protein comprises a single transmembrane helix and a cytoplasmic domain that contains highly conserved phosphorylation sites and a C-terminal PDZ (postsynaptic density protein) binding motif.[210,213] The PDZ binding motif of CD34 recognizes Crk-like protein, which is an adaptor protein that further interacts with the N terminus of NHERF (Na^+/H^+ exchange regulatory cofactor) scaffolding proteins. The C terminus of NHERFs contains an ERM binding domain, which facilitates the indirect interaction of actin cytoskeleton with other binding partners of NHERF proteins.[214] CD34 has been proposed to be involved in enhancing proliferation,[213] blocking differentiation,[215] promoting lymphocyte adhesion,[211] and the trafficking of

hematopoietic cells.[206,216] Because of the ubiquitous expression pattern of CD44 on the surface of both cancerous and normal cells, it has not been utilized for drug delivery to CSCs.

1.4.6 ABCB5

ATP-binding cassette sub-family B member 5 is a member of ABC transporter proteins that contains two transmembrane domains and two nucleotide binding domains.[217] ABC transporter proteins are part of the p-glycoprotein family and are responsible for the transport of a large array of substrates across cellular membranes. Due to these characteristics, ABC transporter proteins are responsible for the multidrug resistance profiles of cancer cells due to their ability to export drugs from cells. ABCB5 exists in two isoforms, α and β, and is a cell surface marker that is currently known to be expressed on skin cancer cells and is closely associated with the chemoresistance of malignantmelanoma-initiating cells (MMICs).[218]

3C2-1D12 is a monoclonal anti-ABCB5 antibody. Systematic administration of 3C2-1D12 into nude mice revealed an increase in ADCC in $ABCB5^+$ MMICs, as well as tumor-inhibitory effects.[107] This anti-ABCB5 monoclonal antibody has not yet reached preclinical testing status.

1.4.7 CD13

CD13 (alanine aminopeptidase N) is a 967-amino acid single-transmembrane peptidase, consisting of a small N terminus and a large C terminus that contains the

active site.[219] CD13 is found ubiquitously in various organs, such as the kidneys, small intestines, and the liver. CD13 plays an important role in antigen processing for the immune response and is expressed in T and B cells as well as macrophages.[220] CD13 has been reported as a diagnostic cell surface marker in liver CSCs.[94]

Ubenimex is a small molecule inhibitor of CD13. Ubenimex (bestatin) is a dipeptide isolated from Streptomyces olivoreticuli[221] and is known to have antitumor effects through augmentation of the host immune system.[222,223] Ubenimex is a competitive protease inhibitor and deters the growth of lung cancer and leukemic cell lines.[224,225] A mechanism of action has been proposed by the co-crystallization of ubenimex with leukotriene A4 hydrolase (PDB 1HS6),[226] which is structurally homologous to cell surface antigen CD13.[227] Studies have shown that, in mouse xenograft models, the combination of CD13 inhibitor and cell proliferation inhibitor fluorouracil dramatically reduces tumor size, as well as tumor progression, as compared with either single agent therapy.[94] Ubenimex is not under clinical investigation at the present time.

1.4.8 CD123

CD123 is the α subunit of the interleukin-3 cell surface receptor. It has been elucidated as a CSC marker in AML[42] but also has been identified as a marker of normal hematopoietic stem cells, where it plays an important role in proliferation.[228] Structural information for CD123 is not well established.

7G3 is a monoclonal anti-CD123 antibody. Targeting of CD123 by this antibody has been shown to significantly reduce $CD34^{+}/CD38^{-}$ AML CSC cell populations and tumor engraftment in NOD/SCID mice. However, the efficacy of the antibody in established AML disease treatment models is still limited, and optimization is required before this strategy is suitable for clinical investigations. The proposed mechanism of anti-CD123 antibodies (e.g., 7G3) includes the inhibition of AML CSC homing to bone marrow and prevention of activation of human CD123 by IL-3.[157] To our knowledge, molecules of this class are not yet in clinical trials.

1.4.9 CD47

The leukocyte surface antigen CD47 plays an important role in cell adhesion by acting as a platelet adhesion receptor.[229] CD47 is widely expressed at low levels in many tissues and highly expressed on AML CSCs, where increased CD47 expression is indicative of poor prognosis.[51] One functional ligand of CD47 is signal regulatory protein-α (SIRPα), which is expressed on phagocytes. The interaction between CD47 and SIRPα activates a signal transduction cascade that results in the inhibition of phagocytosis.[230] The ectodomain of CD47 was crystallized in 2008 (PDB 2JJS).[231]

Clone B6H12.2 is a monoclonal antibody that blocks the interaction between CD47 and SIRPα. It has been demonstrated that B6H12.2 enables phagocytosis of human AML CSCs in vitro and has therapeutic potential.[51] In NOD/SCID mice, B6H12.2 treatment depleted AML cells in peripheral blood.[232] In a preclinical in vivo mouse treatment model with high levels of engraftment, treatment with anti-CD47

antibodies resulted in the rapid clearance of AML and targeting of the CSC population.[51,232]

1.5 Summary and conclusions

Numerous studies have reported the existence of tumor cell populations with abilities to self-renew, differentiate, and potently initiate tumorigenesis. These cell populations, termed cancer stem cells (CSCs), are strongly implicated in disease propagation and, if not addressed during drug therapy, can facilitate disease relapse. Consequently, there is a significant and unmet need to better characterize the unique biology of CSCs as well as develop therapies to eradicate them. CSC markers, which are macromolecules (e.g., proteins, carbohydrates, etc.) that are uniquely expressed on the surface or in the cytoplasm of CSCs, are essential for the isolation and characterization of CSC populations. Additionally, these CSC markers provide targets for the specific delivery of therapeutic molecules into CSCs. In this chapter, we reviewed those cell surface macromolecules that are presented on the surfaces of many tumor CSCs, described the unique chemical and structural features of the most common markers, and reported recent efforts to target CSC surface markers as part of drug delivery efforts. Clearly, the field of CSC biology is still in its infancy and even less advanced are efforts to target those cells with therapeutic molecules. However, given that the elimination of CSCs may result in significantly enhanced therapy outcomes in patients, the focus of cancer drug discovery scientists should shift, at least in part, to designing next generation drugs that target CSC populations.

Table 1.15. Alternative names of CSC surface markers that appear in this chapter.

CSC marker	Other common names	Cancerous tissue where expressed
A2B1	α2β1 Integrin; a2b1 integrin; CD49b	Prostate
A2B5	α2β5 Integrin; a2b5 integrin	Brain
ABCB5	ABCB5 P-gp; ATP-binding cassette sub-family B member 5	Melanoma
ABCG2	ABC transporter G family member 2	Skin, bladder
CD4	Leu-3; T4	ALL
CD7	GP40; Leu-9; TP41	ALL
CD9	BTCC-1; DRAP-27; MIC3; MRP-1; TSPAN-29; 5H9 antigen; p24	ALL
CD10	Atriopeptidase; CALLA; Enkephalinase; Neprilysin; SFE	ALL
CD13	Aminopeptidase N; Alanyl aminopeptidase; gp150; Lap1	Liver
CD19	B-lymphocyte surface antigen B4; Leu-12	ALL
CD24	Small cell lung carcinoma cluster 4 antigen	Breast, colorectal, ovarian, pancreatic
CD25	Interleukin-2 receptor subunit alpha; TAC antigen; p55	AML
CD29	Integrin beta-1; Fibromectin receptor subunit beta; VLA-4 subunit beta	Breast
CD32	Low affinity IgG Fc receptor II-b; CDw32; Fc-gamma RIIb	AML
CD33	Siglec-3; gp67	AML, ALL
CD34	Hematopoietic progenitor cell antigen CD34	AML, ALL, CML
CD38	ADP-ribosyl cyclase 1; cADPr hydrolase 1; T10	AML, ALL, CML
CD44	CDw44; Epican; ECMR-III; GP90 receptor; HUTCH-I; Heparan sulfate proteoglycan; Hermes antigen; PGP-1; Hyaluronate receptor	AML, bladder, breast, colorectal, liver, ovarian, pancreatic, prostate
CD45	Receptor-type tyrosine-protein phosphatase C; Leukocyte common antigen; T200	AML, liver
CD47	Leukocyte surface antigen CD47; antigenic surface determinant protein OA3; integrin-associated protein; MER6	AML, bladder

Table 1.15. (Continued)

CSC marker	Other common names	Cancerous tissue where expressed
CD49f	Integrin alpha-6; VLA-6	Breast, colorectal, prostate
CD71	Transferrin receptor protein 1; T9; p90	AML, breast, liver
CD90	Thy-1 membrane glycoprotein	ALL, AML, breast, liver
CD96	T cell surface protein tactile; T cell-activated increased late expression protein	AML
CD110	Thrombopoietin receptor; Myeloproliferative leukemia protein; Proto-oncogene c-Mpl	ALL
CD117	Mast/stem cell growth factor receptor kit; Piebald trait protein; c-kit; p145; Tyrosine-protein kinase kit	AML, ovarian
CD133	Prominin-1; antigen AC133; Prominin-like protein 1	ALL, brain, breast, colorectal, liver, lung, melanoma, ovarian, pancreatic, prostate
CD166	Activated leukocyte cell adhesion molecule	Colorectal
CD173	H2	Breast
CD174	Lewis Y	Breast
CD176	Thomsen-Friedenreich antigen (TF)	Breast, liver, lung
CD201	Endothelial protein C receptor; PROCR; APC receptor	Breast
CK20	Cytokeratin-20; Protein IT	Bladder
CK5	Type II keratin Kb5; Cytokeratin-5; 58 kDa cytokeratin; Keratin-5; Type II cytoskeletal 5	Bladder
CLL-1	C-type lectin domain family 12 member A; DCAL-2; MICL	AML
CXCR4	FB22; Fusin; HM89; LCR1; LESTR; NPYRL; SDF-1 receptor; CD184; C-X-C chemokine receptor type 4	Pancreatic
Cytokeratin	Keratin	Breast

Table 1.15. (Continued)

CSC marker	Other common names	Cancerous tissue where expressed
EMA	Epithelial membrane antigen; MUC-1; CD227; PEM; PUM; KL-6; H23AG; Episialin; Carcinoma-associated mucin; Breast carcinoma associated antigen DF3	Bladder
EpCAM	CD326; GA733-2; KSA; KS1/4 antigen; ESA; EGP314; EGP-2; Adenocarcinoma-associated antigen; Cell surface glycoprotein Trop-1	Breast, colorectal, liver, ovarian, pancreatic
HLA-DR	CD74; p33; Ia antigen-associated invariant chain	AML
L1CAM	CD171	Brain
Lin	Cell lineage protein	AML, bladder, breast, prostate
OV6	-	Liver
Sca-1	Stem cell antigen-1	Prostate
SSEA-1	Stage-specific embryonic antigen-1; CD15	Brain

Chapter 2. Development of novel parthenolide analogues and evaluation of their anticancer activities

2.1 Introduction

Sesquiterpene lactones are a large family of natural products that have broad therapeutic applications as anti-inflammatory, antimicrobial, antiviral and antitumor agents. Currently, there are over 5000 known natural sesquiterpene lactones from four different families;[233-236] only three sesquiterpene lactones (and their adducts) have made it to clinical trials. These sesquiterpene lactones are thapsigargin, artemisinin, and parthenolide which were evaluated as antimalarial (artemisinin) and anticancer agents respectively (Thapsigargin and LC-1, **Figure 2.1**).[237]

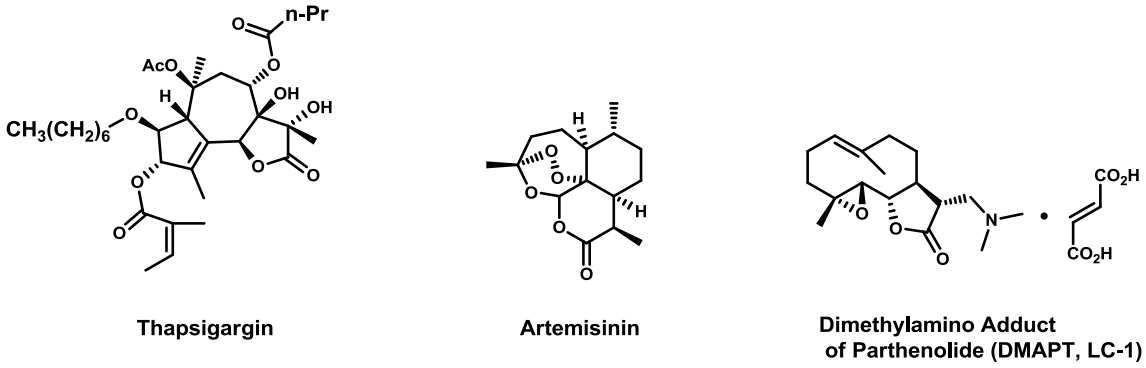

Thapsigargin | Artemisinin | Dimethylamino Adduct of Parthenolide (DMAPT, LC-1)

Figure 2.1 Structure of the three sesquiterpene lactones that have gone to clinical trials: thapsigargin, artemisinin, and the dimethylamino adduct of parthenolide.

Parthenolide (**PTL, 1**) is a germacranolide sesquiterpene lactone from the feverfew plant *Tanacetum parthenium*, a known medical herb utilized for centuries.[238]

Originally isolated by Sorm et al in 1961, **PTL** can comprise up to 1% of dried feverfew leaves.[239] Out of all the natural products contained in feverfew leaves, **PTL** is the major natural product.[238] Although known for many therapeutic uses, **PTL** has been predominately investigated as an anticancer agent against numerous cancer types, both *in vitro* and *in vivo*. Specifically, **PTL** has been tested against cervical cancer,[240] glioblastoma,[241] breast cancer,[242,243] leukemia,[234,244-246] pancreatic cancer,[247] prostate cancer,[248,249] lung cancer,[250-252] melanomas,[253-255] and colon cancer.[256]

Although the mechanism of anticancer activity of **PTL** is not fully elucidated, it has been demonstrated that **PTL** has strong NF-κB inhibition.[233,257] It has been found that the NF-κB pathway is constitutively active or dysregulated in numerous disorders, including cancer.[237] Currently, two mechanisms of inhibition have been elucidated for **PTL**: inhibition by preventing the phosphorylation and degradation of IκBα,[235] and direct binding to the p65 transcription factor subunit.[258] By binding directly to IκB kinase, the degradation of IκBα is prevented, sequestering the NF-κB transcription factors in the cytoplasm and activation of the pathway is prevented.[259] Additionally, **PTL** can bind directly to the p65 subunit of the NF-κB transcription factors preventing DNA binding.[258]

Recently, a publication by Jordan et al. has brought **PTL** into the forefront of anticancer therapeutic development.[246] They discovered that **PTL** displayed selectivity against the AML stem cell population (CSC), but when dosed at the same concentration to normal hematopoietic stem cells, **PTL** had no cytotoxic effect.[246] This selectivity was due to **PTL** inhibiting a constitutively active NF-κB pathway previously observed in

AML, but is regulated in normal hematopoietic cells.[260] In contrast, Cytarabine, a first line chemotherapeutic for AML, displayed cytotoxicity against both AML cells and normal hematopoietic stem cells, while sparing the AML CSC population due to their quiescent nature.[246] The ability for a chemotherapeutic to selectively target the CSC population versus the non-cancerous cell population is a rare characteristic that could potentially make chemotherapy less toxic to patients. Due to this unique trait, **PTL** is an attractive natural product for chemotherapeutic development. (for a comprehensive background on the CSC model please see Chapter 1).

Unfortunately, **PTL** is not an ideal drug candidate. **PTL** suffers from poor bioavailability and modest *in vitro* cytotoxicity (low micromolar at best).[243,249] Previous clinical trials investigating the extract of the feverfew plant yielded no detectable serum concentration of **PTL** in cancer patients.[261] In a similar study in an *in vivo* mouse model, a maximum serum concentration of 0.169 μM was detected after an oral gavage of feverfew dose of 40 mg/kg, far below the required concentration to reach the IC_{50} which is in the low micromolar range.[261] One way to address the bioavailability is to improve the aqueous solubility of **PTL** by conversion to a prodrug. One such compound (dimethylamino PTL, **Figure 2.1**) was found to be 1000-times more water soluble than **PTL**. However, the modest potency of the compound remains problematic.[248]

In addition to development of a prodrug, structure activity relationships (SAR) have been previously investigated on sesquiterpene lactones in an effort to develop clinical candidates.[262-267] Previous SAR studies of **PTL** have predominately focused on the exocyclic methylene (**Figure 2.2**).[234,240,268] This is due to the ease of synthetic

accessibility of the exocyclic methylene, although it is the primary pharmacophore of **PTL**.[234,265,269,270] To improve the bioavailability and cytotoxicity of **PTL** against cancer cells, we envisioned an SAR study against the various reactive functional groups of the molecule and to expand on the limited previous investigations in this regard (**Figure 2.3)**. This task will be accomplished through the development of a small library of **PTL** analogues.

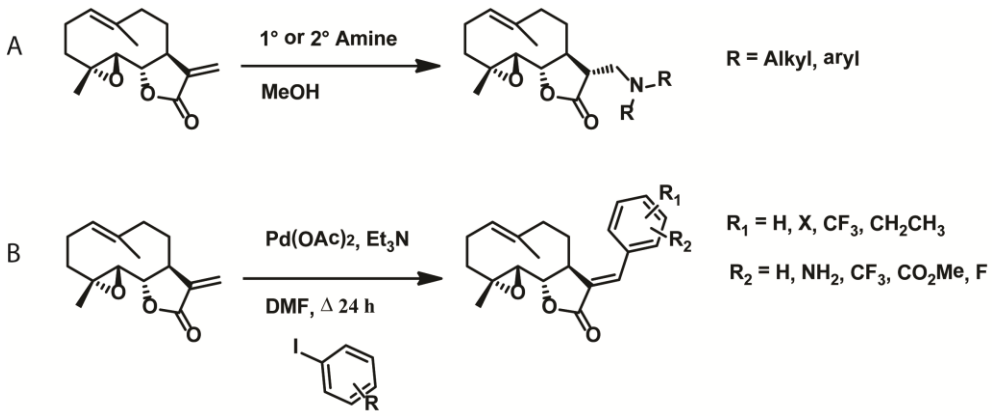

Figure 2.2 Previous SAR studies of the exocyclic methylene of Parthenolide. **A**. Modification of the exocyclic methylene via Michael addition of primary and secondary amines. Neelakantan et al. focused on aliphatic R groups, while Nasim et al. focused on aromatic R groups.[234,268] **B**. Palladium-catalyzed arylation with aryl iodides to yield R-alkylidene-γ-butyrolactones by Han et al.[240]

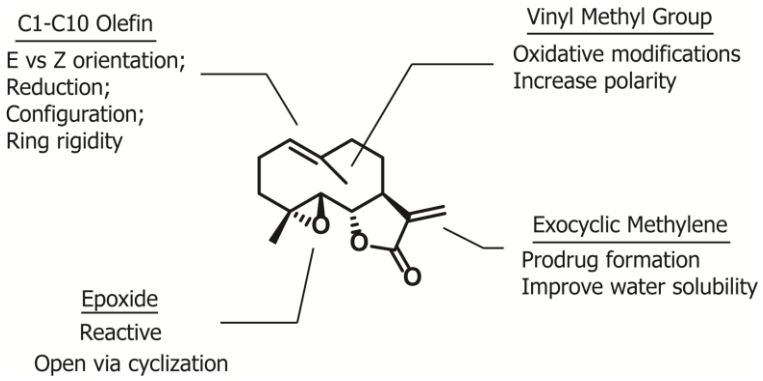

Figure 2.3 Functional group modifications investigated for their contributions to the anticancer activities of parthenolide (**1, PTL**) across a panel of cancer cell types.

2.2 Research Objectives

Using a semi-synthetic approach, we have developed a small library of **PTL** analogues (**Figure 2.4**). With this library of compounds, we elucidated the key structural features that confer **PTL's** cytotoxicity, and developed **PTL** analogues that possess less off-target cytotoxicity (toxicity to normal cells). Each compound was screened against nine cell lines to determine their IC_{50}. Described herein is the syntheses and biological evaluation of each **PTL** analogue, and its implications to the development of a more potent and selective antiproliferative agent.

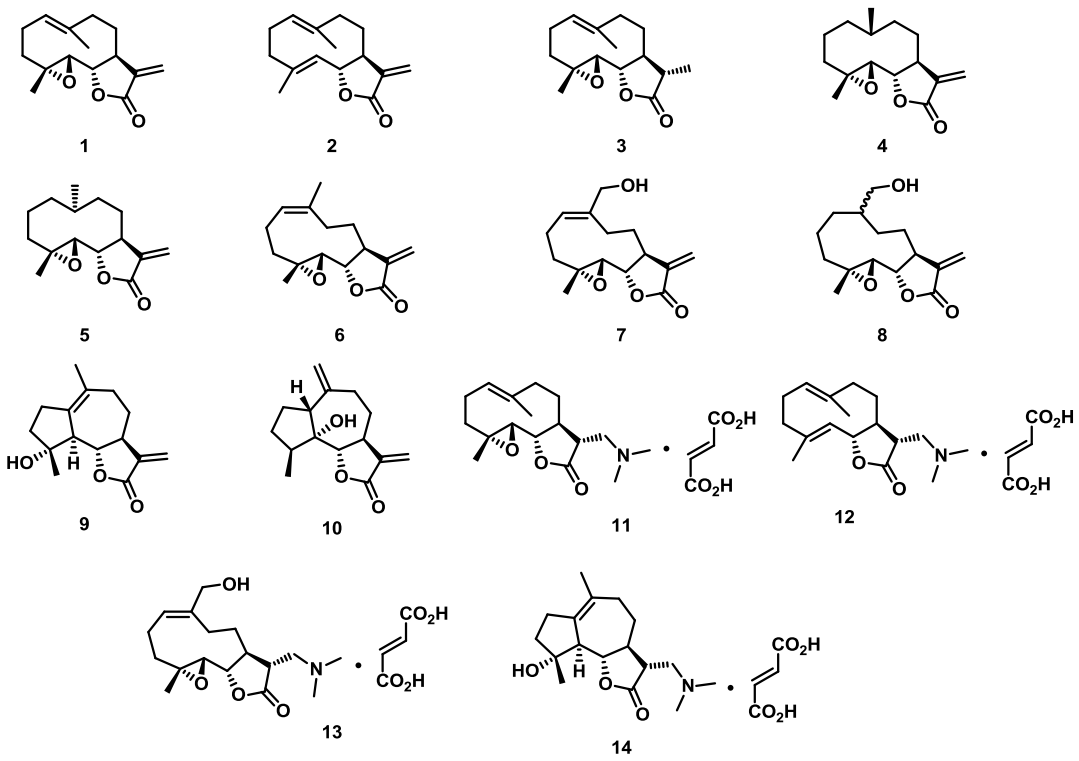

Figure 2.4. Synthesized library of parthenolide analogues.

2.3 Results and Discussion

2.3.1 Synthesis of a Library of Parthenolide Analogues

The development of a library of **PTL** analogues began with the synthesis of dimethylamino prodrugs DMAPT (**LC-1**, **1a**) and costunolide (**CTL, 2**) to deduce the importance of the exocyclic olefin (**Scheme 2.1**). A dimethylamino modification to the Michael acceptor allows increased water solubility while maintaining the activity due to elimination of the dimethylamino group within cells to the parent compound.[271,272] Following a published procedure to synthesize DMAPT, **PTL** was reacted with an excess of dimethylamine to afford **1a** in 97% yield.[234] **CTL** was refluxed with dimethylamine to yield **2a** in 82% yield.[273]

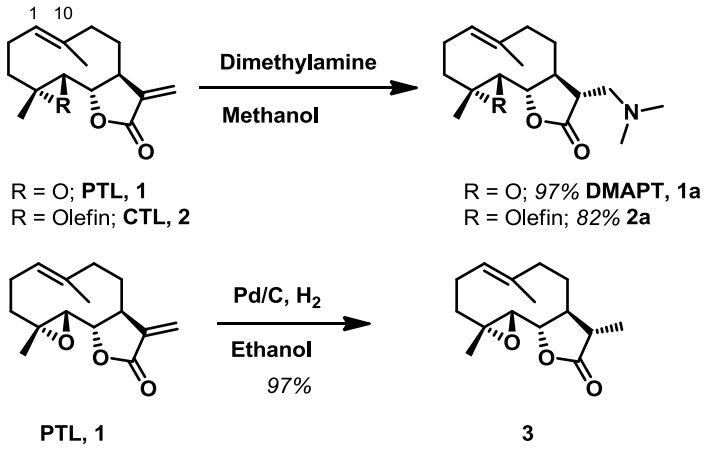

Scheme 2.1 Synthesis of exocyclic olefin modified analogues **1a**, **2a**, and **3**.

In addition to the prodrugs, a reduced exocyclic methylene analogue of **PTL**, dihydroparthenolide (**3**) was synthesized as previously reported.[235,274,275] **PTL** was hydrogenated in the presence of palladium on carbon under a hydrogen atmosphere. After 45 min complete reduction of the exocyclic methylene of **PTL** yielded **3** in 97% yield (**Scheme 2.1**), with no reduction of the C1-C10 olefin. We envisioned this **PTL** analogue would have no biological activity due to the removal of the Michael acceptor, the primary pharmacophore of **PTL**.

The role of the C1-C10 olefin to the cytotoxicity profile of **PTL** was investigated by synthesizing compounds **4-6** (**Scheme 2.2**). In order to synthesize compounds **4** and **5**, without reduction of the exocyclic olefin, the **PTL** prodrug **1a** was used. Initially, the reaction was attempted utilizing palladium on carbon in 1 atm of hydrogen gas, however no product was observed. The hydrogen pressure was increased to 50 psi with a Parr shaker which allowed for product formation; however, even after 5 days of shaking under pressure the reaction did not fully go to completion. Instead, the catalyst was

switched to platinum oxide (PtO_2) under 50 psi of hydrogen gas to afford the reduced product **1b** (99% yield) after 2 days. Reinstallation of the exocyclic methylene was achieved by reacting **1b** with iodomethane to afford the quaternary iodonium salt. Heating of this intermediate with deionized water promoted Hofmann elimination yielding a mixture of diastereomers **4** and **5**. Currently, the separation of these two diastereomers by HPLC is underway to provide ample material for testing and accurate reaction yeild. Previously, our lab separated a small portion of **4** and **5** by HPLC and crystallized diastermer **5**. X-ray analysis allowed us to assign the relative stereochemistry of the methyl group (**Appendix 1**). Absolute stereochemistry was assigned due to the rest of the stereochemistry of **PTL** was known.

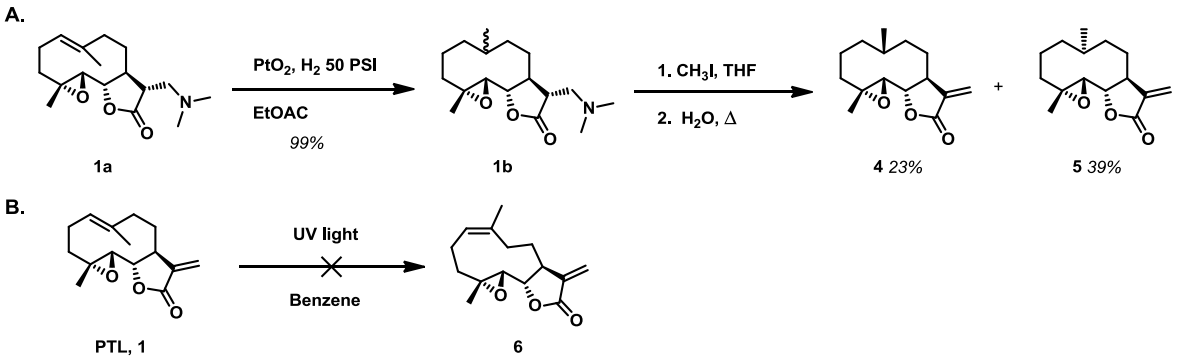

Scheme 2.2. Synthesis of C1-C10 olefin modified **PTL** analogues. **A.** Hydrogenated C`-C10 diastereomers **4** and **5**. **B.** Attempted photoisomerization of **PTL** to provide Z-isomer **6**.

In addition to eliminating the C1-C10 olefin, the stereochemistry of the C1-C10 olefin was investigated. Previously reported syntheses of the Z-isomer of **PTL** (**6,**

Scheme 2.2) have been accomplished by photoisomerization using uv light radiation at 254 nm.[274,276] After multiple attempts, this method of isomerization could not be reliably executed in our hands. Instead we acquired the Z-isomer of **PTL** as a by-product during the synthesis of melampomagnolide B (**7, Scheme 2.3**). During the allylic oxidation of the C1-C10 olefin, a rotation of the vinyl methyl group must occur for the final [2,3]-sigmatropic rearrangement to occur. Instead of the sigmatropic shift occurring, selenium is eliminated yielding the Z-isomer of **PTL** (**6**) as a byproduct in 4% yield. We used this material for screening.

Oxidative modifications to the C1-C10 allylic metyl group of **PTL** were also investigated. According to an established protocol, **PTL** was reacted with selenium dioxide and *tert*-butyl hydroperoxide in an allylic oxidation of the C1-C10 olefin to yield melampomagnolide B (**7, Scheme 2.3)** in 74% yield.[277,278] Compound **7** was then reacted with dimethylamine to produce **7a** in 97% yield, protecting the exocyclic olefin. Compound **7a** was then reacted with palladium on carbon under 50 psi of hydrogen gas to reduce the C1-C10 olefin. Deprotection of the exocyclic olefin was achieved to yield **8** *via* a Hofmann elimination as previously described for preparation of **4** and **5**.

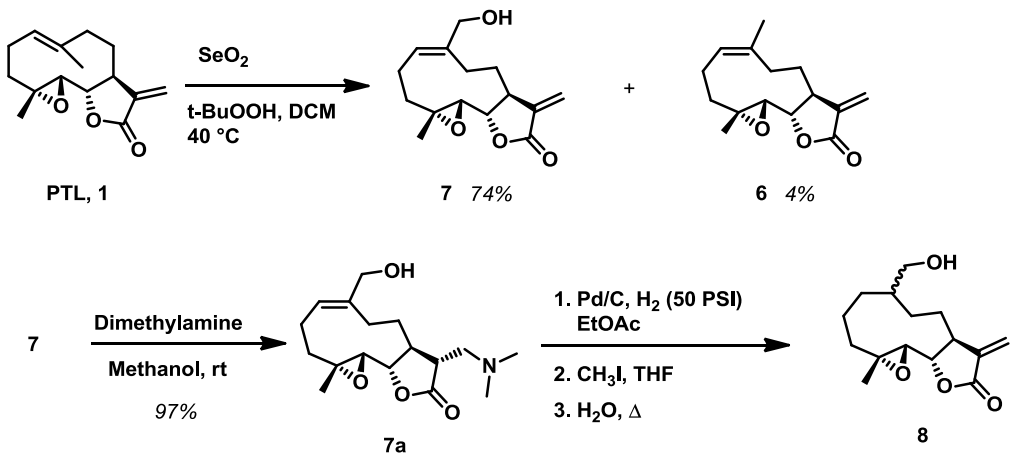

Scheme 2.3. Synthesis of melampomagnolide analogues of **PTL**. Melampomagnolide B (**7**) was synthesized as previously described.[278,279]

The guaianolide analogues (**Figure 2.5**) were provided by co-worker Dan Wang (**9** and **10**). The 5-7-5 ring structure of guaianolide was achieved by reacting **PTL** with boron trifluoride diethyl etherate, *via* reaction of the C1-C10 olefin with the epoxide, yielding analogues **9** and **10** as previously described.[280,281]

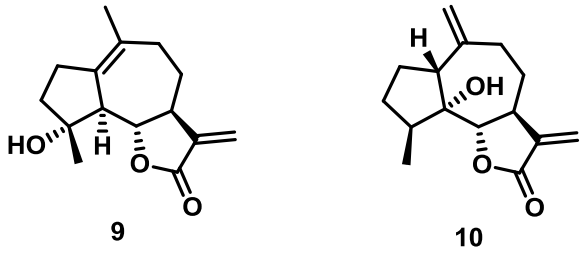

Figure 2.5 Synthesized rearranged guaianolide analogues of Parthenolide.

In addition to structural modifications of **PTL,** the fumarate salts of all dimethylamino analogues of the exocyclic methylene (**1a**, **2a**, **7a**, and **9)** were

synthesized to afford greater water solubility (**Scheme 2.4**). Generally, the dimethylamino compounds were reacted with fumaric acid to afford **11**-**14**, in high yields (range 82% - quant).

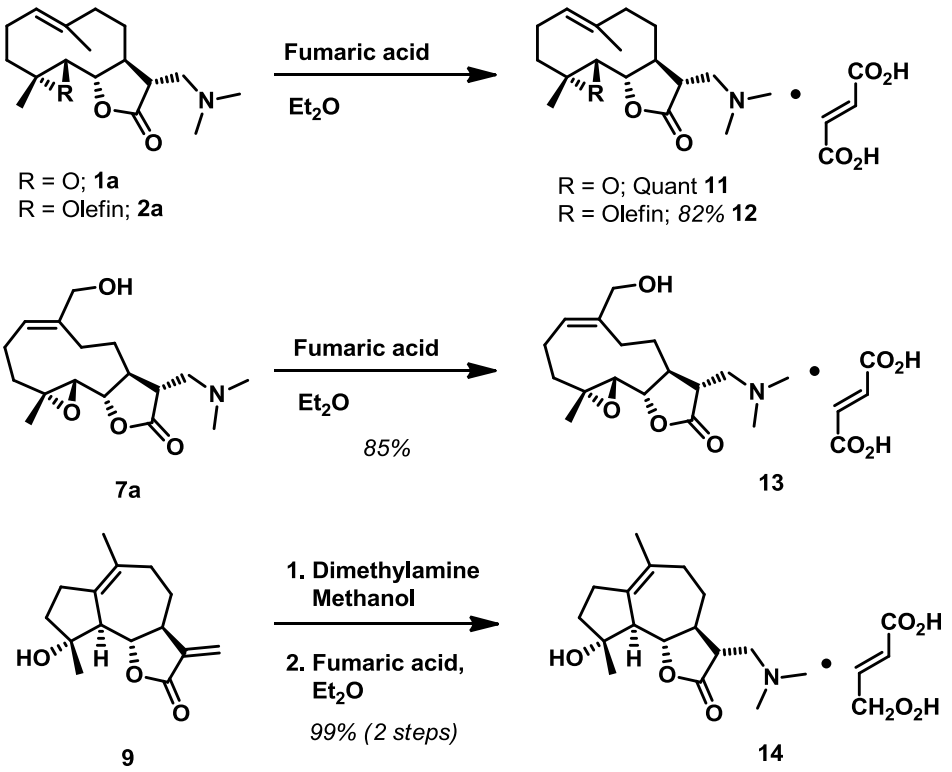

Scheme 2.4. Synthesis of fumarate salt analogues of **PTL** dimethylamino prodrugs.

2.3.2 Biological Evaluation of Parthenolide Analogues

The synthesized analogues of **PTL** were evaluated for their cytotoxicity in nine cell lines to probe the effect of structural modification on cellular cytotoxicity profiles (**Table 2.1**). Cancer cell lines investigated were DU-145 (prostate cancer), CCRF-CEM (acute lymphoblastic leukemia), HL-60 (promyelocytic leukemia), HeLa (cervical

cancer), MCF-7 (breast cancer), GBM6 (glioblastoma multiforme), U-87MG (glioblastoma multiforme), and NCI-ADR-RES (multidrug-resistant ovarian cancer[273,282]). Vero cells (African green monkey epithelial kidney cells) were utilized to gauge cytotoxicity against normal cells. Each compound evaluated for antiproliferative activity was verified to be ≥ 95% pure by HPLC. Stock solutions were made by dissolving compounds into molecular biology grade DMSO and were stored at -20 °C. Cells were plated in 96 well plates and allowed to incubate for 24 hours. The next day, plates were dosed with molecules, each concentration dosed in triplicate, and then incubated for 48 hours. The plates were stained with Alamar Blue® metabolic viability reagent during the final 1-3 hours of dosing. Reaction time with Alamar blue® varied between cell type, but fluorescent readout was only accepted above 1000 AFU. For HeLa, DU-145, U-87MG, MCF-7 and Vero cell lines, deoxidative metabolism of the reagent was observed to be rapid and required an incubation time of 1.5 hours. HL-60 cells metabolized Alamar Blue® at a much slower rate requiring a 3 h incubation time to observe fluorescence above 1000 AFU. For all remaining cell lines, an incubation time of 2 h for Alamar Blue® was used. Data collected was normalized by subtracting blank wells (contained no cells) and dividing by control wells (cells with no drug). Normalized values were graphed using GraphPad prism using a sigmoidal dose-response equation to determine the IC_{50}. Sigmoidal dose-response curves were generated in triplicate to determine the average IC_{50} and standard deviation. **PTL** was dosed above and below its IC_{50} as a control for each plate.

2.3.2.1 Biological Evaluation of Parthenolide, Costunolide, and Reduced Parthenolide

We found that **PTL** conveys modest low micromolar cytotoxity against six of the eight cancer cell lines tested (DU-145, IC_{50} = 8.9 ± 4.6 μM; CCRF-CEM, IC_{50} = 4.7 ± 1.6 μM; U-87MG, IC_{50} = 5.8 ± 2.3 μM; GBM6, IC_{50} = 3.4 ± 1.1 μM; HL-60, IC_{50} = 9.3 ± 3.8 μM; MCF-7, IC_{50} = 9.7 ± 2.8 μM **Table 2.1**). HeLa and NCI/ADR-RES cell lines required higher concentrations to achieve an IC_{50} (HeLa, IC_{50} = 44.1 ± 6.4 μM; NCI/ADR-RES, IC_{50} = 57.6 ± 8.9 μM). **PTL** also conveyed the same cytotoxicity against the normal Vero cell line (IC_{50} = 12.4 ± 0.6 μM) when compared to the cancer cell lines, reinforcing the need for a **PTL** analogue that can spare normal cells. Previous studies of **PTL** against cell lines MCF-7, HL-60, U-87MG, and HeLa were in general agreement withour data, revealing low micromolar inhibitory activity, with some variability resulting from different incubation times and methods of viability measurements.[281,283,284]

Compound	DU-145	CCRF-CEM	U-87MG	GBM6	HL-60	HeLa	MCF-7	NCI/ADR-RES	Vero
1, PTL	8.9 ± 4.6	4.7 ± 1.6	5.8 ± 2.3	3.4 ± 1.1	9.3 ± 3.8	44.1 ± 6.4	9.7 ± 2.8	57.6 ± 8.9	12.4 ± 0.6
2	7.5 ± 3.1	2.3 ± 0.2	9.6 ± 0.8	7.0 ± 1.8	35.4, 37.8	TBD	16.7, 14.3	44.8 ± 7.4	25.7 ± 0.9
3	> 500	> 500	> 500	> 500	> 500	> 500	> 500	> 500	> 500

Table 2.1. Half maximal inhibitory concentration (IC_{50} in μM) of Parthenolide (**1**), Costunolide (**2**), and reduced parthenolide (**3**) in nine different cancer cell lines. IC_{50} values are averages (n > 3) ± Standard deviation. TBD = To be deterimined.

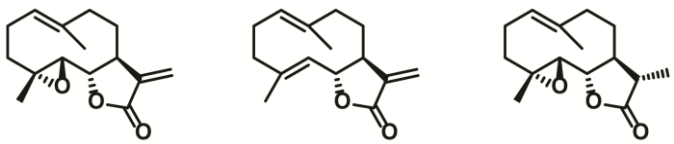

Biological evaluation of **CTL** (**2**) demonstrated that the loss of the epoxide from **PTL** was highly tolerated across five cancer cell lines (IC_{50} for DU-145, CCRF-CEM, U-87MG, and GBM6 = 2.3 – 9.6 μM vs. **PTL** = 3.4 – 8.9 μM; IC_{50} for NCI/ADR-RES = 44.8 ± 7.4 μM vs. **PTL** = 57.6 ± 8.9 μM). Loss of the epoxide was not tolerated in the two remaining cancer cell lines evaluated (HL-60 35.4/37.8 μM vs. **PTL** = 9.3 ± 3.8 μM; MCF-7, 16.7/14.3 μM vs. **PTL** = 1.4/6.7 μM) indicating a need for this functional group for maintaining activity to the level of **PTL**. Additionally, loss of activity against Vero cells (IC_{50} = 25.7 ± 0.9 μM vs. **PTL** = 12.4 ± 0.6 μM). Costunolide was previously reported to inhibit growth of DU-145 cells at IC_{50} = 4.8 μM, verifying our observation of IC_{50} = 7.5 ± 3.1 μM.[285] HL-60 results were consistent with previous reports of **CTL** being dosed up to 8 μM and greater than 97% cell viability observed.[286]

Reduced **PTL** analogue **3** was observed to be biologically inactive (IC_{50} > 500 μM) in all cell lines tested, indicating that the exocyclic olefin must remain intact for biological activity of **PTL**. These results are consistant with previous reports of biological activity of reduced **PTL** in other cell lines as well as antiviral activity.[234,275,287] Additionally, complete loss of activity of reduced **PTL** was observed when dosed to primary leukemia cells.[234]

2.3.2.2 Biological Evaluation of C1-C10 Olefin Modified Parthenolide Analogues

Analogues with modifications to the C1-C10 olefin (compounds **4-6**) were highly tolerated and demonstrated similar biological activity to the parent compound,

PTL (**Table 2.2**). Diastereomers **4** and **5** were equipotent to **PTL** in all cancer cell lines tested (DU-145, CCRF-CEM, U-87MG, and GBM6; IC_{50} for **4** and **5** = 1.6 – 7.7 ± 0.4 – 2.8 μM vs. **PTL** = 3.4 – 8.9 ± 1.1 – 4.6 μM). Compounds **4** and **5** also demonstrated the same cytotoxicity against the normal Vero cell line (IC_{50} = 13.9 ± 2.2 and 12.1 ± 3.3 μM, respectively) when compared to **PTL** (IC_{50} = 12.4 ± 0.6). Biological testing in HeLa, MCF-7, NCI/ADR-RES, and HL-60 still need to be completed for analogues **4** and **5**.

Compound	DU-145	CCRF-CEM	U-87MG	GBM6	HL-60	HeLa	MCF-7	NCI/ADR-RES	Vero
1, PTL	8.9 ± 4.6	4.7 ± 1.6	5.8 ± 2.3	3.4 ± 1.1	9.3 ± 3.8	44.1 ± 6.4	1.4, 6.7	57.6 ± 8.9	12.4 ± 0.6
4	6.2 ± 2.8	1.6 ± 0.4	7.7 ± 1.1	2.0 ± 0.3	7.0, 8.7	TBD	TBD	TBD	13.9 ± 2.2
5	5.5 ± 1.5	2.5 ± 2.1	7.5 ± 0.4	2.0 ± 0.3	7.7, 7.0	TBD	TBD	TBD	12.1 ± 3.3
6	5.16 ± 2.4	2.2 ± 1.0	9.1 ± 4.4	2.6, 3.1	8.0 ± 1.1	18.7, 18.1	7.7 ± 0.3	9.4 ± 2.1	TBD

Table 2.2. Half maximal inhibitory concentration (IC_{50} in μM) of C1-C10 Olefin Modified Parthenolide Analogues **4** – **6** in nine different cancer cell lines. IC_{50} values are averages (n > 3) ± Standard deviation. TBD = To be determined.

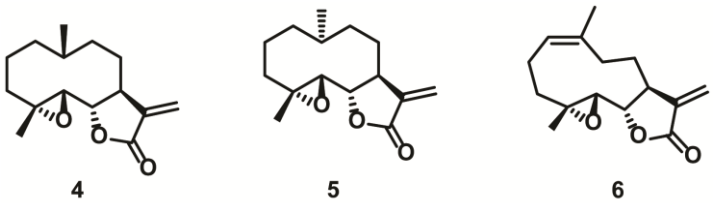

Similar to diastereomers **4** and **5**, the Z-olefin isomer of **PTL**, compound **6,** has been evaluated for anticancer activity. Analogue **6** demonstrated the same biological activity when compared to the parent compound **PTL** in cancer cell lines DU-145, CCRF-CEM, U-87MG, and HL-60 (IC_{50} for **6** = 2.2 – 9.1 ± 1.0 – 4.4 μM vs. IC_{50} for **PTL** = 4.7 – 9.3 ± 1.6 – 4.6 μM respectively) demonstrating that the orientation of the vinyl methyl group is not vital to the anticancer activity in these cell lines. In the chemoresistant cell line NCI/ADR-RES **6** gained activity when compared to **PTL** (IC_{50} for **6** = 9.4 ± 2.1 vs. **PTL** = 57.6 ± 8.9). GBM6, HeLa, and Vero cell lines still require testing of **6** in triplicate. From these observations of C1-C10 modified analogues, the presence of the C1-C10 olefin is not vital to the anticancer activity of **PTL**.

2.3.2.3 Biological Evaluation of Oxidative Modified Parthenolide Analogues

Melampomagnolide B (**7**) was found to have similar cytotoxicity to **PTL** in the cancer cell lines DU-145, CCRF-CEM, HL-60, HeLa, and MCF-7 (IC_{50} for **7** = 14.1 ± 5.7, 5.5 ± 1.2, 7.5 ± 3.0, 36.1 ± 3.2, and 9.5 ± 1.9 μM vs. **PTL** = 8.9 ± 4.6, 4.7 ± 1.6, 9.3 ± 3.8, 44.1 ± 6.4, and 1.4,6.7 μM). Unfortunately **7** also conveyed the same cytotoxicity for normal Vero cells as **PTL** (IC_{50} for **7** = 15.6 ± 3.5 μM vs. **PTL** = 12.4 ± 0.6 μM) indicating that oxidation of the vinylogous methyl group does not help with off-target biological activity. Loss of activity was observed for **7** in the glioblastoma cell line U-87MG (IC_{50} for **7** = 16.3 ± 6.8 μM vs. **PTL** = 5.8 ± 2.3 μM). Additional testing is still required for GBM6 and NCI/ADR-RES. Data from our screening in leukemia cell lines

matches previous reported IC_{50} results observed from dosing **7** to primary leukemia cells.[278]

Compound	DU-145	CCRF-CEM	U-87MG	GBM6	HL-60	HeLa	MCF-7	NCI/ADR-RES	Vero
1, PTL	8.9 ± 4.6	4.7 ± 1.6	5.8 ± 2.3	3.4 ± 1.1	9.3 ± 3.8	44.1 ± 6.4	1.4, 6.7	57.6 ± 8.9	12.4 ± 0.6
7	14.1 ± 5.7	5.5 ± 1.2	16.3 ± 6.8	3.5, 6.6	7.5 ± 3.0	36.1 ± 3.2	9.5 ± 1.9	12.8, 19.9, 20.6	15.6 ± 3.5
8	26.7 ± 6.5	5.9, 1.5	26.8 ± 2.3	17.6, 16.6	41.6, 42.0	TBD	TBD	TBD	TBD

Table 2.3. Half maximal inhibitory concentration (IC_{50} in μM) of oxidative modified parthenolide analogues **7** and **8** in nine different cancer cell lines. IC_{50} values are averages (n > 3) ± Standard deviation. TBD = To be determined.

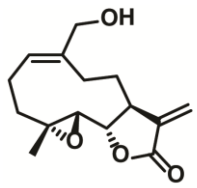

7

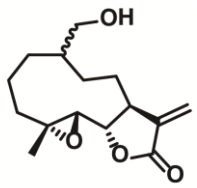

8

Reduction of the C1-C10 olefin of Melampomagnolide B (**7**) was also performed to investigate if the orientation of the alcohol had an impact on the anticancer activity of **PTL**. After hydrogenation, the two diastereomers were tested as a mixture (**8**). A loss of activity in DU-145 and U-87MG cells was observed for **8** (IC_{50} = 26.7 ± 6.5, and 26.8 ± 2.3 μM, respectively) when compared to **PTL** (IC_{50} = 8.9 ± 4.6 and 5.8 ± 2.3 μM, respectively). Data has been collected for CCRF-CEM, GBM6, and HL-60 but not yet in triplicate. HeLa, MCF-7, NCI/ADR-RES and Vero all still require triplicate evaluation of **8**.

2.3.2.4 Biological Evaluation of Rearranged Guaianolide Parthenolide Analogues

Rearranged guaianolide analogue **9** demonstrated equipotent cytotoxicity in three cancer cell lines (DU-145, CCRF-CEM, and HL-60: IC_{50} = 14.8 ± 4.0, 5.2 ± 1.8, and 7.1 ± 1.3 μM respectively) when compared to **PTL** (DU-145, CCRF-CEM, and HL-60: **PTL** = 8.9 ± 4.6, 4.7 ± 1.6, and 9.3 ± 3.8 μM respectively). It was observed with the glioblastoma cell lines (U-87MG and GBM6), as well as the metastatic breast cancer cell line MCF-7, that a higher concentration were required to achieve IC_{50} when compared to **PTL** (IC_{50} for U-87MG, GBM6, and MCF-7 for **9**: 16.2 ± 3.6, 8.7 ± 0.6, 9.6 ± 1.0 μM vs. **PTL** = 5.8 ± 2.3, 3.4 ± 1.1, and 1.4/6.7 μM, respectively). Interestingly, **9** also demonstrated less cytotoxicity against the normal Vero cell line (IC_{50} = 36.1 ± 9.4 μM vs. **PTL** = 12.4 ± 0.6 μM)

Compound	DU-145	CCRF-CEM	U-87MG	GBM6	HL-60	HeLa	MCF-7	NCI/ADR-RES	Vero
1, PTL	8.9 ± 4.6	4.7 ± 1.6	5.8 ± 2.3	3.4 ± 1.1	9.3 ± 3.8	44.1 ± 6.4	1.4, 6.7	57.6 ± 8.9	12.4 ± 0.6
9	14.8 ± 4.0	5.2 ± 1.8	16.2 ± 3.6	8.7 ± 0.6	7.1 ± 1.3	35.6, 34.0	9.6 ± 1.0	12.5, 103, 102	36.1 ± 9.4
10	13.9 ± 3.7	4.8 ± 1.5	29.3 ± 2.97	8.4 ± 1.8	11.6 ± 0.2	44.2	25.0 ± 4.3	18.1, 97.1, 131	54.5 ± 3.0

Table 2.4. Half maximal inhibitory concentration (IC_{50} in μM) of rearranged guaianolide analogues **9** and **8** in nine different cancer cell lines. IC_{50} values are averages (n > 3) ± Standard deviation. TBD = To be determined.

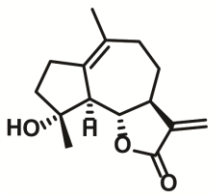

9

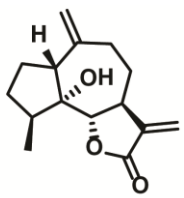

10

Rearranged guaianolide analogue **10** was also found to have similar cytotoxicity in three cancer cell lines (DU-145, CCRF-CEM, and HL-60: IC_{50} = 13.9 ± 3.7, 4.8 ± 1.5, 11.6 ± 0.2 μM respectively) when compared to **PTL** (DU-145, CCRF-CEM, and HL-60: **PTL** = 8.9 ± 4.6, 4.7 ± 1.6, and 9.3 ± 3.8 μM respectively). Similar to **9**, analogue **10** lost activity against the glioblastoma cell lines U-87MG and GBM6 (IC_{50} = 29.3 ± 3.0, and 8.4 ± 1.8 μM respectively) when compared to **PTL** (IC_{50} = 5.8 ± 2.3 and 3.4 ± 1.1 μM respectively). A decrease in activity was also observed in the breast cancer cell line MCF-7 (IC_{50} = 25.0 ± 4.3 μM) as compared to **PTL** (IC_{50} = 1.4, 6.7 μM). Analogue **10** also showed the lowest cytotoxicity against the normal cell line Vero (IC_{50} = 54.5 ± 3.0 μM) out of all the other analogues when compared to **PTL** (IC_{50} = 12.4 ± 0.6 μM). Triplicate data has not been completed yet for HeLa and NCI/ADR-RES.

2.3.2.5 Biological Evaluation of Dimethylamino Fumarate Parthenolide Analogues.

Dimethylamino furmarate salts were highly tolerated as modifications of **PTL**. LC-1 fumarate salt (**11**) displayed the same cytotoxicity against all the cancer cell lines when compared to **PTL** (IC_{50} for **11** = 1.9 – 63.5 ± 0.4 – 11.8 μM vs. IC_{50} for **PTL** = 3.4 – 44.1 ± 1.6 – 6.4 μM). Unfortunately, the same cytotoxicity was observed for **11** against the normal Vero cell line (IC_{50} = 15.6 ± 7.8 μM vs. **PTL** = 12.4 ± 0.6 μM). Although not primary leukemia cell lines themselves, HL-60 and CCRF-CEM leukemia cell lines match previous data performed in primary leukemia cell lines.[234] Although not

tested *in vivo* for our studies, LC-1 has been previously investigated in pancreatic and prostate murine models resulting in tumor suppression.[288,289]

Compound	DU-145	CCRF-CEM	U-87MG	GBM6	HL-60	HeLa	MCF-7	NCI/ADR-RES	Vero
1, PTL	8.9 ± 4.6	4.7 ± 1.6	5.8 ± 2.3	3.4 ± 1.1	9.3 ± 3.8	44.1 ± 6.4	1.4, 6.7	57.6 ± 8.9	12.4 ± 0.6
11	8.4 ± 4.5	1.9 ± 0.4	8.8 ± 1.9	3.5 ± 1.1	7.1 ± 0.4	63.8 ± 11.8	10.4 ± 1.2	38.5 ± 2.1	15.6 ± 7.8
12	205 ± 4.7	6.6 ± 2.5	25.2 ± 2.4	14.6 ± 0.9	35.1 ± 5.5	82.3 ± 1.9	23.7 ± 1.2	118 ± 18	21.1 ± 1.2
13	12.0	2.9, 3.3	28.3 ± 2.3	5.8 ± 1.2	36.2 ± 6.1	118, 104, 442	16.7 ± 0.9	19.6, 39, 40.6	20.6, 28.0
14	60.7 ± 7.5	45.0 ± 7.4	77.5 ± 7.3	27.8 ± 4.8	32.3 ± 10.4	> 250	3.3	74.5, 20.8, 22.9	48.7 ± 5.9

Table 2.5 Half maximal inhibitory concentration (IC_{50} in μM) of dimethylamino fumarate salt compounds **11** – **14** in nine different cancer cell lines. IC_{50} values are averages (n > 3) ± Standard deviation. TBD = To be determined.

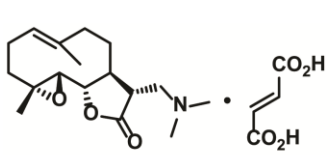

11

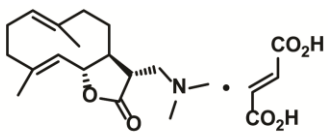

12

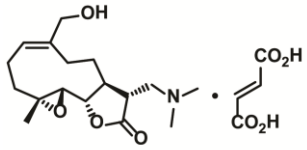

13

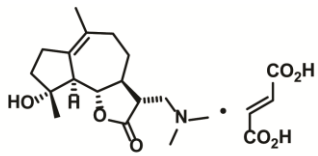

14

CTL fumarate salt **12** only retained the same activity as **11** in the leukemia cell line CCRF-CEM and normal Vero cells (CCRF-CEM and Vero IC_{50}s for **12** = 6.6 ± 2.5 and 21.1 ±1.2 μM vs. **11** =1.9 ± 0.4 and 15.6 ± 7.8 μM respectively). **12** lost activity against seven other cancer cell lines (IC_{50} for DU-145, U-87MG, HL-60, HeLa, MCF-7, NCI/ADR-Res, and GBM6 = 6.6 -118 ± 0.9 - 18 μM vs. **11** (IC_{50} = 3.5 – 63.8 ± 0.4 – 11.8 μM). Previous DU-145 cytotoxicity data for only the dimethylamino compound **2a**, and not the fumarate salt was available. Our findings agreed with the previous DU-145 anticancer data.[273]

The Melampomagnolide B fumarate salt **13** is currently under additional biological evaluation to determine its IC_{50} values in all nine cell lines. It has been elucidated that it has lower cytotoxicity in U-87MG, HL-60, and MCF-7 (IC_{50} = 28.3 ± 2.3, 36.2 ± 6.1, and 16.7 ± 0.9 μM vs. **PTL** = 5.8 ± 2.3, 9.3 ± 3.8, and 1.4, 6.7 respectively). Compound **13** was found to be equipotent as **PTL** in the glioblastoma cell line GBM6 (IC_{50} for **13** = 5.8 ± 1.2 vs. **PTL** = 3.4 ± 1.1).

The dimethylamino fumarate salt of guaianolide **9** (**14)** was not as well tolerated as other dimethylamino fumarates. Guaianolide fumarate salt **14** lost activity against all cell lines tested to date (IC_{50} for DU-145, CCRF-CEM, U-87MG, HL-60, and GBM6 = 27.8 – 77.5 ± 7.3 – 10.4 μM vs. **PTL** = 3.4 – 9.3 ± 1.1 – 4.6 μM; NCI/ADR-RES = 74.5 μM vs. **PTL** = 57.6 ± 8.9 μM). In HeLa cells 100% cell viability was not achievable with 500 μM being the largest concentration dosed. The extrapolated IC_{50} value was >

250 μM. Additionally, activity was also lost against the normal Vero cell line (IC_{50} for **14** = 48.7 ± 5.9 μM vs. **PTL** = 12.4 ± 0.6 μM).

2.4 Conclusion and Future Direction

In summary, we have synthesized a library of **PTL** analogues to elucidate the importance of various functional groups to its cytotoxicity profile. The modified functional groups of **PTL** included alterations to the exocyclic olefin, C1-C10 olefin, the vinyl methyl group, as well as loss of the epoxide. In addition, rearranged 5-7-5 guainanolide analogues were synthesized to observe the importance of the ring structure of **PTL** to its cytotoxicity profile. Dimethylamino prodrugs were synthesized to address the water solubility issues of PTL and evaluated as fumarate salts for their biological activity. The only modification to completely ablate activity of **PTL** across all cell lines was removal of the exocyclic olefin, the primary pharmacophore of **PTL**.

Modifications to the C1-C10 olefin were tolerated across all cell lines tested for analogues **4-6** indicating that alteration or complete removal of the internal olefin of **PTL** has no effect on the biological activity. Oxidative modifications to the vinyl methyl group were also highly tolerated with slight loss of activity observed in the glioblastoma cell line U-87MG. Tolerance of the installation of the allylic alcohol can allow for further modifications to this site to prepare **PTL** probe compounds and additional analogues. Dimethylamino fumarate salt analogues **11-14** all displayed low cytotoxicity within 5-fold of **PTL** against the cancer cell lines tested, confirming that the

dimethylamino prodrug of **PTL** is a viable modification to improve water solubility while retaining biological activity.

The rearranged guaianolide analogues **9** and **10** demonstrated the most interesting biological activity of all the **PTL** analogues. Although analogues **9** and **10** displayed similar activity when compared to **PTL** in most cancer cell lines (except U-87MG, **10** was 6-fold less potent than **PTL**), the greatest finding was a loss in activity against the normal cell line Vero. Both rearranged **PTL** analogues **9** and **10** had up to a 5-fold loss in activity against Vero cells, indicating that the more ridged 5-7-5 guaianolide ring structure was not as cytotoxic to normal cells. From these results we can conclude that the guaianolide ring structure should serve as a new basis for further SAR studies. Other future direction for this SAR could include modifications to the butyrolactone, as well alterations in ring sizes for new potential clinical leads. Re-synthesis and purification of analogues **4**, **5** and **8** to finish biological testing is currently underway.

2.5 Experimental

2.5.1 General

All reactions were performed under an anhydrous nitrogen atmosphere unless otherwise noted. Parthenolide was purchased from Enzo Life Sciences and repurified by SiO_2 chromatography prior to biological studies. Costunolide was purchased from Tocris Biosciene (Boston, MA) and was used without further purification. Commercial grade reagents (Aldrich, Acros, Alfa Aesar) were used without further purification

unless otherwise noted. Tetrahydrofuran and dichloromethane were rendered anhydrous by passing through the resin column of a solvent purification system. Benzene was purified by distillation over calcium hydride. Methanol and N,N-dimethylformamide were purchased as anhydrous solvent. High pressure hydrogenation reactions were performed in a Parr hydrogenation apparatus (Moline, IL; model # 3916). All reactions were monitored by thin-layer chromatography (TLC) using silica gel 60-F_{254} TLC plates (Merck), and visualized using cerium ammonium molybdate stain. Silica gel chromatography was performed using a Teledyne-Isco Combiflash R_f 200 instrument using Redisep R_f Gold High-Performance silica gel columns (Teledyne-Isco). HPLC purification was performed using an Agilent 1200 series instrument equipped with a Zorbax (Agilent) preparatory column (21.2 x 250 mm, 7 μm). Analysis of compound purity was conducted on the aforementioned HPLC, using a Zorbax analytical column (4.6 x 150 mm, 5 μm). Nuclear magnetic resonance (NMR) spectroscopy employed a Bruker Avance instrument operating at 400 MHz (for ^{1}H) and 100 MHz (for ^{13}C) at ambient temperature. Internal solvent peaks were referenced in each case. Mass spectral data was obtained from the University of Minnesota Department of Chemistry Mass Spectrometry lab, employing a Bruker BioTOF II instrument.

2.5.2 Synthesis of Parthenolide Analogues

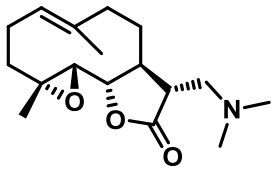

Dimethylamino Parthenolide 1a.

Known compound **1a** was prepared by the method of Neelakantan et al.[234] Parthenolide (16.90 mg, 0.07 mmol) was dissolved in methanol (4 mL) and dimethylamine was added (0.10 mL, 0.20 mmol). The reaction was allowed to stir for 5 h at rt, and then concentrated *in vacuo* to yield compound **4** (19.90 mg, 97%) as an off white crystalline solid. ^{1}H NMR (400 MHz, $CDCl_3$) δ = 5.19 (dd, *J* = 12.3, 3.8 Hz, 1H), 3.81 (t, *J* = 9.0 Hz, 1H), 2.78 – 2.68 (m, 2H), 2.62 (dd, *J* = 13.2, 4.8 Hz, 1H), 2.45 – 2.31 (m, 2H), 2.25 (s, 6H), 2.22 (s, 1H) , 2.21 – 2.01 (m, 5H), 1.68 (t, *J* = 1.2 Hz, 3H), 1.66 – 1.57 (m, 1H), 1.28 (s, 3H), 1.21 (td, *J* = 13.0, 5.8 Hz, 1H). ^{13}C NMR (100 MHz, $CDCl_3$) δ = 176.6, 134.8, 125.2, 82.3, 66.7, 61.6, 57.8, 48.0, 46.6, 46.3, 46.3, 41.2, 36.8, 30.1, 24.2, 17.3, 17.1. MS-ESI$^+$ m/z [M+H] calcd for $C_{17}H_{28}NO_3$: 294.2, found: 294.2. MS-ESI$^+$ m/z [M+Na] calcd for $C_{17}H_{27}NO_3Na$: 316.1, found: 316.2.

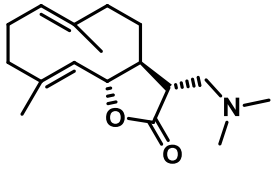

Dimethylamino Costunolide 2a

The known compound **2a** was prepared by as described by Srivastava et al.[273] Costunolide (10.0 mg, 0.04 mmol) was dissolved into ethanol (15 mL). An excess of dimethylamine (0.1 mL, 0.2 mmol) was added and the reaction was refluxed at 90 °C

overnight. The reaction was concentrated *in vacuo* after reacting for 12 h. The crude product was purified by flash chromatography over SiO_2 (gradient 0-10% methanol in dichloromethane) to yield compound **2a** (9.8 mg, 82%) as an off-white crystalline solid. ^{1}H NMR (400 MHz, $CDCl_3$) δ 4.82 (dd, *J* = 11.5, 4.5 Hz, 1H), 4.66 (d, *J* = 9.7 Hz, 1H), 4.55 (t, *J* = 9.3 Hz, 1H), 2.74 (dd, *J* = 13.2, 5.1 Hz, 1H), 2.60 (dd, *J* = 13.2, 4.8 Hz, 1H), 2.39 – 2.29 (m, 2H), 2.27 (s, 6H), 2.25 – 2.12 (m, 2H), 2.12 – 1.91 (m, 4H), 1.68 (d, *J* = 1.4 Hz, 3H), 1.64 – 1.54 (m, 1H), 1.40 (s, 3H), 1.25 (s, 1H). ^{13}C NMR (100 MHz, $CDCl_3$) δ 177.7, 140.6, 137.2, 127.5, 127.0, 81.5, 58.1, 51.3, 46.3, 46.2, 41.2, 39.7, 28.5, 26.3, 17.4, 16.3. MS-ESI$^+$ m/z [M+H] calcd for $C_{17}H_{28}NO_2$: 278.2, found: 278.2.

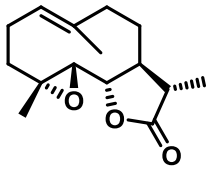

Reduced Parthenolide 3

Known compound **3** was prepared by the method of Govindachari et al.[282] Parthenolide (13.50 mg, 0.054 mmol) and palladium on carbon (14.20 mg, 0.13 mmol) were added to a flask and ethanol (10 mL). The reaction was placed under 1 atm of H_2, and allowed to stir for 45 mins. Upon completion, the reaction was filtered through celite and the solvent was removed *in vacuo*. The product was purified by flash chromatography over SiO_2 (10-50% ethyl acetate in hexanes gradient) to yield compound 3 (13.30 mg, 97% yield). ^{1}H NMR (400 MHz, $CDCl_3$) δ = 5.19 (dd, *J* = 11.8, 1.8 Hz, 1H), 3.81 (t, *J* = 9.1 Hz, 1H), 2.70 (d, *J* = 9.0 Hz, 1H), 2.46 – 2.22 (m, 3H), 2.16 (m, 2H), 2.05 (t, *J* = 12.3 Hz, 1H), 1.95 – 1.79 (m, 3H), 1.70 (s, 3H), 1.68 – 1.35 (m, 3H), 1.29 (s, 3H). MS-ESI$^+$

m/z [M+H] calcd for $C_{15}H_{23}O_3Na$: 273.1, Found: 273.1. MS-ESI$^+$ m/z [M+H] calcd for $C_{15}H_{22}O_3K$: 289.1, found: 289.1.

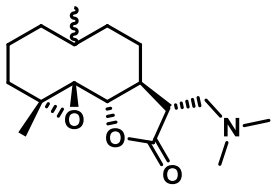

Reduced C1-C10 Olefin of Dimethylamino Parthenolide 1b

Compound **1a** (29.10 mg, 0.10 mmol) was dissolved into ethyl acetate, and PtO_2 (29.50 mg, 0.28 mmol) was added. The reaction was placed under an atmosphere of H_2 (50 psi) and the reaction was shook for 2 days with a Parr shaker. The reaction was then filtered through a celite plug and washed with ethyl acetate (5 × 5 ml) and dichloromethane (5 x 4 ml). The solvent was removed *in vacuo* to yield compound **1b** (29.30 mg, 99%) as a white crystalline solid. ^{1}H NMR (400 MHz, $CDCl_3$) δ = 3.82 (t, *J* = 9.4 Hz, 1H), 3.00 (d, *J* = 9.6 Hz, 1H), 2.72 (dd, *J* = 12.9, 4.0 Hz, 1H), 2.58 (dd, *J* = 12.9, 5.0 Hz, 1H), 2.37 (m, 2H), 2.25 (s, 6H), 2.15 (m, 2H), 1.73 (m, 2H), 1.66 – 1.52 (m, 2H), 1.49 (s, 3H), 1.47 – 1.36 (m, 3H), 1.10 (m, 2H), 0.88 (d, *J* = 6.4 Hz, 3H). ^{13}C NMR (100 MHz, $CDCl_3$) δ= 177.1, 80.8, 76.7, 66.6, 61.1, 58.2, 46.2, 45.6, 44.3, 36.6, 35.7, 30.8, 27.6, 25.7, 21.2, 20.5, 19.0. HRMS-ESI$^+$ *m/z* [M+H] calcd for $C_{17}H_{30}NO_3$: 296.2220, found: 296.2229.

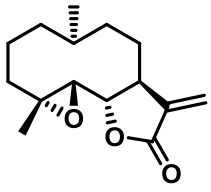 and 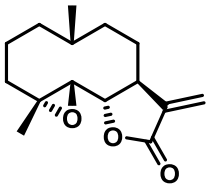

C1-C10 Reduced PTL Analogues 4 and 5

Compound **1b** (28.70 mg, 0.01 mmol) was dissolved into THF (2 ml) and iodomethane was added in excess (0.10 ml, 1.60 mmol). The reaction was allowed to stir at rt for 20 h. The solvent and excess iodomethane was removed *in vacuo* resulting in 30.6 mg of yellowish solid. Distilled water (10 mL) was added and the reaction was heated to 45 °C. Complete solvation of the yellowish material resulted within minutes of heating. The reaction was allowed to stir with heating for 3 h, and then solvent was removed *in vacuo*. Saturated $NaHCO_3$ aqueous solution (5 mL) was added to the reaction mixture, and the product was extracted with DCM (3 × 20 mL). The combined organic layers were washed with brine (20 mL), and dried with Na_2SO_4. The reaction was purified by flash chromatography over SiO_2 (10%-50% ethyl acetate in hexanes gradient) to yield 12.3 mg of crude product. HPLC separation and characterization is currently underway.

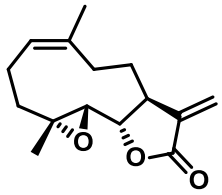

Cis Parthenolide 6

Previously reported synthesis of cis parthenolide were attempted but could not be replicated in my hands.[274,279] *Cis* parthenolide was isolated as a side product from

synthesis of melampomagnolide B (**7**). Crude material was purified by SiO_2 (gradient 10 – 50% ethyl acetate in Hexanes) to yield compound **6** (7.90 mg, 4% yield) as a white crystalline solid. ^{1}H NMR (400 MHz,$CDCl_3$) δ = 6.24 (d, *J* = 3.5 Hz, 1H), 5.53 (d, *J* = 3.2 Hz, 1H), 5.33 (t, *J* = 7.3 Hz, 1H), 3.83 (t, *J* = 9.3 Hz, 1H), 2.90 (d, *J* = 9.4 Hz, 1H), 2.77 (M, 1H), 2.50 – 2.18 (m, 3H), 2.10 (m, 3H), 1.71 (s, 3H), 1.69 – 1.58 (m, 1H), 1.53 (s, 3H), 1.07 (t, *J* = 12.1 Hz, 1H). MS-ESI$^+$ *m/z* [M+Na] calcd for $C_{15}H_{20}NaO$: 271.1, Found: 271.1. MS-ESI$^+$ *m/z* [M+K] calcd for $C_{15}H_{20}KO$: 287.1, found: 287.1.

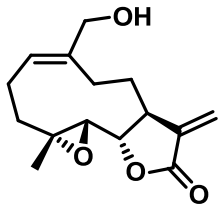

Melampomagnolide B (7)

Known compound **7** was prepared by the method of Nasim et al.[277,278] Parthenolide (49 mg, 0.20 mmol) and selenium dioxide (22 mg, 0.20 mmol) were suspended in anhydrous dichloromethane (15 mL) and *t*-BuOOH (0.32 mL, 3.33 mmol, 70% in H_2O) and refluxed at 40 °C for 4.5 h. The reaction mixture was cooled to rt, and water (15 mL) was added to the reaction. The crude material was extracted with DCM (3 × 15 mL). The combined organics were dried over Na_2SO_4. The solvent was then removed *in vacuo*, and the product was purified by chromatography over SiO_2 (gradient 10-50% ethyl acetate in hexanes) to yield compound 3 (38.60 mg, 74%) as an off-white crystalline solid. ^{1}H NMR (400 MHz, $CDCl_3$) δ = 6.25 (d, *J* = 3.5 Hz, 1H), 5.66 (t, *J* = 8.3 Hz, 1H), 5.55 (d, *J* = 3.2 Hz, 1H), 4.23 – 4.04 (q, *J* = 12.6 Hz, 2H), 3.86 (t, *J* = 9.3

Hz, 1H), 2.92 – 2.76 (m, 2H), 2.42 (s, 2H), 2.37 – 2.11 (m, 3H), 1.74 – 1.61 (m, 1H), 1.56 (s, 3H), 1.18 – 1.04 (m, 1H). ^{13}C NMR (100 MHz, $CDCl_3$) δ= 169.6, 139.7, 139.0, 127.7, 120.4, 81.3, 66.0, 63.5, 60.2, 43.0, 37.0, 25.7, 24.1, 23.8, 18.2 ppm; MS-ESI$^+$ *m/z* [M+Na] calcd for $C_{15}H_{20}NaO_4$: 287.1, found: 287.1.

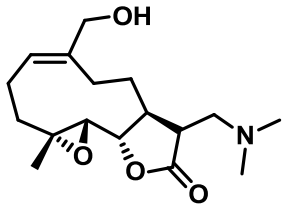

Dimethylamino adduct of Melampomagnolide B (7a)

Melampomagnolide B, **7**, (32.50 mg, 0.10 mmol) was dissolved in methanol (4 ml) and dimethylamine was added (0.10 mL, 0.20 mmol). The reaction was allowed to stir overnight, and was then concentrated *in vacuo* to yield compound **7a** (32.70 mg 86%) as a white solid. ^{1}H NMR (400 MHz, CDCl3) δ = 5.59 (t, *J* = 7.9 Hz, 1H), 4.10 (q, *J* = 13.0 Hz, 2H), 3.85 (t, *J* = 9.2 Hz, 1H), 2.80 (d, *J* = 9.4 Hz, 1H), 2.73 (dd, *J* = 12.9, 5.1 Hz, 1H), 2.61 (dd, *J* = 12.9, 5.4 Hz, 1H), 2.51 – 2.35 (m, 4H), 2.25 (m, 2H), 2.21 (s, 6H), 2.12 (m, 2H), 1.59 (m, 1H), 1.52 (s, 3H), 1.07 (t, *J* = 11.4 Hz, 1H). ^{13}C NMR (100 MHz, $CDCl_3$) δ = 177.0, 141.1, 127.2, 81.6, 77.5, 66.0, 64.1, 60.0, 57.7, 45.7, 44.3, 42.2, 37.1, 27.5, 25.8, 23.8, 18.0. HRMS-ESI$^+$ *m/z* [M+H] calcd for $C_{17}H_{28}NO_4$: 310.2013, found: 310.1999.

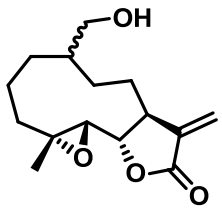

Reduced C1-C10 olefin of Melampomagnolide B 8

Compound **7a** (46.90 mg, 0.15 mmol) was dissolved into ethyl acetate (10 mL), and 10% palladium on carbon (46.30 mg, 0.44 mmol) was added to the reaction mixture. The reaction was put under an atmosphere of 50 psi hydrogen gas, and shook for 5 days. The reaction mixture was filtered through a celite plug and washed with ethyl acetate (5 × 5 mL) and DCM (5 × 5 mL). The solvent was removed *in vacuo* and the crude material was purified by flash chromatography over SiO_2 (0 to 10% Methanol in DCM) to yield (14.00 mg) as a white solid. The compound was then dissolved into THF (2 ml) and iodomethane was added in excess (0.10 mL, 1.60 mmol). The reaction was allowed to stir at rt for 20 h. The solvent and excess methyl iodine was removed *in vacuo* resulting in a yellowish solid. Distilled water (10 mL) was added and the reaction and was heated to 45°C. Complete solvation of the yellowish material resulted within minutes of heating. The reaction was allowed to stir with heating for 3 h, then solvent was removed *in vacuo*. Saturated $NaHCO_3$ aqueous solution (10 mL) was added to the reaction mixture, and the product was extracted with DCM (3 × 20 mL). The combined organic layers were washed with brine, and dried over Na_2SO_4. Purification and characterization is currently underway.

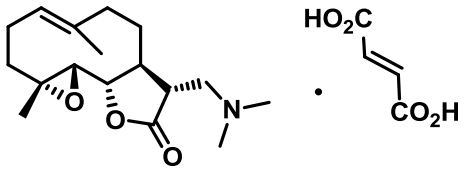

LC-1 (11)

Known compound **11** was prepared by the method of Neelakantan et al.[234] Compound **1a** (14.20 mg, 0.05 mmol) was dissolved into ethyl ether (5 mL) and fumaric acid (5.62 mg, 0.05 mmol) was added. The reaction was allowed to stir for two days and solvent was removed *in vacuo* to yield compound **11** (16.30 mg, 82 %) as a white solid. ^{1}H NMR (400 MHz, DMSO-d_6) δ = 13.00 (s, 2H), 6.62 (s, 2H), 5.22 (dd, *J* = 11.9, 2.4 Hz, 1H), 3.97 (t, *J* = 9.0 Hz, 1H), 2.80 (d, *J* = 9.0 Hz, 1H), 2.63 (m, 3H), 2.42 – 2.26 (m, 2H) 2.21 (s, 6H), 2.14 (m, 1H), 2.10 – 1.91 (m, 4H), 1.64 (s, 3H), 1.20 (s, 3H), 1.17 – 1.05 (m, 2H). Spectral data matches previously reported.[234]

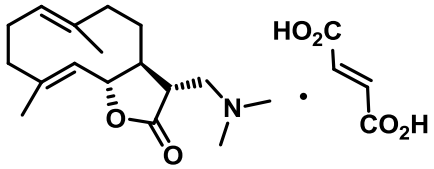

Costunolide Fumarate Salt 12

Compound **1b** (15.10 mg, 0.055 mmol) was dissolved into ethyl ether (5 mL) and fumaric acid (6.34 mg, 0.06 mmol) was added. The reaction was allowed to stir for two days, at which time solvent was removed *in vacuo* to yield compound **12** (22.20 mg, quantitative yield) as an off white solid. ^{1}H NMR (400 MHz, DMSO-d_6) δ = 6.60 (s, 2H), 4.78 (dd, *J* = 10.6, 2.2 Hz, 1H), 4.70 (t, *J* = 9.7 Hz, 1H), 4.64 (d, *J* = 10.2 Hz, 1H), 2.70 – 2.52 (m, 4H), 2.35 – 2.21 (m, 3H), 2.18 (s, 6H), 2.12 – 1.88 (m, 5H), 1.63 (d, *J* =

1.3 Hz, 3H), 1.36 (s, 3H). ^{13}C NMR (100 MHz, DMSO-d6) δ = 177.1, 166.2, 139.5, 136.9, 134.1, 127.5, 126.2, 80.5, 57.0, 50.3, 45.3, 45.2, 44.4, 40.5, 27.1, 25.8, 16.9, 15.9. HRMS-ESI$^+$ *m/z* [M+H] Calcd for $C_{17}H_{28}NO_2$ (without salt): 278.2115, found: 278.2126.

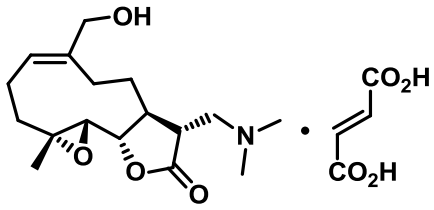

Melampomagnolide B fumarate salt 13

7a (40.50 mg, 0.15 mmol) was dissolved into DCM (5 mL) and fumaric acid (17.70 mg, 0.15 mmol) was added. The reaction was allowed to stir overnight, at which time solvent was removed *in vacuo* to yield compound **13** (55.30 mg, 85%) as a white solid. ^{1}H NMR (400 MHz, DMSO-d_6) δ 6.61 (s, 2H), 5.49 (t, *J* = 7.7 Hz, 1H), 4.01 (t, *J* = 9.6 Hz, 1H), 3.92 (q, *J* = 13.3 Hz, 2H), 2.73 – 2.55 (m, 4H), 2.31-2.14 (m, 10H), 2.13 – 1.99 (m, 3H), 1.57 (t, *J* = 10.6 Hz, 1H), 1.47 (s, 3H), 0.96 – 0.86 (m, 1H). ^{13}C NMR (100 MHz, DMSO-d6) δ = 177.1, 166.2, 141.0, 134.1, 123.5, 123.4, 80.6, 63.3, 59.9, 57.6, 45.2, 45.2, 43.4, 42.7, 40.2, 36.9, 25.7, 24.0, 23.0, 17.5. HRMS-ESI$^+$ *m/z* [M+H] calcd for $C_{17}H_{28}NO_4$ (without salt): 310.2013, found: 310.2015.

2.5.3 Protocol for Mammalian Cell Culture

All cell lines were maintained in a humidified 5% CO_2 environment at 37 °C in culture flasks (Corning). Adherent cells were dissociated using 0.25% Trypsin-EDTA solution (Gibco). CCRF-CEM cells (ATCC, CCL-119) and NCI/ADR-RES were

cultured in RPMI-1640 media (Cellgro) supplemented with 10% fetal bovine serum (FBS, Gibco), penicillin (100 I.U./mL), and streptomycin (100 μg/mL, ATCC) at a density of 2×10^5 - 2×10^6 cells/mL. DU-145 cells (ATCC, HTB-81), Vero cells (ATCC, CCL-81), U-87MG cells (ATCC, HTB-14**)**, and HeLa cells (ATCC, CCL-2) were cultured in MEM media (Cellgro) supplemented with 10% FBS (Gibco), penicillin (100 I.U./mL), and streptomycin (100 μg/mL, ATCC). HL-60 cells (ATCC, CCL-240) were cultured in IMDM media (Cellgro) supplemented with 20% FBS (Gibco), penicillin (100 I.U./mL), and streptomycin (100 μg/mL, ATCC). MCF-7 cells (ATCC, HTB-22) were cultured in MEM media (Cellgro) supplemented with 10% FBS (Gibco), bovine insulin (0.01 mg/mL, Sigma) penicillin (100 I.U./mL), and streptomycin (100 μg/mL, ATCC). GBM6 cells (gift from the lab of professor John Ohlfest) were cultured with DMEM/F12 (1:1) with L-Glutamine, without HEPES (Thermo Scientific) supplemented with Normocin (100 μg/mL, Invivogen), 50X B-27 supplement (10 mL, Gibco), 100X N-2 supplement (5 mL, Gibco), human EGF (20 ng/μL, Peprotech), human FGF-basic (20 ng/μL, PeproTech), penicillin (50 I.U./mL), and streptomycin (50 μg/mL, ATCC).

2.5.4 Protocol for Cell Culture Cytotoxicity Assays

The protocol for cellular cytotoxicity assays was previously published by our laboratory (Hexum et al).[264] CCRF-CEM and HL-60 cells were cultured at a density of 10,000 cells/well in cell culture media (50 μL) in standard 96-well plates (Costar) 24 h prior to treatment. DU-145, Vero, U-87MG, GBM6, HeLa, MCF-7, and NCI/ADR-RES

cells were seeded at a density of 5,000 cells/well in cell culture media (50 μL) in standard 96-well plates (Costar). Blank (no cells) wells and control (vehicle control treated) wells were prepared for every experiment to normalize the data. All **PTL** analogues were serially diluted in pre-warmed media and dosed to 96 well plates (final volume/well = 100 μL; final DMSO concentration = 0.5%). Approximately 1-3 h before the end of the treatment period (48 h), Alamar Blue (Invitrogen) cell viability reagent was added to the 96 well plates (10 μL). A quantitative measure of cell viability can be achieved from evaluating the ability of metabolically active cells (which are proportional to the number of living cells) to convert resazurin (non-fluorescent dye) to red-fluorescent resorufin. Fluorescence data were obtained on either a Molecular Devices SpectraMax M2 plate reader or an LJL BioSystems HT Analyst plate reader. Background fluorescence (no cell controls) was subtracted from each well and cellular viability values following compound treatment were normalized to vehicle-only treated wells (control wells only treated with aqueous DMSO, which were arbitrarily assigned 100% viability). Individual IC_{50} curves were generated by fitting data to the sigmoidal (dose response) function of varied slope in GraphPad Prism (v. 5.0) software. Only curve fits with $R^2 > 0.95$ were deemed sufficient. Each experiment was performed in biological triplicate and mean IC_{50} values were calculated from the individual IC_{50} values obtained from each replicate. Standard deviation was calculated from the individual IC_{50} values obtained for each biological replicate.

Dimethylamino Parthenolide 1a
^{1}H NMR ($CDCl_3$):

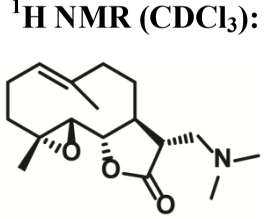

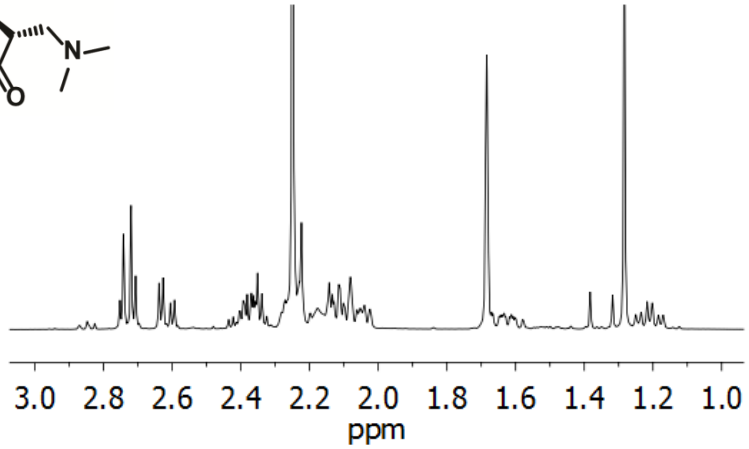

2.6 NMR

Dimethylamino Parthenolide 1a
^{13}C NMR ($CDCl_3$):

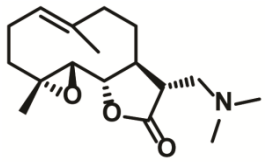

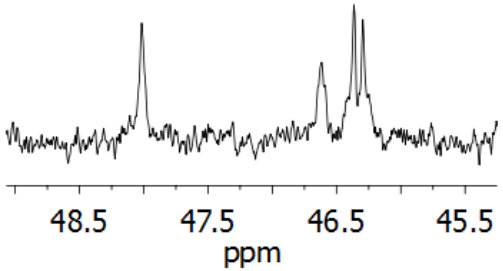

Dimethylamino Costunolide 2a
^{1}H NMR ($CDCl_3$):

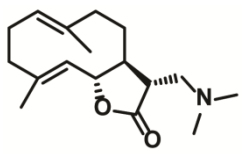

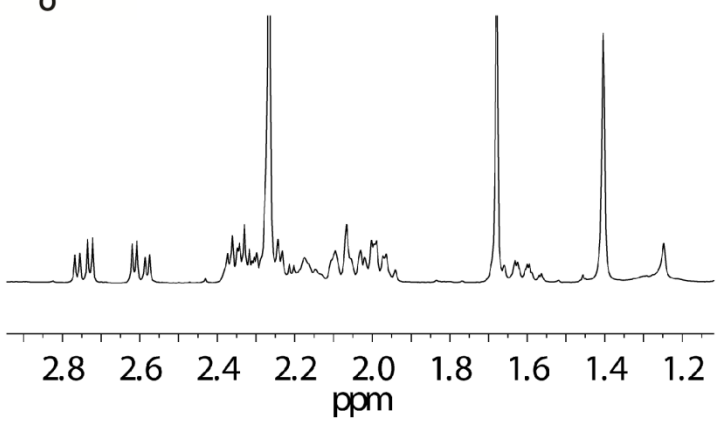

Dimethylamino Costunolide 2a
^{13}C NMR ($CDCl_3$):

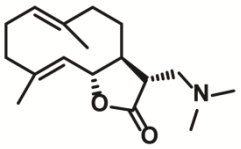

Reduced Parthenolide 3

^{1}H NMR ($CDCl_3$):

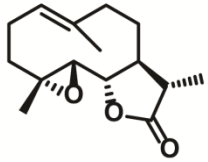

Reduced C1-C10 Olefine of Dimthylamino Parthenolide 1b
^{1}H NMR ($CDCl_3$):

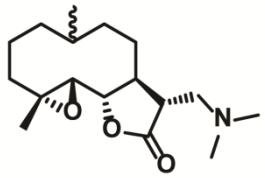

Reduced C1-C10 Olefine of Dimthylamino Parthenolide 1b
^{13}C NMR ($CDCl_3$):

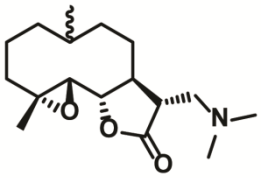

Cis Parthenolide 6
^{1}H NMR ($CDCl_3$):

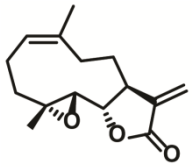

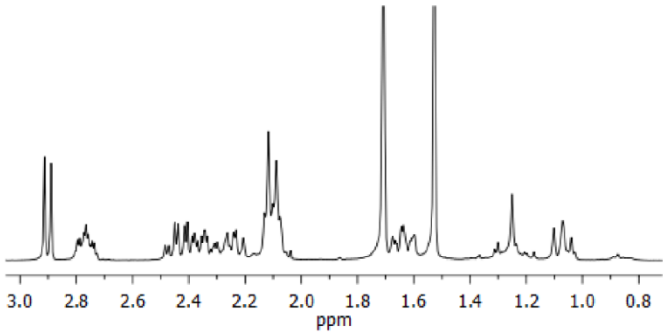

Melampomagnolide B (7)
^{1}H NMR ($CDCl_3$):

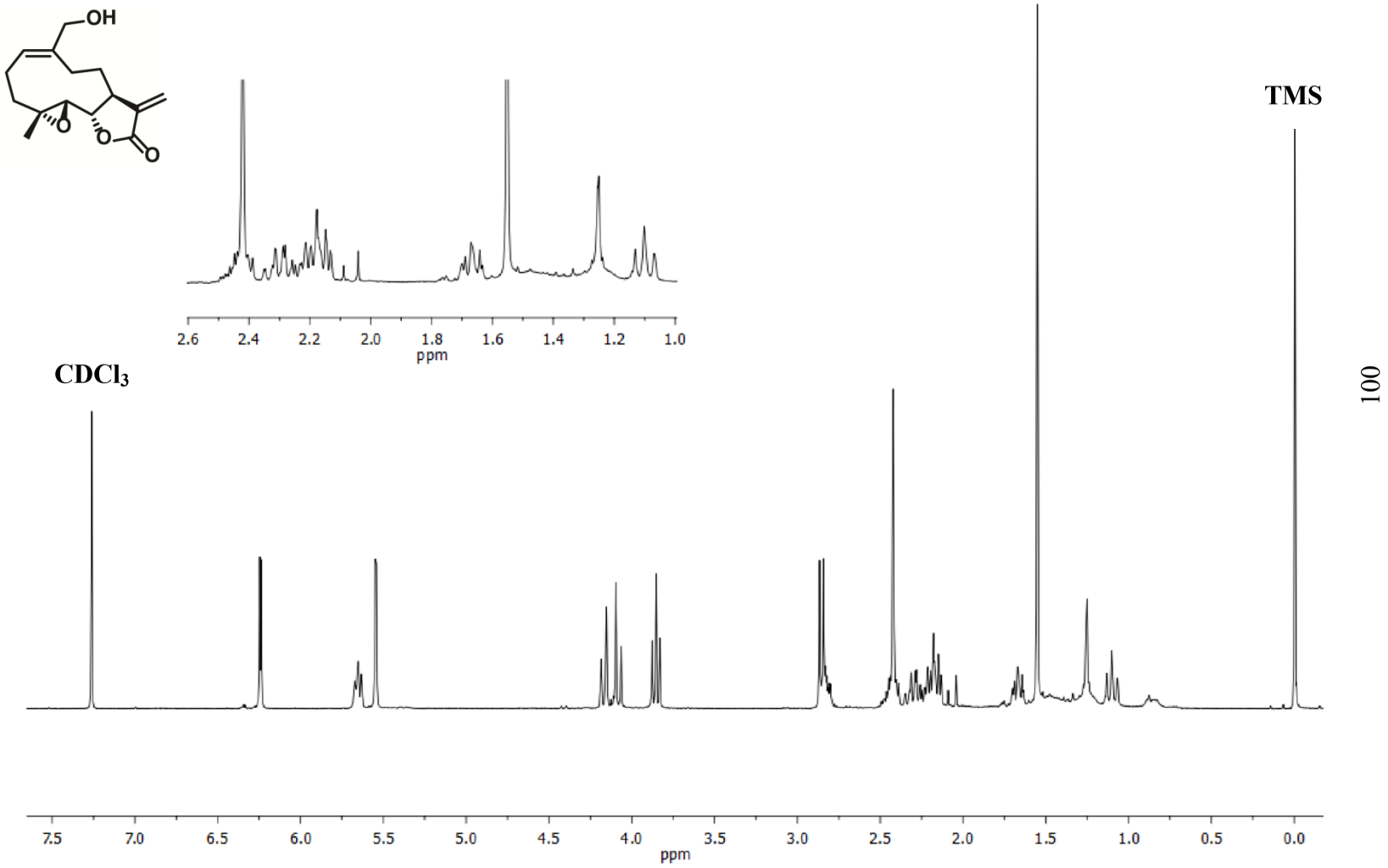

Dimethylamino adduct of Melampomagnolide B (7a)

^{1}H NMR ($CDCl_3$):

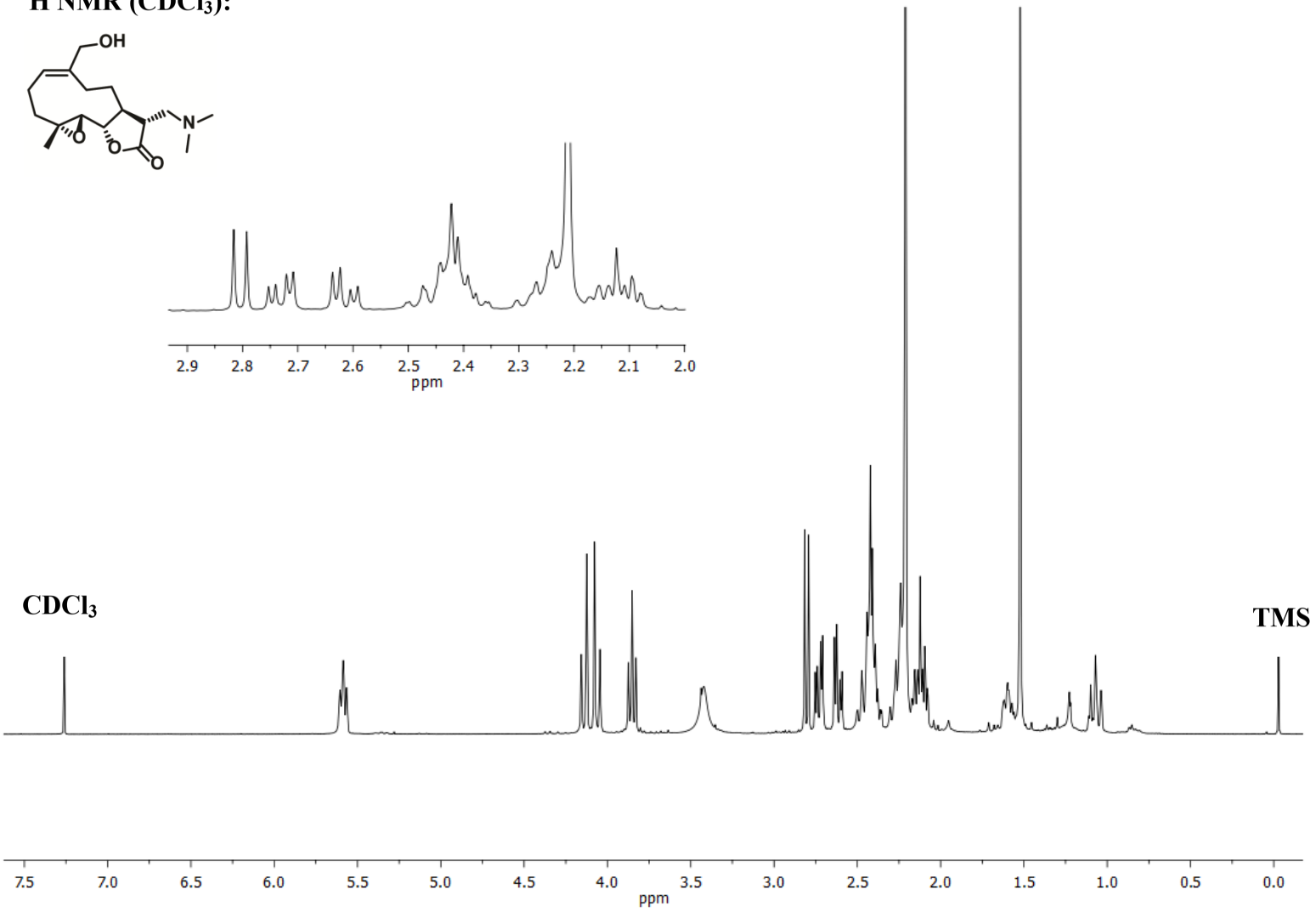

Dimethylamino adduct of Melampomagnolide B (7a)
^{13}C NMR ($CDCl_3$):

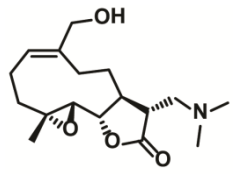

LC-1 (11)
^{1}H NMR (DMSO-d_6):

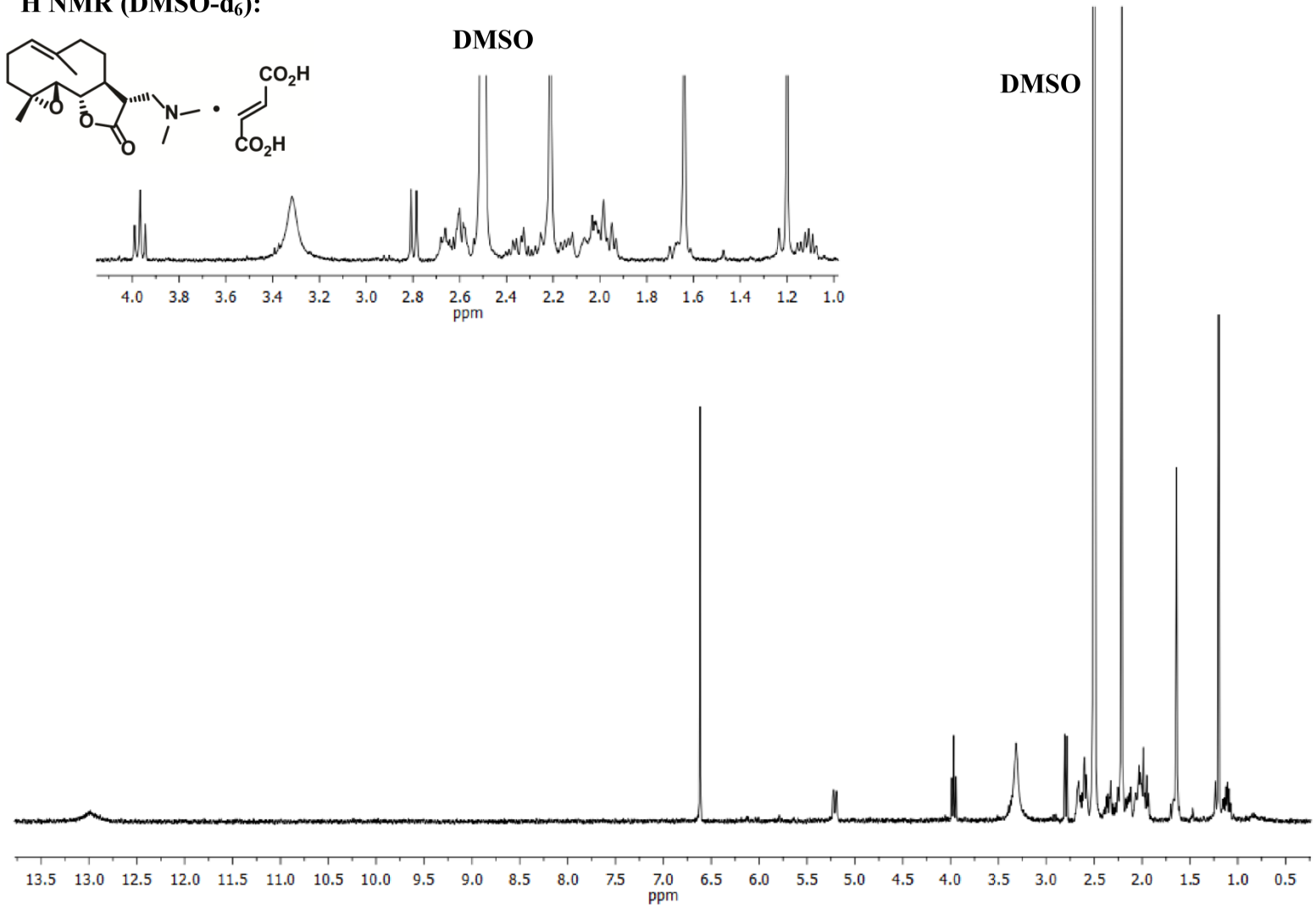

Costunolide Fumarate Salt 12
^{1}H NMR (DMSO-d_6):

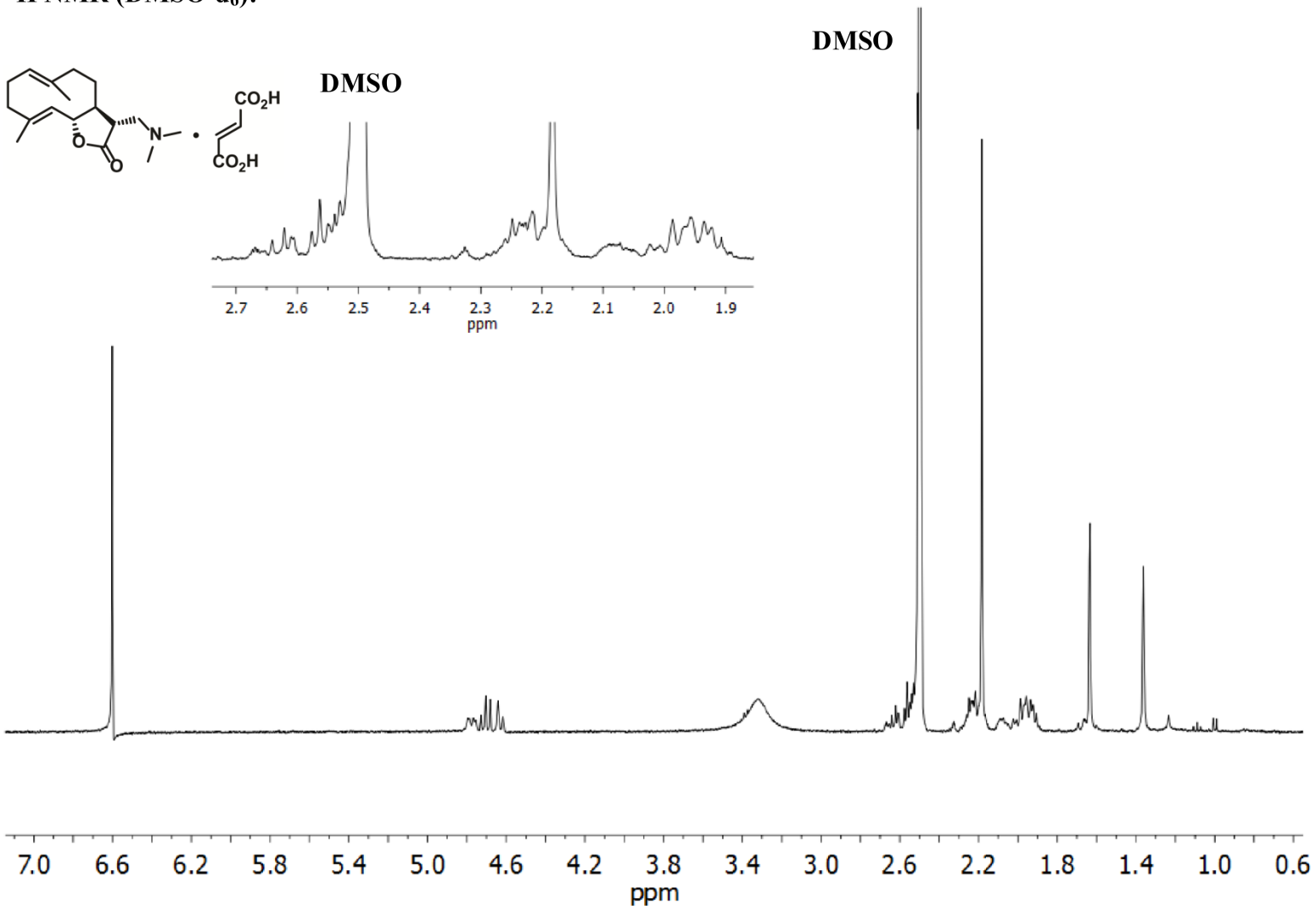

Costunolide Fumarate Salt 12
^{13}C NMR (DMSO-d_6):

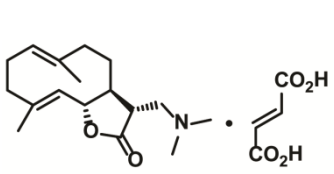

Melampomagnolide B Fumarate Salt 13
^{1}H NMR (DMSO-d_6):

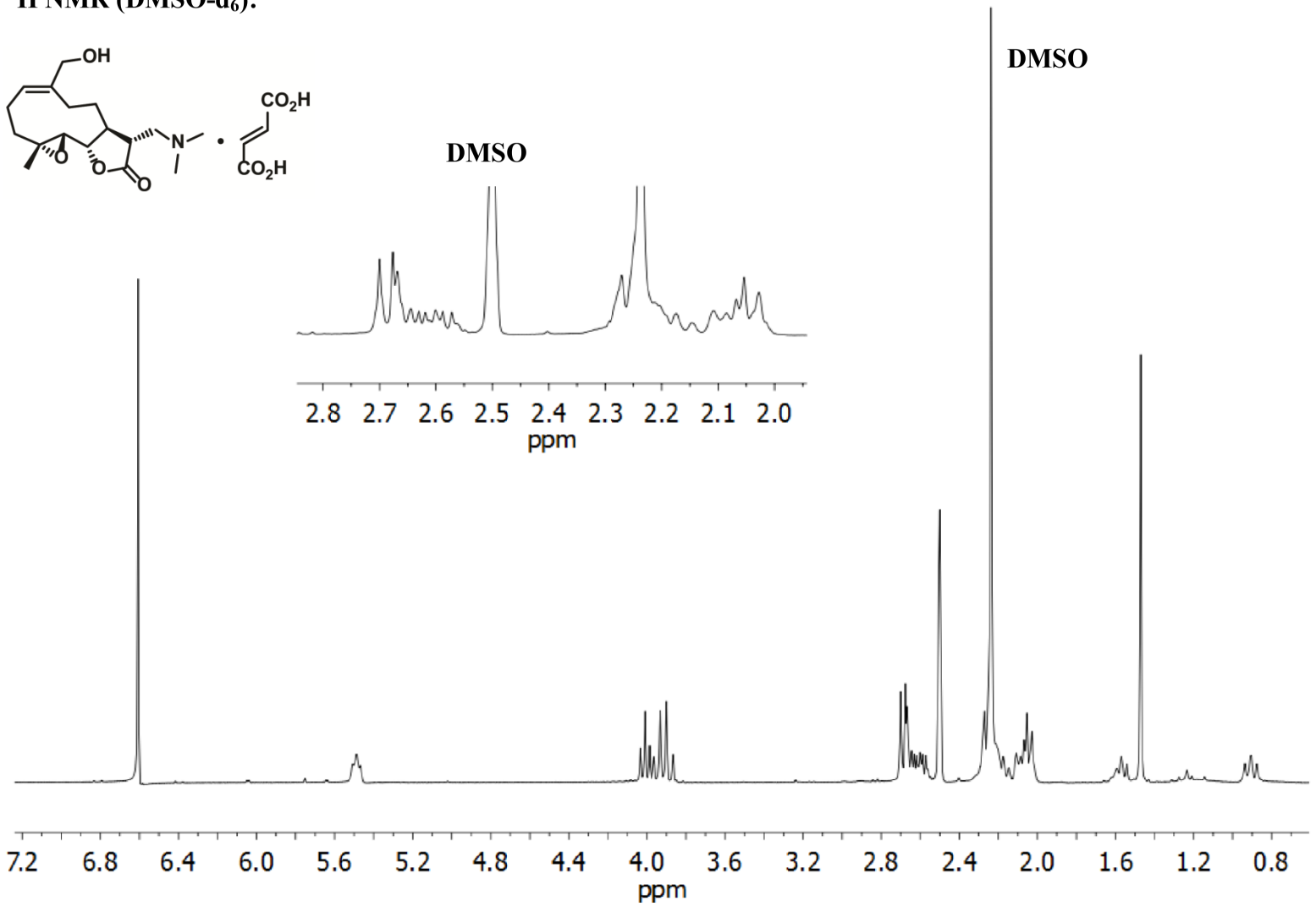

Melampomagnolide B Fumarate Salt 13

^{13}C NMR (DMSO-d_6):

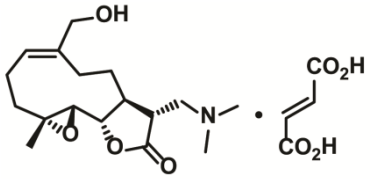

Chapter 3. Raising the Effective Intracellular Concentration of Parthenolide Utilizing a Gold Nanoparticle Delivery System.

3.1 Introduction

Nanoparticles are particles on the order of nanometers made out of various metals (copper, platinum, silver, or gold) or semiconductors (titanium dioxide, cadmium selenide, cadmium sulfide, silver sulfide, and lead sulfide).[290] Ligands are used during the synthesis of nanoparticles to control growth and prevent aggregation.[291] Compared to the size of a cell, nanoparticles are up to ten thousand times smaller, around the size of receptors, enzymes, and antibodies.[292] Due to their small size, nanoparticles are capable of interactions both extracellular and intracellular.[292]

Nanoparticles have been intensely investigated as potential drug carriers for targeted delivery.[291,293-295] Nanoparticle delivery systems take advantage of pathophysiological alterations observed in tumors, such as increased diffusion and permeability due to leaky vasculature of tumors.[296] Nanoparticles ranging between 20-100 nm can take advantage of the enhanced permeability and retention effect (EPR), allowing passive diffusion into tumors, thereby permitting greater accumulation when compared to free drugs.[297] Moreover, nanoparticle delivery systems can increase drug solubility and allow for timed release of drugs conjugated to them.[298,299]

However, nanoparticles do have their flaws. The reticuloendothelial system (RES) will opsonize large nanoparticles (> 100 nm) and eliminate them through the liver.[292,300,301] To avoid excretion through the RES, smaller particles functionalized with

a secondary layer of hydrophilic polymer are used.[301] Polyethylene glycol (PEG) has been widely used to mask nanoparticles from the RES, while also improving water solubility.[302]

Out of all the nanomaterials utilized today, gold nanoparticles (AuNP) have become a primary interest in drug delivery research.[295,303,304] Gold has excellent properties that lead to ease of synthesis and functionalization of nanoparticles.[303,305] Compared to other materials used, gold has greater chemical stability.[305] Gold also has intrinsic characterization properties that include visible light scattering/absorption, low biological concentrations, and large electron density that allows for easy quantification, location, and imaging in biological organisms.[305,306] Additionally, routes have been developed for controlled synthesis of AuNP allowing the shape and size of the AuNP to be regulated.[307-310]

AuNPs have been previously loaded with anticancer drugs, such as paclitaxel,[301,311] methotrexate,[312] daunorubicin,[313] gemcitabine,[314] 5-fluoruracil,[315] cisplatin,[316] tamoxifen,[317] trastuzumab,[318] and doxorubicin.[319] Agasti et al demonstrated that by conjugation to a AuNP delivery system, a 100-fold decrease in the IC_{50} value of 5-fluorouracil (5-FU) was observed, from 11.9 μM to 0.7 μM in MCF-7 cells. AuNP in this study were used to cage 5-FU, and upon photolysis, 5-FU was released.[315]

Gold is also readily functionalized by thiols. Utilization of an alkanethiol linker to anchor drug payloads to the AuNP is often observed in the literature.[303,320,321] Thiol ligand exchange is a fairly rapid conversion that depends on chain length and sterics.[320,322] Because of these characteristics we have chosen to synthesize parthenolide

(**PTL**) functionalized AuNPs utilizing a PEG-thiol, similar to that of a previously reported functionalization of paclitaxel to a AuNP.[311] By conjugating **PTL** to a AuNP we hope to improve the water solubility of the drug and increase the effective concentration delivered to the target cancer cells.

3.2 Research Objectives

Current progress on the synthesis and anticancer evaluation of a **PTL** functionalized AuNP is herein reported. We have envisioned three different linkers (**Figure 3.1**) to investigate the effects of conjugating **PTL** to AuNP: melampomagnolide B linker **15**, a non-functional linker **16** and a dimethylamino analogue of **PTL** (DMAPT) linker **17**. Once synthesized, we will investigate the AuNP's ability to address two major problems with **PTL**: its poor water solubility and low micromolar anticancer activity. A AuNP delivery system should increase the effective concentration of **PTL** delivered to cancer cells allowing detectable levels of **PTL**, and ultimately reaching the IC_{50} *in vivo*. Additionally, water solubility of the drug would improve by utilization of a PEG linker as well as the innate characteristic of AuNP to improve drug solubility. Described here are the efforts made towards the synthesis of a **PTL** functionalized AuNP.

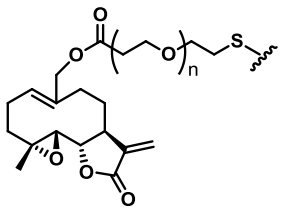

15

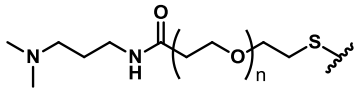

16

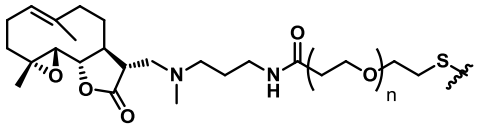

17

Figure 3.1 Proposed linkers for conjugation of **PTL** to AuNP. Conjugation of **PTL** via ester linker **15,** a nonfunctional control linker **16**, and a DMAPT inspired linker **17**. N ranges from 36-55 PEG units $CTPEG_{2000}$.

3.3 Results and Discussion

3.3.1 Synthesis of 2 nm Gold Nanoparticles

2 nm gold nanoparticles were synthesized from a known procedure.[307] Tetrachloroaurate trihydrate and p-mercaptophenol were dissolved into methanol. Acetic acid was added to the stirring reaction to prevent deprotonation of p-mercaptophenol. Next, $NaBH_4$ was added to the reaction gradually, causing a brown precipitate to form, which was a clear indication of formation of 2 nm gold nanoparticles. After complete addition of $NaBH_4$ the reaction was allowed to stir for 30 minutes then the solvent was removed *in vacuo*. The brown solid was washed with ethyl ether and distilled and deionized H_2O to remove any excess reagent. Transition electron microscopy was

utilized to image the nanoparticles verifying the size of the particles and to observe if aggregation had occurred. Particles were found to have an average of 2 nm in diameter (**Figure 3.2**).

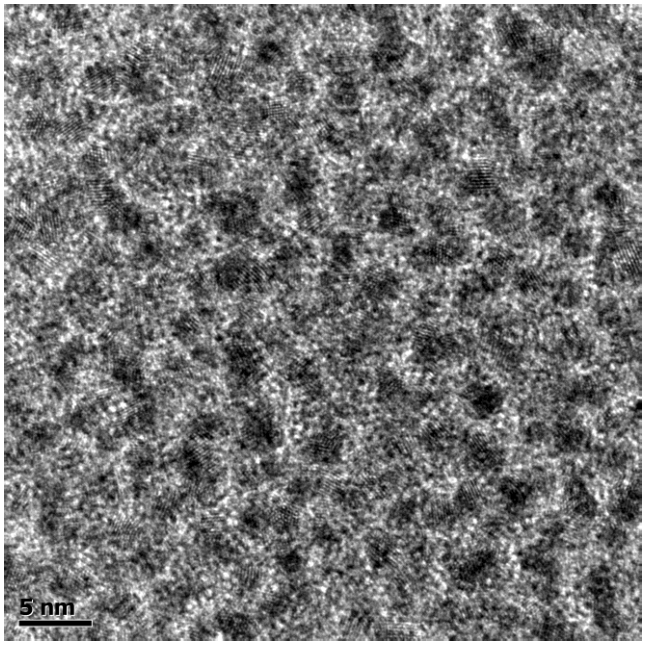

Figure 3.2 Transition electron microscopy image of synthesized 2 nm gold nanoparticles.

3.3.2 Solution Phase Functionalization of Gold Nanoparticles

Originally, use of 2 nm AuNP for conjugation of **PTL** was planned; however, concerns were raised. Two nm AuNP fall short of the requirements for the EPR effect. Additionally, TEM images of larger AuNP are easier to resolve. We opted to purchase 15 nm tannic acid capped AuNP to continue our studies. Tannic acid capped 15 nm AuNPs were reacted with the 2,000 mw (Da) carboxyl thiol polyethylene glycol ($CTPEG_{2000}$) at rt for 12 h to yield **18** (**Scheme 3.1**). AuNPs were then filtered through a 10,000 kDa molecular weight filter to remove excess thiol and tannic acid.

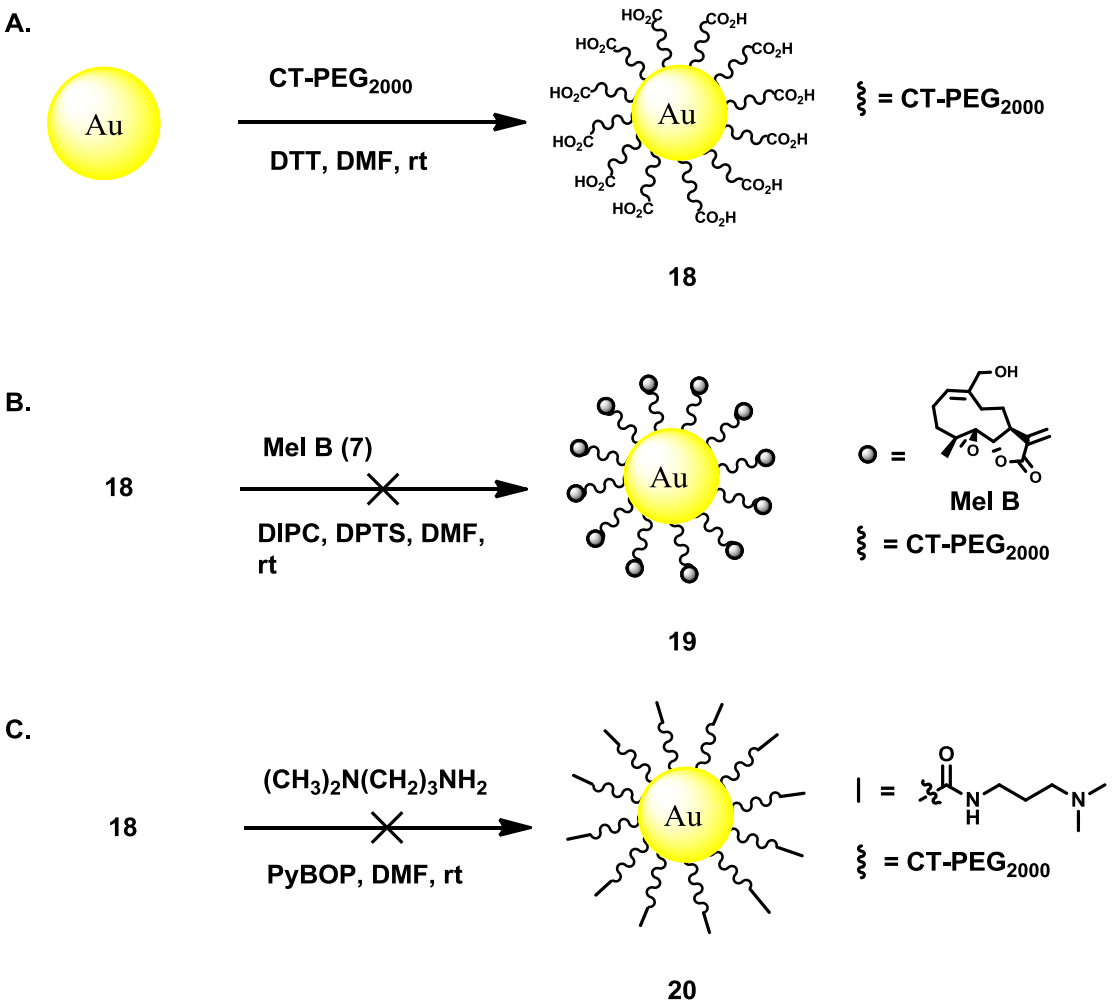

Scheme 3.1 Solution phase synthesis of **PTL** functionalized AuNP. **A**. Thiol functionalization of AuNP. **B**. Attempted Mitsunobu conditions to synthesize Melampomagnolide B (Mel B) functionalized AuNP. **C**. Attempted synthesis of non-functional AuNP.

After resuspension of the AuNP **18** in Millipore water, UV-Vis full spectrum analysis was performed. We observed that functionalization of the AuNP via ligand exchange of the thiol for tannic acid had occurred due to an observed reduction in the wavelength max (520 nm) of 15 nm AuNPs (**Figure 3.3**).[306] Additionally, we could confirm a 15 nm core particle size (**Figure 3.4**).

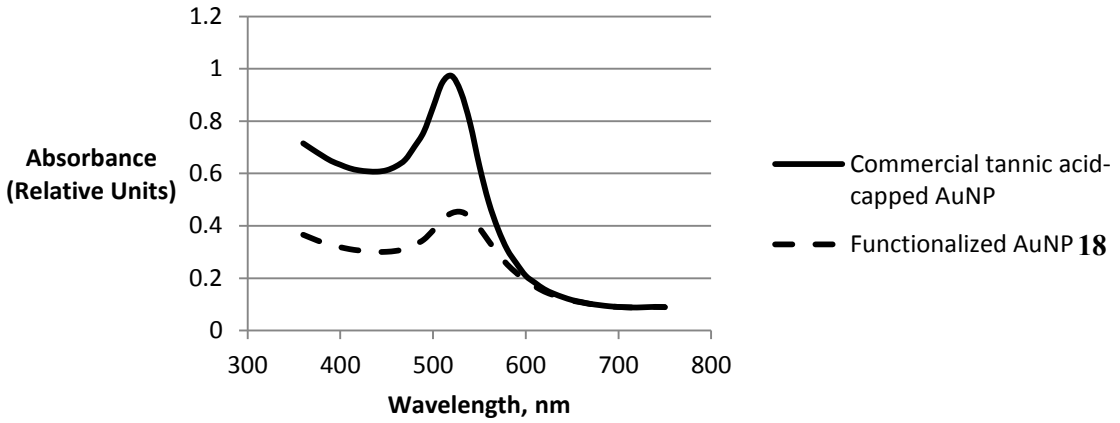

Figure 3.3 Full spectrum UV-Vis absorption of functionalized **18** and non-functionalized gold nanoparticles. A reduction of absorbance at the wavelength max of 15 nm AuNP (λ = 520 nm) was observed upon functionalizing with thiols.

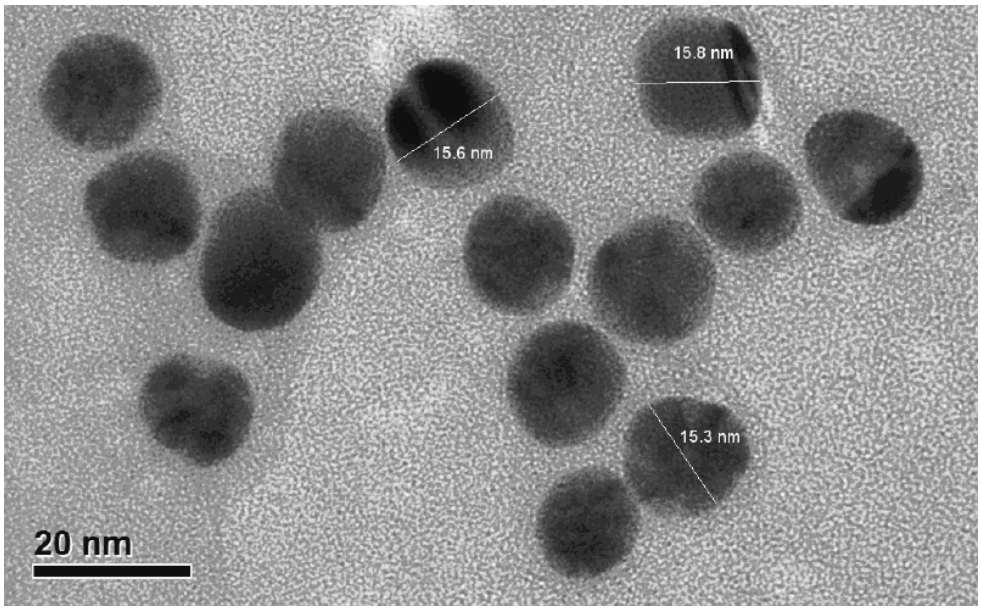

Figure 3.4 Transition electron microscopy image of 15 nm AuNP after funtionalization with carboxyl thiol PEG **18**. Core particle size was 15 nm.

Following the protocol to conjugate paclitaxel to a AuNP, Mitsunobu conditions were performed to conjugate melampomagnolide B (**7**) to **18** (**Scheme 3.1**).[311] DMF was added to the solution of **18**, and the water was removed *in vacuo*. 4-(*N,N*-Dimethylamino)pyridinium-4-toluenesulfonate and *N,N'*-diisopropylcarbodiimide was added to the reaction and left to stir overnight. Irreversbile Aggregation of the AuNP was observed the next day.

In an effort to synthesize the non-functional AuNP, peptide coupling conditions were performed to conjugate 3-(dimethylamino)-1-propylamine to the free carboxylic acid of **18**. PyBOP and dimethylamine were reacted with **18** overnight. Aggregation of the AuNP was observed similar to that observed with coupling to melampomagnolide B. Based on these unexpected difficulties, it was decided to first synthesize the **PTL**-linker-thiol reagent, and then couple the pre-assembled payload to the nanoparticle.

3.3.3 Solid Phase Synthesis of DMAPT Linker for Gold Nanoparticle Functionalization

In an effort to avoid the aggregation issues of solution phase synthesis of the PTL functionalized linker on a AuNP, solid phase synthesis was performed. FMOC protected Rink amide MHBA resin was deprotected with piperidine. After washing the resin with DMF, it was reacted with mercaptoacetic acid in the presence of EDCI and TEA to yield the free thiol on resin **(Scheme 3.1)**.

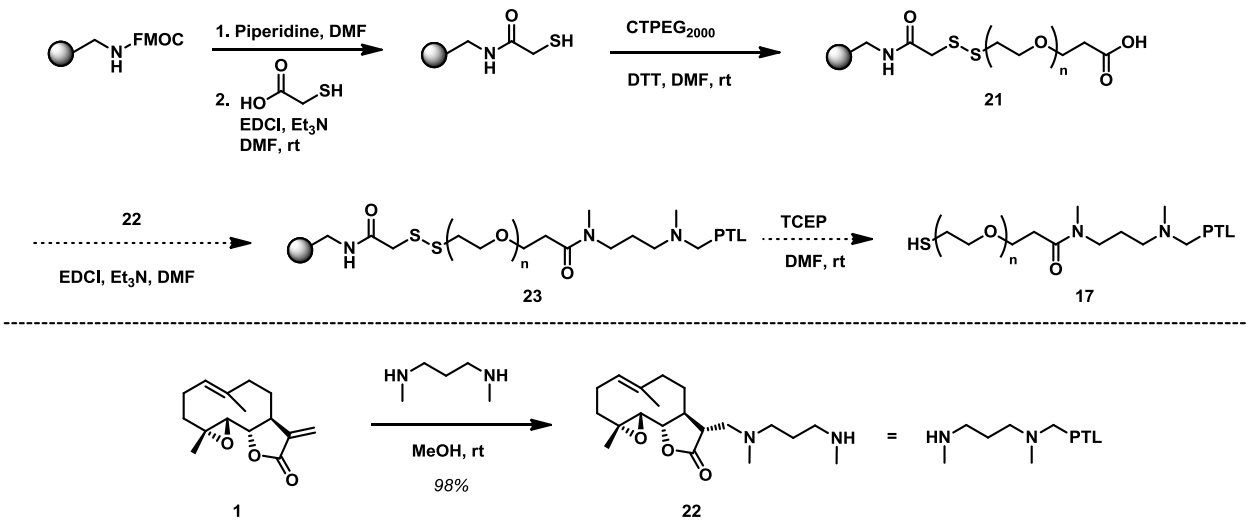

Scheme 3.2 Solid phase synthesis of dimethylamino analogue of **PTL** (DMAPT) PEG linker **17**. N ranges from 36-55 PEG units $CTPEG_{2000}$.

Any disulfide bonds formed from the free thiol of mercaptoacetic acid were then cleaved with DTT. Rigourous washing to remove the DTT was performed and the resulting free thiol was reacted with the 2000 MW thiol carboxyl PEG ($CTPEG_{2000}$) yielding compound **21**. In an effort to prevent linkers on resin to react with each other during peptide synthesis with N,N-dimethyl-1,3-propanediamine, the diamine was monofunctionalized beforehand with **PTL** in a Michael addition to yield compound **22** in 98% yield. Current effort are focused on exploring peptide coupling reagents to conjugate **22** to **21**, and then cleaving **23** from resin to yield the DMAPT linker **17**.

3.4 Conclusion and Future Direction

In summary, we have attempted to synthesize a **PTL** functionalized AuNP. Initial solution phase synthetic routes lead to irreversible aggregation of the AuNP *via*

Mitsunobu and peptide coupling reactions. Functionalization of the AuNP with $CTPEG_{2000}$ was achieved by a thiol exchange reaction to replace the tannic acid capping the AuNP. To circumvent the observed aggregation, we have begun solid phase synthesis of the **PTL** functionalized linkers. Once synthesized, we will react the linkers with tannic acid capped AuNP for a facile thiol exchange reaction. Anticancer activity of the **PTL** functionalized AuNP will be evaluated *in vitro* upon completion of the synthesis.

3.5 Experimental

Parthenolide was purchased from Enzo Life Sciences. Commercial grade reagents (Aldrich, Acros, Alfa Aesar) were used without further purification unless otherwise noted. 15 nm gold nanoparticles were purchased from Ted Pella Inc (Redding, CA). Carboxyl thiol polyethylene glycol (mw = 2000) was purchased from JenKem Technology USA (Allen, TX). Centrifuge filters were purchased from Millipore (Billerica, MA). 2 nm Transition electron microscopy images were peformed by the UMN characterization facilty on a on a Tecnai G^2 F30 microscope. 15 nm AuNP Transition electron microscopy images were also performed by the UMN characterization facility on a Tecnai T12 microscope. UV-Vis full specrum analysis was performed on a Molecular Devices SpectraMax M2 plate reader using millipore water as a solvent Nuclear magnetic resonance (NMR) spectroscopy employed a Bruker Avance instrument operating at 400 MHz (for ^{1}H) and 100 MHz (for ^{13}C) at ambient temperature. Internal solvent peaks were referenced in each case.

3.5.1 Synthesis of 2nm Gold Nanoparticles

Two nm gold nanoparticles were synthesized from the Brust method.[307] Tetrachloroauric(III) acid (298.5 mg, 0.88 mmol) and p-mercaptophenol (230 mg, 1.82 mmol) were dissolved into 150 mL of MeOH. AcOH (3 mL) was then added. $NaBH_4$ (30 mL, 0.4 M) was added slowly (1 mL every 30 seconds) affording a brown ppt. Reaction was then allowed to stir for 30 minutes after complete addition of $NaBH_4$. Solvent was then removed *in vacuo* and the remaining brown solid was washed with ethyl ether (20 mL) and then deionized water (20 mL) to yield a brown solid (1.26 g). Transition electron microscopy images showed an average size of 2 nm of the particles (**Figure 3.2**).

3.5.2 Synthesis of Parthenolide Functionalized Gold Nanoparticles in Solution.

Synthesis of $CTPEG_{2000}$ Functionalized AuNP (18)

A 15 nm tannic acid-capped gold nanoparticle solution in distilled and deionized water (2mL, $1.1x10^{12}$ particles/mL) was reacted with a non-discrete $CTPEG_{2000}$ (50.0 mg, 0.03 mmol) overnight. The next day, the reaction was filtered through a 10,000 mw centrifuge filter, washed with distilled and deionized water (3 x 0.5 mL) through the centrifuge filter. Remaining nanoparticle solution that did not filter was removed from the centrifuge filter and resuspended into distilled and deionized water (total volume of 2 mL). A total volue of 2 mL was required to be compare the UV-Vis spectrum of the functionalized AuNP to the starting tannic acid-capped AuNP. Full spectrum UV-Vis

was performed to gauge functionalization. ^{1}H NMR (400 MHz, D_2O) δ = 3.71 (s, 189H) 2.74 (t, *J* = 6.3 Hz, 2 H, -CH_2-SH). 189 protons correlates to 47 repeat PEG units, which falls into the range of PEG repeat units observed by maldi of $CTPEG_{2000}$ starting material.

3.5.3 Solid Phase Synthesis of DMAPT Linker 17

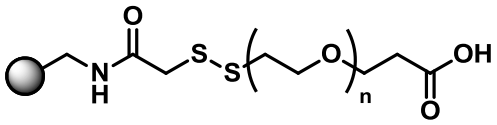

Synthesis of 21.

Rink amide MHBA resin (21.4 mg) was swelled in DMF (1 mL) for 10 minutes in a solid phase reaction vessel. Piperidine (0.2 mL, 0.002 mmol) was added and allowed to shake for 1 h. The reaction was filtered and washed with DMF (5 x 1 mL) with manual shaking between washes. Kaiser test verified deprotection of the amine was achieved. The resin was swelled with DMF (1 mL) for 10 minutes. Mercaptoacetic acid (0.01 mL, 0.14 mmol), EDCI (24.3 mg, 0.16 mmol), and Et_3N (0.02 mL, 0.14 mmol) were added to the reaction vessel and left to shake over night. Reaction was filtered and washed with DMF (5 x 1 mL) with manual shaking between washes to form the amide bond on resin.

The resin was then swelled with DMF (1 mL) for 10 minutes. Dithiothreitol (28.5 mg, 0.19 mmol) was added and reaction was allowed to shake for 15 minutes. Reaction was filtered and washed with DMF (5 x 1 mL) with manual shaking between washes. The resin was reswelled with DMF (1 mL) for 10 minutes, and $CTPEG_{2000}$

(23.4 mg, 0.0117 mmol) was added to the reaction vessel and left to shake over night. Next day reaction was filtered and washed with DMF (5 x 1 mL) with manual shaking between washes to yield compound **21**. Future direction would involve peptide coupling with **22** to anchor **PTL** to resin. Cleavage of the disulfide bond would then yield the DMAPT Linker which can be functionalized to a gold nanoparticle.

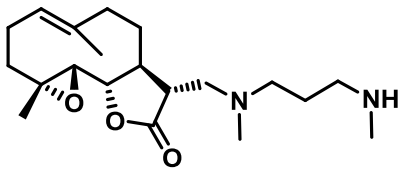

Dimethyl-Propanediamine Parthenolide 22

Parthenolide (32.6 mg, 0.13 mmol) as dissolved into MeOH (5 mL) and an excess of N,N'-Dimethyl-1,3-propanediamine (0.1 mL, 0.80 mmol) was added and the reaction was allowed to stir overnight at rt. The next day solvent and excess N,N'-Dimethyl-1,3-propanediamine was removed in vacuo to yield compound **23** (45.2 mg, 98%) as a clear oil. ^{1}H NMR (400 MHz, $CDCl_3$) δ = 5.17 (d, *J* = 11.5 Hz, H), 3.79 (t, *J* = 9.0 Hz, 1H), 2.77 (dd, *J* = 13.4, 4.8 Hz, 1H), 2.69 (m, 2H), 2.60 (t, *J* = 6.9 Hz, 2H), 2.45 – 2.32 (m, 7H), 2.26 (m, 2H), 2.20 (s, 3H), 2.16 – 2.01 (m, 5H), 1.67 (s, 3H), 1.63 (m, 2H), 1.27 (s, 3H), 1.20 (td, *J* = 13.0, 5.6 Hz, 1H). ^{13}C NMR (100 MHz, $CDCl_3$) δ = 176.6, 134.7, 125.2, 125.1, 82.2, 66.7, 61.4, 57.0, 56.5, 50.5, 48.0, 46.6, 42.7, 41.3, 36.8, 30.1, 27.7, 24.2, 17.1. MS-ESI$^+$ *m/z* calcd for $C_{20}H_{35}N_2O_3$: 351.2648, found: 351.2611.

3.6 NMR

CTPEG$_{2000}$ Functionalized AuNP (18)
^{1}H NMR (D_2O):

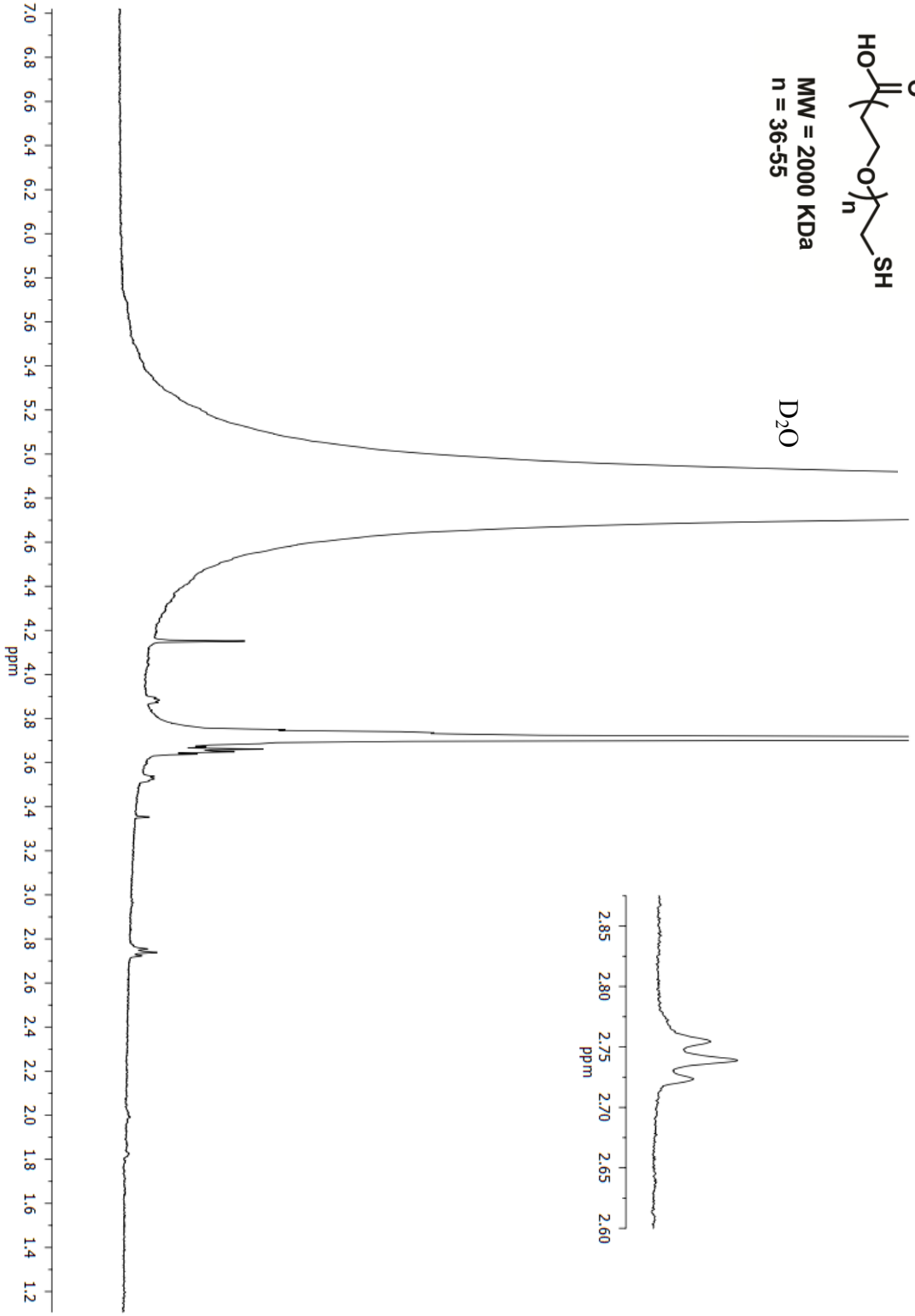

Dimethyl-Propanediamine Parthenolide 22

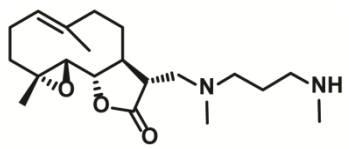

^{1}H NMR ($CDCl_3$):

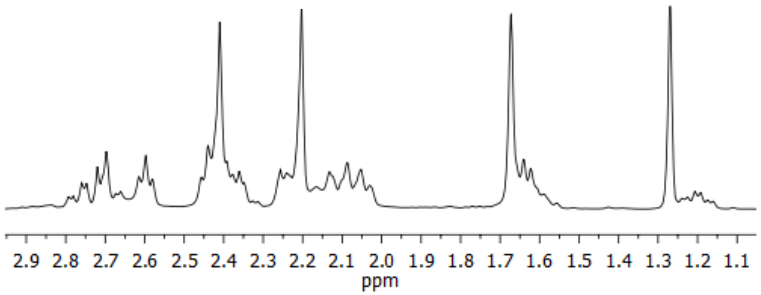

Dimethyl-Propanediamine Parthenolide 22

^{13}C NMR ($CDCl_3$):

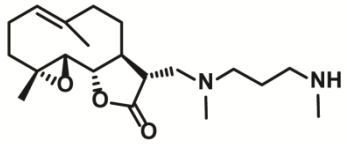

Bibliography

(1) Al-Hajj, M. Cancer stem cells and oncology therapeutics *Curr. Opin. Oncol.* **2007**, *19*, 61.
(2) Behbod, F.; Rosen, J. M. Will cancer stem cells provide new therapeutic targets? *Carcinogenesis* **2005**, *26*, 703.
(3) Dick, J. E. Stem cell concepts renew cancer research *Blood* **2008**, *112*, 4793.
(4) Reya, T.; Morrison, S. J.; Clarke, M. F.; Weissman, I. L. Stem cells, cancer, and cancer stem cells *Nature* **2001**, *414*, 105.
(5) Saini, V.; Shoemaker, R. H. Potential for therapeutic targeting of tumor stem cells *Cancer Sci.* **2010**, *101*, 16.
(6) Wang, J. C. Y. Evaluating therapeutic efficacy against cancer stem cells: New challenges posed by a new paradigm *Cell Stem Cell* **2007**, *1*, 497.
(7) Ward, R. J.; Dirks, P. B. Cancer Stem Cells: At the Headwaters of Tumor Development *Annu. Rev. Pathol-Mech.* **2007**, *2*, 175.
(8) Zhou, B. B. S.; Zhang, H. Y.; Damelin, M.; Geles, K. G.; Grindley, J. C.; Dirks, P. B. Tumour-initiating cells: challenges and opportunities for anticancer drug discovery *Nat. Rev. Drug Discov.* **2009**, *8*, 806.
(9) Bonnet, D.; Dick, J. E. Human acute myeloid leukemia is organized as a hierarchy that originates from a primitive hematopoietic cell *Nat. Med.* **1997**, *3*, 730.
(10) Lapidot, T.; Sirard, C.; Vormoor, J.; Murdoch, B.; Hoang, T.; Caceres cortes, J.; Minden, M.; Paterson, B.; Caligiuri, M. A.; Dick, J. E. A Cell initiating human acute myeloid leukemia after transplantation into SCID mice *Nature* **1994**, *367*, 645.
(11) Fialkow, P. J.; Singer, J. W.; Raskind, W. H.; Adamson, J. W.; Jacobson, R. J.; Bernstein, I. D.; Dow, L. W.; Najfeld, V.; Veith, R. Clonal development, stem-cell differentiation, and clinical remission in acute nonlymphocytic leukemia *New Engl. J. Med.* **1987**, *317*, 468.
(12) Griffin, J. D.; Lowenberg, B. Clonogenic cells in acute myeloblastic leukemia *Blood* **1986**, *68*, 1185.
(13) McCulloch, E. A. Stem cells in normal and leukemic hematopoiesis (Henry Stratton Lecture) *Blood* **1983**, *62*, 1.
(14) Li, L.; Bhatia, R. Stem Cell Quiescence *Clin. Cancer Res.* **2011**, *17*, 4936.
(15) Sehl, M.; Zhou, H.; Sinsheimer, J. S.; Lange, K. L. Extinction models for cancer stem cell therapy *Math. Biosci.* **2011**, *234*, 132.
(16) Dey, M.; Ulasov, I. V.; Tyler, M. A.; Sonabend, A. M.; Lesniak, M. S. Cancer Stem Cells: The Final Frontier for Glioma Virotherapy *Stem Cell Rev. Rep.* **2011**, *7*, 119.
(17) Natarajan, K.; Xie, Y.; Baer, M. R.; Ross, D. D. Role of breast cancer resistance protein (BCRP/ABCG2) in cancer drug resistance *Biochem. Pharmacol.* **2012**, *83*, 1084.

(18) American Cance Society. Cancer Facts & Figures 2011 *ACS* **2011**.
(19) Guzman, M. L.; Rossi, R. M.; Karnischky, L.; Li, X. J.; Peterson, D. R.; Howard, D. S.; Jordan, C. T. The sesquiterpene lactone parthenolide induces apoptosis of human acute myelogenous leukemia stem and progenitor cells *Blood* **2005**, *105*, 4163.
(20) Jin, L.; Hope, K. J.; Zhai, Q.; Smadja-Joffe, F.; Dick, J. E. Targeting of CD44 eradicates human acute myeloid leukemic stem cells *Nat. Med.* **2006**, *12*, 1167.
(21) Chen, Q.; Du, L.; Wang, H. Y.; He, L. Y.; Zhang, J. Y.; Ni, B. Y.; Wang, X. H.; Jin, H. J.; Cahuzac, N.; Mehrpour, M.; Lu, Y. Y. CD44 is of Functional Importance for Colorectal Cancer Stem Cells *Clin. Cancer Res.* **2008**, *14*, 6751.
(22) Druker, B. J.; Talpaz, M.; Resta, D. J.; Peng, B.; Buchdunger, E.; Ford, J. M.; Lydon, N. B.; Kantarjian, H.; Capdeville, R.; Ohno-Jones, S.; Sawyers, C. L. Efficacy and safety of a specific inhibitor of the BCR-ABL tyrosine kinase in chronic myeloid leukemia. *New Engl. J. Med.* **2001**, *344*, 1031.
(23) Kantarjian, H.; Talpaz, M.; O'Brien, S. S.; Garcia-Manero, G.; Verstovsek, S.; Giles, F.; Rios, M. B.; Shan, J. Q.; Letvak, L.; Thomas, D.; Faderl, S.; Ferrajoli, A.; Cortes, J. High-dose imatinib mesylate therapy in newly diagnosed Philadelphia chromosome-positive chronic phase chronic myeloid leukemia *Blood* **2004**, *103*, 2873.
(24) Nicholson, E.; Holyoake, T. The Chronic Myeloid Leukemia Stem Cell *Clin. Lymphoma Myeloma* **2009**, *9*, S376.
(25) Graham, S. M.; Jorgensen, H. G.; Allan, E.; Pearson, C.; Alcorn, M. J.; Richmond, L.; Holyoake, T. L. Primitive, quiescent, Philadelphia-positive stem cells from patients with chronic myeloid leukemia are insensitive to STI571 in vitro *Blood* **2002**, *99*, 319.
(26) Zoeller, M. CD44: can a cancer-initiating cell profit from an abundantly expressed molecule? *Nat. Rev. Cancer* **2011**, *11*, 254.
(27) Garvalov, B. K.; Acker, T. Cancer stem cells: a new framework for the design of tumor therapies *J. Mol. Med-Jmm* **2011**, *89*, 95.
(28) Collins, A. T.; Berry, P. A.; Hyde, C.; Stower, M. J.; Maitland, N. J. Prospective Identification of Tumorigenic Prostate Cancer Stem Cells *Cancer Res.* **2005**, *65*, 10946.
(29) Clayton, S.; Mousa, S. A. Therapeutics formulated to target cancer stem cells: Is it in our future? *Cancer Cell Int.* **2011**, *11*.
(30) Klonisch, T.; Wiechec, E.; Hombach-Klonisch, S.; Ande, S. R.; Wesselborg, S.; Schulze-Osthoff, K.; Los, M. Cancer stem cell markers in common cancers – therapeutic implications *Trends Mol. Med.* **2008**, *14*, 450.
(31) Liu, H.-G.; Chen, C.; Yang, H.; Pan, Y.-F.; Zhang, X.-H. Cancer stem cell subsets and their relationships *J. Transl. Med.* **2011**, *9*.
(32) Visvader, J. E.; Lindeman, G. J. Cancer stem cells in solid tumours: accumulating evidence and unresolved questions *Nat. Rev. Cancer* **2008**, *8*, 755.
(33) Gilbert, C. A.; Ross, A. H. Cancer Stem Cells: Cell Culture, Markers, and Targets for New Therapies *J. Cell Biochem.* **2009**, *108*, 1031.

(34) Alison, M. R.; Lim, S. M. L.; Nicholson, L. J. Cancer stem cells: problems for therapy? *J. Pathol.* **2011**, *223*, 147.
(35) Jordan, C. T. Cancer sten cell biology: from leukemia to solid tumors *Curr. Opin. Cell Biol.* **2004**, *16*, 708.
(36) Jemal, A.; Bray, F.; Center, M. M.; Ferlay, J.; Ward, E.; Forman, D. Global Cancer Statistics *CA-A Cancer Journal for Clinicians* **2011**, *61*, 69.
(37) Siegel, R.; Ward, E.; Brawley, O.; Jemal, A. Cancer statistics, 2011: the impact of eliminating socioeconomic and racial disparities on premature cancer deaths *CA Cancer J Clin* **2011**, *61*, 212.
(38) Testa, U. Leukemia stem cells *Ann. Hematol.* **2011**, *90*, 245.
(39) Blair, A.; Hogge, D. E.; Ailles, L. E.; Lansdorp, P. M.; Sutherland, H. J. Lack of expression of Thy-1 (CD90) on acute myeloid leukemia cells with long-term proliferative ability in vitro and in vivo *Blood* **1997**, *89*, 3104.
(40) Blair, A.; Hogge, D. E.; Sutherland, H. J. Most acute myeloid leukemia progenitor cells with long-term proliferative ability in vitro and in vivo have the phenotype CD34(+)/CD71(-)/HLA-DR *Blood* **1998**, *92*, 4325.
(41) Blair, A.; Sutherland, H. J. Primitive acute myeloid leukemia cells with long-term proliferative ability in vitro and in vivo lack surface expression of c-kit (CD 117) *Exp. Hematol.* **2000**, *28*, 660.
(42) Jordan, C. T.; Upchurch, D.; Szilvassy, S. J.; Guzman, M. L.; Howard, D. S.; Pettigrew, A. L.; Meyerrose, T.; Rossi, R.; Grimes, B.; Rizzieri, D. A.; Luger, S. M.; Phillips, G. L. The interleukin-3 receptor alpha chain is a unique marker for human acute myelogenous leukemia stem cells *Leukemia* **2000**, *14*, 1777.
(43) Florian, S.; Sonneck, K.; Hauswirth, A. W.; Krauth, M. T.; Schernthaner, G. H.; Sperr, W. R.; Valent, P. Detection of molecular targets on the surface of CD34+/CD38-stem cells in various myeloid malignancies *Leukemia Lymphoma* **2006**, *47*, 207.
(44) Dinndorf, P. A.; Andrews, R. G.; Benjamin, D.; Ridgway, D.; Wolff, L.; Bernstein, I. D. Expression of normal myeloid-associated antigens by acute leukemia cells *Blood* **1986**, *67*, 1048.
(45) Hauswirth, A. W.; Florian, S.; Printz, D.; Sotlar, K.; Krauth, M. T.; Fritsch, G.; Schernthaner, G. H.; Wacheck, V.; Selzer, E.; Sperr, W. R.; Valent, P. Expression of the target receptor CD33 in CD34(+)/CD38(-)/CD123(+) AML stem cells *European Journal of Clinical Investigation* **2007**, *37*, 73.
(46) de Figueiredo-Pontes, L. L.; Pintao, M.-C. T.; Oliveira, L. C. O.; Dalmazzo, L. F. F.; Jacomo, R. H.; Garcia, A. B.; Falcao, R. P.; Rego, E. M. Determination of P-glycoprotein, MDR-related protein 1, breast cancer resistance protein, and lung-resistance protein expression in leukemic stem cells of acute myeloid leukemia *Cytom. Part B-Clin. Cy.* **2008**, *74B*, 163.
(47) van Rhenen, A.; van Dongen, G. A. M. S.; Kelder, A.; Rombouts, E. J.; Feller, N.; Moshaver, B.; Stigter-van Walsum, M.; Zweegman, S.; Ossenkoppele, G. J.; Schuurhuis, G. J. The novel AML stem cell-associated antigen CLL-1 aids in discrimination between normal and leukemic stem cells *Blood* **2007**, *110*, 2659.

(48) Hosen, N.; Park, C. Y.; Tatsumi, N.; Oji, Y.; Sugiyama, H.; Gramatzki, M.; Krensky, A. M.; Weissman, I. L. CD96 is a leukemic stem cell-specific marker in human acute myeloid leukemia *Proc. Natl. Acad. Sci. USA.* **2007**, *104*, 11008.
(49) Bendall, L. J.; Bradstock, K. F.; Gottlieb, D. J. Expression of CD44 variant exons in acute myeloid leukemia is more common and more complex than that observed in normal blood, bone marrow or CD34(+) cells *Leukemia* **2000**, *14*, 1239.
(50) Saito, Y.; Kitamura, H.; Hijikata, A.; Tomizawa-Murasawa, M.; Tanaka, S.; Takagi, S.; Uchida, N.; Suzuki, N.; Sone, A.; Najima, Y.; Ozawa, H.; Wake, A.; Taniguchi, S.; Shultz, L. D.; Ohara, O.; Ishikawa, F. Identification of Therapeutic Targets for Quiescent, Chemotherapy-Resistant Human Leukemia Stem Cells *Sci. Transl. Med.* **2010**, *2*.
(51) Majeti, R.; Chao, M. P.; Alizadeh, A. A.; Pang, W. W.; Jaiswal, S.; Gibbs, K. D., Jr.; van Rooijen, N.; Weissman, I. L. CD47 Is an Adverse Prognostic Factor and Therapeutic Antibody Target on Human Acute Myeloid Leukemia Stem Cells *Cell* **2009**, *138*, 286.
(52) Quijano, C. A.; Moore, D.; Arthur, D.; Feusner, J.; Winter, S. S.; Pallavicini, M. G. Cytogenetically aberrant cells are present in the CD34(+)CD33(-)38(-)19(-) marrow compartment in children with acute lymphoblastic leukemia *Leukemia* **1997**, *11*, 1508.
(53) Cobaleda, C.; Gutierrez-Cianca, N.; Perez-Losada, J.; Flores, T.; Garcia-Sanz, R.; Gonzalez, M.; Sanchez-Garcia, I. A primitive hematopoietic cell is the target for the leukemic transformation in human Philadelphia-positive acute lymphoblastic leukemia *Blood* **2000**, *95*, 1007.
(54) Advani, A. S.; Pendergast, A. M. Bcr-Abl variants: biological and clinical aspects *Leukemia Res.* **2002**, *26*, 713.
(55) Faderl, S.; Garcia-Manero, G.; Thomas, D. A.; Kantarjian, H. M. Philadelphia chromosome-positive acute lymphoblastic leukemia– current concepts and future perspectives *Rev. Clin. Exp. Hematol.* **2002**, *6*, 142.
(56) Castor, A.; Nilsson, L.; Astrand-Grundstrom, I.; Buitenhuis, M.; Ramirez, C.; Anderson, K.; Strombeck, B.; Garwicz, S.; Bekassy, A. N.; Schmiegelow, K.; Lausen, B.; Hokland, P.; Lehmann, S.; Juliusson, G.; Johansson, B.; Jacobsen, S. E. W. Distinct patterns of hematopoietic stem cell involvement in acute lymphoblastic leukemia *Nat. Med.* **2005**, *11*, 630.
(57) Yeoh, E. J.; Ross, M. E.; Shurtleff, S. A.; Williams, W. K.; Patel, D.; Mahfouz, R.; Behm, F. G.; Raimondi, S. C.; Relling, M. V.; Patel, A.; Cheng, C.; Campana, D.; Wilkins, D.; Zhou, X. D.; Li, J. Y.; Liu, H. Q.; Pui, C. H.; Evans, W. E.; Naeve, C.; Wong, L. S.; Downing, J. R. Classification, subtype discovery, and prediction of outcome in pediatric acute lymphoblastic leukemia by gene expression profiling *Cancer Cell* **2002**, *1*, 133.
(58) Cox, C. V.; Evely, R. S.; Oakhill, A.; Pamphilon, D. H.; Goulden, N. J.; Blair, A. Characterization of acute lymphoblastic leukemia progenitor cells *Blood* **2004**, *104*, 2919.

(59) Cox, C. V.; Martin, H. M.; Kearns, P. R.; Virgo, P.; Evely, R. S.; Blair, A. Characterization of a progenitor cell population in childhood T-cell acute lymphoblastic leukemia *Blood* **2007**, *109*, 674.
(60) Cox, C. V.; Diamanti, P.; Evely, R. S.; Kearns, P. R.; Blair, A. Expression of CD133 on leukemia-initiating cells in childhood ALL *Blood* **2009**, *113*, 3287.
(61) Nishida, H.; Yamazaki, H.; Yamada, T.; Iwata, S.; Dang, N. H.; Inukai, T.; Sugita, K.; Ikeda, Y.; Morimoto, C. CD9 correlates with cancer stem cell potentials in human B-acute lymphoblastic leukemia cells *Biochem. Bioph. Res. Co.* **2009**, *382*, 57.
(62) Yamazaki, H.; Nishida, H.; Iwata, S.; Dang, N. H.; Morimoto, C. CD90 and CD110 correlate with cancer stem cell potentials in human T-acute lymphoblastic leukemia cells *Biochem. Bioph. Res. Co.* **2009**, *383*, 172.
(63) Holyoake, T.; Jiang, X. Y.; Eaves, C.; Eaves, A. Isolation of a highly quiescent subpopulation of primitive leukemic cells in chronic myeloid leukemia *Blood* **1999**, *94*, 2056.
(64) DeSantis, C.; Siegel, R.; Bandi, P.; Jemal, A. Breast cancer statistics, 2011 *CA Cancer J Clin* **2011**, *61*, 409.
(65) Takahashi, R. T., Fumitaka; Fujiwara,Tomohiro; Ono, Makiko and Ochiya, Takahiro Cancer stem cells in breast cancer *Cancers* **2011**, *3*, 1311.
(66) Al-Hajj, M.; Wicha, M. S.; Benito-Hernandez, A.; Morrison, S. J.; Clarke, M. F. Prospective identification of tumorigenic breast cancer cells *Proc. Natl. Acad. Sci. USA.* **2003**, *100*, 3983.
(67) Phillips, T. M.; McBride, W. H.; Pajonk, F. The response of CD24(-/low)/CD44(+) breast cancer-initiating cells to radiation *J. Natl. Cancer I.* **2006**, *98*, 1777.
(68) Buess, M.; Rajski, M.; Vogel-Durrer, B. M. L.; Herrmann, R.; Rochlitz, C. Tumor-Endothelial Interaction Links the CD44(+)/CD24(-) Phenotype with Poor Prognosis in Early-Stage Breast Cancer *Neoplasia* **2009**, *11*, 987.
(69) Sheridan, C.; Kishimoto, H.; Fuchs, R. K.; Mehrotra, S.; Bhat-Nakshatri, P.; Turner, C. H.; Goulet, R.; Badve, S.; Nakshatri, H. CD44(+)/CD24(-) breast cancer cells exhibit enhanced invasive properties: an early step necessary for metastasis *Breast Cancer Res.* **2006**, *8*.
(70) Donnelly, D. S.; Zelterman, D.; Sharkis, S.; Krause, D. S. Functional activity of murine CD34(+) and CD34(-) hematopoietic stem cell populations *Exp. Hematol.* **1999**, *27*, 788.
(71) Neumeister, V.; Agarwal, S.; Bordeaux, J.; Camp, R. L.; Rimm, D. L. In Situ Identification of Putative Cancer Stem Cells by Multiplexing ALDH1, CD44, and Cytokeratin Identifies Breast Cancer Patients with Poor Prognosis *Am. J. Pathol.* **2010**, *176*, 2131.
(72) Cho, R. W.; Wang, X.; Diehn, M.; Shedden, K.; Chen, G. Y.; Sherlock, G.; Gurney, A.; Lewicki, J.; Clarke, M. F. Isolation and molecular characterization of cancer stem cells in MMTV-Wnt-1 murine breast tumors *Stem Cells* **2008**, *26*, 364.

(73) Wright, M. H.; Calcagno, A. M.; Salcido, C. D.; Carlson, M. D.; Ambudkar, S. V.; Varticovski, L. Brca1 breast tumors contain distinct CD44(+)/CD24(-) and CD133(+) cells with cancer stem cell characteristics *Breast Cancer Res.* **2008**, *10*.
(74) Zhao, P.; Lu, Y.; Jiang, X.; Li, X. Clinicopathological significance and prognostic value of CD133 expression in triple-negative breast carcinoma *Cancer Sci.* **2011**, *102*, 1107.
(75) Liu, Q.; Li, J.-g.; Zheng, X.-y.; Jin, F.; Dong, H.-t. Expression of CD133, PAX2, ESA, and GPR30 in invasive ductal breast carcinomas *Chinese Med. J-Peking* **2009**, *122*, 2763.
(76) Lin, W.-M.; Karsten, U.; Goletz, S.; Cheng, R.-C.; Cao, Y. Co-expression of CD173 (H2) and CD174 (Lewis Y) with CD44 suggests that fucosylated histo-blood group antigens are markers of breast cancer-initiating cells *Vichows Arch.* **2010**, *456*, 403.
(77) Lin, W.-M.; Karsten, U.; Goletz, S.; Cheng, R.-C.; Cao, Y. Expression of CD176 (Thomsen-Friedenreich antigen) on lung, breast and liver cancer-initiating cells *Int. J. Exp. Pathol.* **2011**, *92*, 97.
(78) Vassilopoulos, A.; Wang, R.-H.; Petrovas, C.; Ambrozak, D.; Koup, R.; Deng, C.-X. Identification and characterization of cancer initiating cells from BRCA1 related mammary tumors using markers for normal mammary stem cells *Int. J. Biol. Sci.* **2008**, *4*, 133.
(79) Shipitsin, M.; Campbell, L. L.; Argani, P.; Werernowicz, S.; Bloushtain-Qimron, N.; Yao, J.; Nikolskaya, T.; Serebryiskaya, T.; Beroukhim, R.; Hu, M.; Halushka, M. K.; Sukumar, S.; Parker, L. M.; Anderson, K. S.; Harris, L. N.; Garber, J. E.; Richardson, A. L.; Schnitt, S. J.; Nikolsky, Y.; Gelman, R. S.; Polyak, K. Molecular definition of breast tumor heterogeneity *Cancer Cell* **2007**, *11*, 259.
(80) Dalerba, P.; Dylla, S. J.; Park, I.-K.; Liu, R.; Wang, X.; Cho, R. W.; Hoey, T.; Gurney, A.; Huang, E. H.; Simeone, D. M.; Shelton, A. A.; Parmiani, G.; Castelli, C.; Clarke, M. F. Phenotypic characterization of human colorectal cancer stem cells *Proc. Natl. Acad. Sci. USA.* **2007**, *104*, 10158.
(81) O'Brien, C. A.; Pollett, A.; Gallinger, S.; Dick, J. E. A human colon cancer cell capable of initiating tumour growth in immunodeficient mice *Nature* **2007**, *445*, 106.
(82) Ricci-Vitiani, L.; Lombardi, D. G.; Pilozzi, E.; Biffoni, M.; Todaro, M.; Peschle, C.; De Maria, R. Identification and expansion of human colon-cancer-initiating cells *Nature* **2007**, *445*, 111.
(83) Shmelkov, S. V.; Butler, J. M.; Hooper, A. T.; Hormigo, A.; Kushner, J.; Milde, T.; St Clair, R.; Baljevic, M.; White, I.; Jin, D. K.; Chadburn, A.; Murphy, A. J.; Valenzuela, D. M.; Gale, N. W.; Thurston, G.; Yancopoulos, G. D.; D'Angelica, M.; Kemeny, N.; Lyden, D.; Rafii, S. CD133 expression is not restricted to stem cells, and both CD133+ and CD133- metastatic colon cancer cells initiate tumors *J Clin Invest* **2008**, *118*, 2111.

(84) Du, L.; Wang, H.; He, L. CD44 is of functional importance for colorectal cancer stem cells. (vol 14, pg 6751, 2008) *Clin. Cancer Res.* **2008**, *14*, 7964.
(85) Horst, D.; Kriegl, L.; Engel, J.; Kirchner, T.; Jung, A. Prognostic Significance of the Cancer Stem Cell Markers CD133, CD44, and CD166 in Colorectal Cancer *Cancer Invest.* **2009**, *27*, 844.
(86) Lugli, A.; Iezzi, G.; Hostettler, I.; Muraro, M. G.; Mele, V.; Tornillo, L.; Carafa, V.; Spagnoli, G.; Terracciano, L.; Zlobec, I. Prognostic impact of the expression of putative cancer stem cell markers CD133, CD166, CD44s, EpCAM, and ALDH1 in colorectal cancer *Brit. J. Cancer* **2010**, *103*, 382.
(87) Vermeulen, L.; Todaro, M.; Mello, F. d. S.; Sprick, M. R.; Kemper, K.; Alea, M. P.; Richel, D. J.; Stassi, G.; Medema, J. P. Single-cell cloning of colon cancer stem cells reveals a multi-lineage differentiation capacity *Proc. Natl. Acad. Sci. USA.* **2008**, *105*, 13427.
(88) Liu, A. Y.; True, L. D.; LaTray, L.; Nelson, P. S.; Ellis, W. J.; Vessella, R. L.; Lange, P. H.; Hood, L.; vandenEngh, G. Cell-cell interaction in prostate gene regulation and cytodifferentiation *Proc. Natl. Acad. Sci. USA.* **1997**, *94*, 10705.
(89) Eguchi, S.; Kanematsu, T.; Arii, S.; Omata, M.; Kudo, M.; Sakamoto, M.; Takayasu, K.; Makuuchi, M.; Matsuyama, Y.; Monden, M.; Liver Canc Study Grp, J. Recurrence-free survival more than 10 years after liver resection for hepatocellular carcinoma *Brit. J. Surg.* **2011**, *98*, 552.
(90) Ma, S.; Chan, K.-W.; Hu, L.; Lee, T. K.-W.; Wo, J. Y.-H.; Ng, I.-L.; Zheng, B.-J.; Guan, X.-Y. Identification and characterization of tumorigenic liver cancer stem/progenitor cells *Gasterenterol.* **2007**, *132*, 2542.
(91) Zhu, Z.; Hao, X.; Yan, M.; Yao, M.; Ge, C.; Gu, J.; Li, J. Cancer stem/progenitor cells are highly enriched in CD133(+)CD44(+) population in hepatocellular carcinoma *Int. J. Cancer* **2010**, *126*, 2067.
(92) Kimura, O.; Takahashi, T.; Ishii, N.; Inoue, Y.; Ueno, Y.; Kogure, T.; Fukushima, K.; Shiina, M.; Yamagiwa, Y.; Kondo, Y.; Inoue, J.; Kakazu, E.; Iwasaki, T.; Kawagishi, N.; Shimosegawa, T.; Sugamura, K. Characterization of the epithelial cell adhesion molecule (EpCAM) plus cell population in hepatocellular carcinoma cell lines *Cancer Sci.* **2010**, *101*, 2145.
(93) Yamashita, T.; Ji, J. F.; Budhu, A.; Forgues, M.; Yang, W.; Wang, H. Y.; Jia, H. L.; Ye, Q. H.; Qin, L. X.; Wauthier, E.; Reid, L. M.; Minato, H.; Honda, M.; Kaneko, S.; Tang, Z. Y.; Wang, X. W. EpCAM-Positive Hepatocellular Carcinoma Cells Are Tumor-Initiating Cells With Stem/Progenitor Cell Features *Gasterenterol.* **2009**, *136*, 1012.
(94) Haraguchi, N.; Ishii, H.; Mimori, K.; Tanaka, F.; Ohkuma, M.; Kim, H. M.; Akita, H.; Takiuchi, D.; Hatano, H.; Nagano, H.; Barnard, G. F.; Doki, Y.; Mori, M. CD13 is a therapeutic target in human liver cancer stem cells *J. Clin. Invest.* **2010**, *120*, 3326.
(95) Yang, Z. F.; Ho, D. W.; Ng, M. N.; Lau, C. K.; Yu, W. C.; Ngai, P.; Chu, P. W. K.; Lam, C. T.; Poon, R. T. P.; Fan, S. T. Significance of CD90(+) cancer stem cells in human liver cancer *Cancer Cell* **2008**, *13*, 153.

(96) Polakis, P. Wnt signaling and cancer *Gene. Dev.* **2000**, *14*, 1837.
(97) Yang, W.; Yan, H.-X.; Chen, L.; Liu, Q.; He, Y.-Q.; Yu, L.-X.; Zhang, S.-H.; Huang, D.-D.; Tang, L.; Kong, X.-N.; Chen, C.; Liu, S.-Q.; Wu, M.-C.; Wang, H.-Y. Wnt/beta-catenin signaling contributes to activation of normal and tumorigenic liver progenitor cells *Cancer Res.* **2008**, *68*, 4287.
(98) Jemal, A.; Siegel, R.; Ward, E.; Hao, Y.; Xu, J.; Murray, T.; Thun, M. J. Cancer statistics, 2008 *Ca-Cancer J. Clin.* **2008**, *58*, 71.
(99) Li, C.; Heidt, D. G.; Dalerba, P.; Burant, C. F.; Zhang, L.; Adsay, V.; Wicha, M.; Clarke, M. F.; Simeone, D. M. Identification of pancreatic cancer stem cells *Cancer Res.* **2007**, *67*, 1030.
(100) Hermann, P. C.; Huber, S. L.; Herrler, T.; Aicher, A.; Ellwart, J. W.; Guba, M.; Bruns, C. J.; Heeschen, C. Distinct populations of cancer stem cells determine tumor growth and metastatic activity in human pancreatic cancer *Cell Stem Cell* **2007**, *1*, 313.
(101) Jemal, A.; Siegel, R.; Xu, J.; Ward, E. Cancer Statistics, 2010 *Ca-Cancer J. Clin.* **2010**, *60*, 277.
(102) Fang, D.; Nguyen, T. K.; Leishear, K.; Finko, R.; Kulp, A. N.; Hotz, S.; Van Belle, P. A.; Xu, X. W.; Elder, D. E.; Herlyn, M. A tumorigenic subpopulation with stem cell properties in melanomas *Cancer Res.* **2005**, *65*, 9328.
(103) Monzani, E.; Facchetti, F.; Galmozzi, E.; Corsini, E.; Benetti, A.; Cavazzin, C.; Gritti, A.; Piccinini, A.; Porro, D.; Santinami, M.; Invernici, G.; Parati, E.; Alessandri, G.; La Porta, C. A. M. Melanoma contains CD133 and ABCG2 positive cells with enhanced tumourigenic potential *Eur. J. Cancer* **2007**, *43*, 935.
(104) Grichnik, J. M.; Burch, J. A.; Schulteis, R. D.; Shan, S.; Liu, J.; Darrow, T. L.; Vervaert, C. E.; Seigler, H. F. Melanoma, a tumor based on a mutant stem cell? *J. Invest. Dermatol.* **2006**, *126*, 142.
(105) Fusi, A.; Reichelt, U.; Busse, A.; Ochsenreither, S.; Rietz, A.; Maisel, M.; Keilholz, U. Expression of the Stem Cell Markers Nestin and CD133 on Circulating Melanoma Cells *J. Invest. Dermatol.* **2011**, *131*, 487.
(106) Schatton, T.; Frank, N. Y.; Frank, M. H. Identification and targeting of cancer stem cells *Bioessays* **2009**, *31*, 1038.
(107) Schatton, T.; Murphy, G. F.; Frank, N. Y.; Yamaura, K.; Waaga-Gasser, A. M.; Gasser, M.; Zhan, Q.; Jordan, S.; Duncan, L. M.; Weishaupt, C.; Fuhlbrigge, R. C.; Kupper, T. S.; Sayegh, M. H.; Frank, M. H. Identification of cells initiating human melanomas *Nature* **2008**, *451*, 345.
(108) Davis, F. G.; Kupelian, V.; Freels, S.; McCarthy, B.; Surawicz, T. Prevalence estimates for primary brain tumors in the United States by behavior and major histology groups *Neuro-Oncology* **2001**, *3*, 152.
(109) Khalatbari, M. R.; Hamidi, M.; Moharamzad, Y. Glioblastoma multiforme with very rapid growth and long-term survival in children: report of two cases and review of the literature *Child. Nerv. Syst.* **2012**, *28*, 9.

(110) Eyler, C. E.; Rich, J. N. Survival of the fittest: Cancer stem cells in therapeutic resistance and angiogenesis *J. Clin. Oncol.* **2008**, *26*, 2839.
(111) Binello, E.; Germano, I. M. Targeting glioma stem cells: A novel framework for brain tumors *Cancer Sci.* **2011**, *102*, 1958.
(112) Singh, S. K.; Clarke, I. D.; Terasaki, M.; Bonn, V. E.; Hawkins, C.; Squire, J.; Dirks, P. B. Identification of a cancer stem cell in human brain tumors *Cancer Res.* **2003**, *63*, 5821.
(113) Singh, S. K.; Hawkins, C.; Clarke, I. D.; Squire, J. A.; Bayani, J.; Hide, T.; Henkelman, R. M.; Cusimano, M. D.; Dirks, P. B. Identification of human brain tumour initiating cells *Nature* **2004**, *432*, 396.
(114) Tchoghandjian, A.; Baeza, N.; Colin, C.; Cayre, M.; Metellus, P.; Beclin, C.; Ouafik, L. H.; Figarella-Branger, D. A2B5 Cells from Human Glioblastoma have Cancer Stem Cell Properties *Brain Pathol.* **2010**, *20*, 211.
(115) Ogden, A. T.; Waziri, A. E.; Lochhead, R. A.; Fusco, D.; Lopez, K.; Ellis, J. A.; Kang, J.; Assanah, M.; McKhann, G. M.; Sisti, M. B.; McCormick, P. C.; Canoll, P.; Bruce, J. N. Identification of A2B5(+)CD133-tumor-initiating cells in adult human gliomas *Neurosurgery* **2008**, *62*, 505.
(116) Wang, J.; Sakariassen, P. O.; Tsinkalovsky, O.; Immervoll, H.; Boe, S. O.; Svendsen, A.; Prestegarden, L.; Rosland, G.; Thorsen, F.; Stuhr, L.; Molven, A.; Bjerkvig, R.; Enger, P. O. CD133 negative glioma cells form tumors in nude rats and give rise to CD133 positive cells *Int. J. Cancer* **2008**, *122*, 761.
(117) Bao, S.; Wu, Q.; Li, Z.; Sathornsumetee, S.; Wang, H.; McLendon, R. E.; Hjehneland, A. B.; Rich, J. N. Targeting cancer stem cells through L1CAM suppresses glioma growth *Cancer Res.* **2008**, *68*, 6043.
(118) Bao, S.; Wu, Q.; Sathornsumetee, S.; Hao, Y.; Li, Z.; Hjelmeland, A. B.; Shi, O.; McLendon, R. E.; Bigner, D. D.; Rich, J. N. Stem cell-like glioma cells promote tumor angiogenesis through vascular endothelial growth factor *Cancer Res.* **2006**, *66*, 7843.
(119) Son, M. J.; Woolard, K.; Nam, D.-H.; Lee, J.; Fine, H. A. SSEA-1 Is an Enrichment Marker for Tumor-Initiating Cells in Human Glioblastoma *Cell Stem Cell* **2009**, *4*, 440.
(120) Read, T.-A.; Fogarty, M. P.; Markant, S. L.; McLendon, R. E.; Wei, Z.; Ellison, D. W.; Febbo, P. G.; Wechsler-Reya, R. J. Identification of CD15 as a Marker for Tumor-Propagating Cells in a Mouse Model of Medulloblastoma *Cancer Cell* **2009**, *15*, 135.
(121) Dean, M.; Fojo, T.; Bates, S. Tumour stem cells and drug resistance *Nat. Rev. Cancer* **2005**, *5*, 275.
(122) Eramo, A.; Lotti, F.; Sette, G.; Pilozzi, E.; Biffoni, M.; Di Virgilio, A.; Conticello, C.; Ruco, L.; Peschle, C.; De Maria, R. Identification and expansion of the tumorigenic lung cancer stem cell population *Cell Death Differ* **2007**, *15*, 504.
(123) Dinney, C. P. N.; McConkey, D. J.; Millikan, R. E.; Wu, X. F.; Bar-Eli, M.; Adam, L.; Kamat, A. M.; Siefker-Radtke, A. O.; Tuziak, T.; Sabichi, A. L.;

Grossman, H. B.; Benedict, W. F.; Czerniak, B. Focus on bladder cancer *Cancer Cell* **2004**, *6*, 111.
(124) Su, Y.; Qiu, Q.; Zhang, X.; Jiang, Z.; Leng, Q.; Liu, Z.; Stass, S. A.; Jiang, F. Aldehyde Dehydrogenase 1 A1-Positive Cell Population Is Enriched in Tumor-Initiating Cells and Associated with Progression of Bladder Cancer *Cancer Epidem. Biomar.* **2010**, *19*, 327.
(125) Chan, K. S.; Espinosa, I.; Chao, M.; Wong, D.; Ailles, L.; Diehn, M.; Gill, H.; Presti, J.; Chang, H. Y.; van de Rijn, M.; Shortliffe, L.; Weissman, I. L. Identification, molecular characterization, clinical prognosis, and therapeutic targeting of human bladder tumor-initiating cells *Proc. Nat. Acad. Sci.* **2009**, *106*, 14016.
(126) Yang, Y. M.; Chang, J. W. Bladder cancer initiating cells (BCICs) are among EMA(-)CD44v6(+) subset: Novel methods for isolating undetermined cancer stem (initiating) cells *Cancer Invest.* **2008**, *26*, 725.
(127) Ning, Z. F.; Huang, Y. J.; Lin, T. X.; Zhou, Y. X.; Jiang, C.; Xu, K. W.; Huang, H.; Yin, X. B.; Huang, J. Subpopulations of Stem-like Cells in Side Population Cells from the Human Bladder Transitional Cell Cancer Cell Line T24 *J. Int. Med. Res.* **2009**, *37*, 621.
(128) Oates, J. E.; Grey, B. R.; Addla, S. K.; Samuel, J. D.; Hart, C. A.; Ramani, V. A. C.; Brown, M. D.; Clarke, N. W. Hoechst 33342 Side Population Identification Is a Conserved and Unified Mechanism in Urological Cancers *Stem Cells Dev.* **2009**, *18*, 1515.
(129) Bostwick, D. G. E., J. N. *Urological Surgical Pathology*; 2nd ed.; Mosby, 2007.
(130) Mulholland, D. J.; Xin, L.; Morim, A.; Lawson, D.; Witte, O.; Wu, H. Lin(-)Sca-1(+)CD49f(high) Stem/Progenitors Are Tumor-Initiating Cells in the Pten-Null Prostate Cancer Model *Cancer Res.* **2009**, *69*, 8555.
(131) Beltran, H.; Beer, T. M.; Carducci, M. A.; de Bono, J.; Gleave, M.; Hussain, M.; Kelly, W. K.; Saad, F.; Sternberg, C.; Tagawa, S. T.; Tannock, I. F. New Therapies for Castration-Resistant Prostate Cancer: Efficacy and Safety *Eur. Urol.* **2011**, *60*, 279.
(132) Patrawala, L.; Calhoun, T.; Schneider-Broussard, R.; Li, H.; Bhatia, B.; Tang, S.; Reilly, J. G.; Chandra, D.; Zhou, J.; Claypool, K.; Coghlan, L.; Tang, D. G. Highly purified CD44(+) prostate cancer cells from xenograft human tumors are enriched in tumorigenic and metastatic progenitor cells *Oncogene* **2006**, *25*, 1696.
(133) Patrawala, L.; Calhoun-Davis, T.; Schneider-Broussard, R.; Tang, D. G. Hierarchical organization of prostate cancer cells in xenograft tumors: The CD44(+)alpha 2 beta 1(+) cell population is enriched in tumor-initiating cells *Cancer Res.* **2007**, *67*, 6796.
(134) Suzuki, A.; Nakano, T.; Mak, T. W.; Sasaki, T. Portrait of PTEN: Messages from mutant mice *Cancer Sci.* **2008**, *99*, 209.
(135) Zhang, S.; Balch, C.; Chan, M. W.; Lai, H.-C.; Matei, D.; Schilder, J. M.; Yan, P. S.; Huang, T. H.-M.; Nephew, K. P. Identification and Characterization

of Ovarian Cancer-Initiating Cells from Primary Human Tumors *Cancer Res.* **2008**, *68*, 4311.
(136) Choi, Y. P.; Shim, H. S.; Gao, M.-Q.; Kang, S.; Cho, N. H. Molecular portraits of intratumoral heterogeneity in human ovarian cancer *Cancer Lett.* **2011**, *307*, 62.
(137) Ferrandina, G.; Bonanno, G.; Pierelli, L.; Perillo, A.; Procoli, A.; Mariotti, A.; Corallo, M.; Martinelli, E.; Rutella, S.; Paglia, A.; Zannoni, G.; Mancuso, S.; Scambia, G. Expression of CD133-1 and CD133-2 in ovarian cancer *Int. J. Gynecol. Cancer* **2008**, *18*, 506.
(138) Curley, M. D.; Therrien, V. A.; Cummings, C. L.; Sergent, P. A.; Koulouris, C. R.; Friel, A. M.; Roberts, D. J.; Seiden, M. V.; Scadden, D. T.; Rueda, B. R.; Foster, R. CD133 Expression Defines a Tumor Initiating Cell Population in Primary Human Ovarian Cancer *Stem Cells* **2009**, *27*, 2875.
(139) Gao, M. Q.; Choi, Y. P.; Kang, S.; Youn, J. H.; Cho, N. H. CD24+ cells from hierarchically organized ovarian cancer are enriched in cancer stem cells *Oncogene* **2010**, *29*, 2672.
(140) Wei, X.; Dombkowski, D.; Meirelles, K.; Pieretti-Vanmarcke, R.; Szotek, P. P.; Chang, H. L.; Preffer, F. I.; Mueller, P. R.; Teixeira, J.; MacLaughlin, D. T.; Donahoe, P. K. Mullerian inhibiting substance preferentially inhibits stem/progenitors in human ovarian cancer cell lines compared with chemotherapeutics *Proc. Natl. Acad. Sci. USA.* **2010**, *107*, 18874.
(141) Gupta, P. B.; Onder, T. T.; Jiang, G. Z.; Tao, K.; Kuperwasser, C.; Weinberg, R. A.; Lander, E. S. Identification of Selective Inhibitors of Cancer Stem Cells by High-Throughput Screening *Cell* **2009**, *138*, 645.
(142) Shmelkov, S. V.; St Clair, R.; Lyden, D.; Rafii, S. AC133/CD133/Prominin-1 *Int J Biochem Cell B* **2005**, *37*, 715.
(143) Griguer, C. E.; Oliva, C. R.; Gobin, E.; Marcorelles, P.; Benos, D. J.; Lancaster, J. R., Jr.; Gillespie, G. Y. CD133 Is a Marker of Bioenergetic Stress in Human Glioma *Plos One* **2008**, *3*.
(144) Weigmann, A.; Corbeil, D.; Hellwig, A.; Huttner, W. B. Prominin, a novel microvilli-specific polytopic membrane protein of the apical surface of epithelial cells, is targeted to plasmalemmal protrusions of non-epithelial cells *Proc. Natl. Acad. Sci. USA.* **1997**, *94*, 12425.
(145) Rappa, G.; Fodstad, O.; Lorico, A. The Stem Cell-Associated Antigen CD133 (Prominin-1) Is a Molecular Therapeutic Target for Metastatic Melanoma *Stem Cells* **2008**, *26*, 3008.
(146) Wu, Y. J.; Wu, P. Y. CD133 as a Marker for Cancer Stem Cells: Progresses and Concerns *Stem Cells Dev.* **2009**, *18*, 1127.
(147) Swaminathan, S. K.; Olin, M. R.; Forster, C. L.; Cruz, K. S. S.; Panyam, J.; Ohlfest, J. R. Identification of a novel monoclonal antibody recognizing CD133 *J. Immunol. Methods.* **2010**, *361*, 110.
(148) Bourseau-Guilmain, E.; Bejaud, J.; Griveau, A.; Lautram, N.; Hindre, F.; Weyland, M.; Benoit, J. P.; Garcion, E. Development and characterization of

immuno-nanocarriers targeting the cancer stem cell marker AC133 *Int. J. Pharm.* **2012**, *423*, 93.
(149) Seimetz, D.; Lindhofer, H.; Bokemeyer, C. Development and approval of the trifunctional antibody catumaxomab (anti-EpCAM x anti-CD3) as a targeted cancer immunotherapy *Cancer Treat. Rev.* **2010**, *36*, 458.
(150) Haas, C.; Krinner, E.; Brischwein, K.; Hoffmann, P.; Lutterbuese, R.; Schlereth, B.; Kufer, P.; Baeuerle, P. A. Mode of cytotoxic action of T cell-engaging BiTE antibody MT110 *Immunobiology* **2009**, *214*, 441.
(151) Hartung, G.; Hofheinz, R. D.; Dencausse, Y.; Sturm, J.; Kopp-Schneider, A.; Dietrich, G.; Fackler-Schwalbe, I.; Bornbusch, D.; Gonnermann, M.; Wojatschek, C.; Lindemann, W.; Eschenburg, H.; Jost, K.; Edler, L.; Hochhaus, A.; Queisser, W. Adjuvant therapy with edrecolomab versus observation in stage II colon cancer: A multicenter randomized phase III study *Onkologie* **2005**, *28*, 347.
(152) Naundorf, S.; Preithner, S.; Mayer, P.; Lippold, S.; Wolf, A.; Hanakam, F.; Fichtner, I.; Kufer, P.; Raum, T.; Riethmuller, G.; Baeuerle, P. A.; Dreier, T. In vitro and in vivo activity of MT201, a fully human monoclonal antibody for pancarcinoma treatment *Int. J. Cancer* **2002**, *100*, 101.
(153) Marangoni, E.; Lecomte, N.; Durand, L.; de Pinieux, G.; Decaudin, D.; Chomienne, C.; Smadja-Joffe, F.; Poupon, M. F. CD44 targeting reduces tumour growth and prevents post-chemotherapy relapse of human breast cancers xenografts *Brit. J. Cancer* **2009**, *100*, 918.
(154) Hamann, P. R.; Hinman, L. M.; Hollander, I.; Beyer, C. F.; Lindh, D.; Holcomb, R.; Hallett, W.; Tsou, H. R.; Upeslacis, J.; Shochat, D.; Mountain, A.; Flowers, D. A.; Bernstein, I. Gemtuzumab ozogamicin, a potent and selective anti-CD33 antibody-calicheamicin conjugate for treatment of acute myeloid leukemia *Bioconjugate chemistry* **2002**, *13*, 47.
(155) Hamann, P. R.; Hinman, L. M.; Beyer, C. F.; Lindh, D.; Upeslacis, J.; Flowers, D. A.; Bernstein, I. An anti-CD33 antibody-calicheamicin conjugate for treatment of acute myeloid leukemia. Choice of linker *Bioconjugate chemistry* **2002**, *13*, 40.
(156) Frank, M. H.; Schatton, T.; Murphy, G. F.; Frank, N. Y.; Yamaura, K.; Waaga-Gasser, A. M.; Gasser, M.; Zhan, Q.; Jordan, S.; Duncan, L. M.; Weishaupt, C.; Fuhlbrigge, R. C.; Kupper, T. S.; Sayegh, M. H. Identification of cells initiating human melanomas *Nature* **2008**, *451*, 345.
(157) Jin, L. Q.; Lee, E. M.; Ramshaw, H. S.; Busfield, S. J.; Peoppl, A. G.; Wilkinson, L.; Guthridge, M. A.; Thomas, D.; Barry, E. F.; Boyd, A.; Gearing, D. P.; Vairo, G.; Lopez, A. F.; Dick, J. E.; Lock, R. B. Monoclonal Antibody-Mediated Targeting of CD123, IL-3 Receptor alpha Chain, Eliminates Human Acute Myeloid Leukemic Stem Cells *Cell Stem Cell* **2009**, *5*, 31.
(158) Bidlingmaier, S.; Zhu, X.; Liu, B. The utility and limitations of glycosylated human CD133 epitopes in defining cancer stem cells *J. Mol. Med-Jmm* **2008**, *86*, 1025.

(159) Wang, C.-H.; Chiou, S.-H.; Chou, C.-P.; Chen, Y.-C.; Huang, Y.-J.; Peng, C.-A. Photothermolysis of glioblastoma stem-like cells targeted by carbon nanotubes conjugated with CD133 monoclonal antibody *Nanomedicine-Nanotechnology Biology and Medicine* **2011**, *7*, 69.
(160) van der Gun, B. T. F.; Melchers, L. J.; Ruiters, M. H. J.; de Leij, L. F. M. H.; McLaughlin, P. M. J.; Rots, M. G. EpCAM in carcinogenesis: the good, the bad or the ugly *Carcinogenesis* **2010**, *31*, 1913.
(161) Winter, M. J.; Nagelkerken, B.; Mertens, A. E. E.; Rees-Bakker, H. A. M.; Briaire-de Bruijn, I. H.; Litvinov, S. V. Expression of Ep-CAM shifts the state of cadherin-mediated adhesions from strong to weak *Exp. Cell Res.* **2003**, *285*, 50.
(162) Litvinov, S. V.; Velders, M. P.; Bakker, H. A. M.; Fleuren, G. J.; Warnaar, S. O. Ep-CAM - A human epithelial antigen is a homophilic cell-cell adhesion molecule *J. Cell Biol.* **1994**, *125*, 437.
(163) Ruf, P.; Gires, O.; Jager, M.; Fellinger, K.; Atz, J.; Lindhofer, H. Characterisation of the new EpCAM-specific antibody HO-3: implications for trifunctional antibody immunotherapy of cancer *Brit. J. Cancer* **2007**, *97*, 315.
(164) Chelius, D.; Ruf, P.; Gruber, P.; Ploscher, M.; Liedtke, R.; Gansberger, E.; Hess, J.; Wasiliu, M.; Lindhofer, H. Structural and functional characterization of the trifunctional antibody catumaxomab *Mabs-Austin* **2010**, *2*, 309.
(165) Lindhofer, H.; Schoberth, A.; Pelster, D.; Hess, J.; Herold, J.; Jager, M. Elimination of cancer stem cells (CD133+/EpCAM+) from malignant ascites by the trifunctional antibody catumaxomab: Results from a pivotal phase II/III study *J. Clin. Oncol.* **2009**, *27*.
(166) Jager, M.; Schoberth, A.; Ruf, P.; Hess, J.; Hennig, M.; Schmalfeldt, B.; Wimberger, P.; Strohlein, M.; Theissen, B.; Heiss, M. M.; Lindhofer, H. Immunomonitoring Results of a Phase II/III Study of Malignant Ascites Patients Treated with the Trifunctional Antibody Catumaxomab (Anti-EpCAM x Anti-CD3) *Cancer Res.* **2012**, *72*, 24.
(167) Brischwein, K.; Schlereth, B.; Guller, B.; Steiger, C.; Wolf, A.; Lutterbuese, R.; Offner, S.; Locher, M.; Urbig, T.; Raum, T.; Kleindienst, P.; Wimberger, P.; Kimmig, R.; Fichtner, I.; Kufer, P.; Hofmeister, R.; da Silva, A. J.; Baeuerle, P. A. MT110: A novel bispecific single-chain antibody construct with high efficacy in eradicating established tumors *Mol. Immunol.* **2006**, *43*, 1129.
(168) Baeuerle, P. A.; Kufer, P.; Bargou, R. BiTE: Teaching antibodies to engage T-cells for cancer therapy *Curr. Opin. Mol. Ther.* **2009**, *11*, 22.
(169) Amann, M.; Brischwein, K.; Lutterbuese, P.; Parr, L.; Petersen, L.; Lorenczewski, G.; Krinner, E.; Bruckmeier, S.; Lippold, S.; Kischel, R.; Lutterbuese, R.; Kufer, P.; Baeuerle, P. A.; Schlereth, B. Therapeutic window of MuS110, a single-chain antibody construct bispecific for murine EpCAM and murine CD3 *Cancer Res.* **2008**, *68*, 143.
(170) Herrmann, I.; Baeuerle, P. A.; Friedrich, M.; Murr, A.; Filusch, S.; Ruttinger, D.; Majdoub, M. W.; Sharma, S.; Kufer, P.; Raum, T.; Munz, M.

Highly Efficient Elimination of Colorectal Tumor-Initiating Cells by an EpCAM/CD3-Bispecific Antibody Engaging Human T Cells *Plos One* **2010**, *5*.
(171) Balzar, M.; Winter, M. J.; de Boer, C. J.; Litvinov, S. V. The biology of the 17-1A antigen (Ep-CAM) *J. Mol. Med-Jmm* **1999**, *77*, 699.
(172) Riethmuller, G.; Schneidergadicke, E.; Schlimok, G.; Schmiegel, W.; Raab, R.; Hoffken, K.; Gruber, R.; Pichlmaier, H.; Hirche, H.; Pichlmayr, R.; Buggisch, P.; Witte, J.; Eigler, F. W.; Facklerschwalbe, I.; Funke, I.; Schmidt, C. G.; Schreiber, H.; Schweiberer, L.; Eibleibesfeldt, B. Randomized Trial of Monoclonal-Antibody for Adjuvant Therapy of Resected Dukes-C Colorectal-Carcinoma *Lancet* **1994**, *343*, 1177.
(173) Braun, S.; Hepp, F.; Kentenich, C. R. M.; Janni, W.; Pantel, K.; Riethmuller, G.; Willgeroth, F.; Sommer, H. L. Monoclonal antibody therapy with Edrecolomab in breast cancer patients: Monitoring of elimination of disseminated cytokeratin-positive tumor cells in bone marrow *Clin. Cancer Res.* **1999**, *5*, 3999.
(174) Schmidt, M.; Ruttinger, D.; Sebastian, M.; Hanusch, C. A.; Marschner, N.; Baeuerle, P. A.; Wolf, A.; Goppel, G.; Oruzio, D.; Schlimok, G.; Steger, G. G.; Wolf, C.; Eiermann, W.; Lang, A.; Schuler, M. Phase IB study of the EpCAM antibody adecatumumab combined with docetaxel in patients with EpCAM-positive relapsed or refractory advanced-stage breast cancer *Ann. Oncol.* **2012**.
(175) Gallatin, W. M.; Weissman, I. L.; Butcher, E. C. A Cell-Surface Molecule Involved in Organ-Specific Homing of Lymphocytes *Nature* **1983**, *304*, 30.
(176) Aruffo, A.; Stamenkovic, I.; Melnick, M.; Underhill, C. B.; Seed, B. CD44 is the Principle Cell-Surface Receptor For Hyaluronate *Cell* **1990**, *61*, 1303.
(177) Stamenkovic, I.; Amiot, M.; Pesando, J. M.; Seed, B. A Lymphocyte Molecule Implicated in Lymph-Node Homing Is a Member of the Cartilage Link Protein Family *Cell* **1989**, *56*, 1057.
(178) Teriete, P.; Banerji, S.; Noble, M.; Blundell, C. D.; Wright, A. J.; Pickford, A. R.; Lowe, E.; Mahoney, D. J.; Tammi, M. I.; Kahmann, J. D.; Campbell, I. D.; Day, A. J.; Jackson, D. G. Structure of the regulatory hyaluronan binding domain in the inflammatory leukocyte homing receptor CD44 *Mol. Cell* **2004**, *13*, 483.
(179) Nagano, O.; Saya, H. Mechanism and biological significance of CD44 cleavage *Cancer Sci.* **2004**, *95*, 930.
(180) Vigetti, D.; Viola, M.; Karousou, E.; Rizzi, M.; Moretto, P.; Genasetti, A.; Clerici, M.; Hascall, V. C.; De Luca, G.; Passi, A. Hyaluronan-CD44-ERK1/2 regulate human aortic smooth muscle cell motility during aging *J. Biol. Chem.* **2008**, *283*, 4448.
(181) Cheng, C. H.; Sharp, P. A. Regulation of CD44 alternative splicing by SRm160 and its potential role in tumor cell invasion *Mol. Cell. Biol.* **2006**, *26*, 362.

(182) Peach, R. J.; Hollenbaugh, D.; Stamenkovic, I.; Aruffo, A. Identification of Hyaluronic-Acid Binding-Sites in the Extracellular Domain of Cd44 *J. Cell Biol.* **1993**, *122*, 257.
(183) Ishii, S.; Ford, R.; Thomas, P.; Nachman, A.; Steele, G.; Jessup, J. M. Cd44 Participates in the Adhesion of Human Colorectal-Carcinoma Cells to Laminin and Type-Iv Collagen *Surg. Oncol.* **1993**, *2*, 255.
(184) Jalkanen, S.; Jalkanen, M. Lymphocyte Cd44 Binds the Cooh-Terminal Heparin-Binding Domain of Fibronectin *J. Cell Biol.* **1992**, *116*, 817.
(185) Konstantopoulos, K.; Thomas, S. N. Cancer Cells in Transit: The Vascular Interactions of Tumor Cells *Ann. Rev. Biomed. Eng.* **2009**, *11*, 177.
(186) Toyamasorimachi, N.; Miyasaka, M. A Novel Ligand for Cd44 Is Sulfated Proteoglycan *Int. Immunol.* **1994**, *6*, 655.
(187) Liu, D. C.; Sy, M. S. Phorbol myristate acetate stimulates the dimerization of CD44 involving a cysteine in the transmembrane domain *J. Immunol.* **1997**, *159*, 2702.
(188) Oliferenko, S.; Paiha, K.; Harder, T.; Gerke, V.; Schwarzler, C.; Schwarz, H.; Beug, H.; Gunthert, U.; Huber, L. A. Analysis of CD44-containing lipid rafts: Recruitment of annexin II and stabilization by the actin cytoskeleton *J. Cell Biol.* **1999**, *146*, 843.
(189) Fehon, R. G.; McClatchey, A. I.; Bretscher, A. Organizing the cell cortex: the role of ERM proteins *Nat. Rev. Mol. Cell Bio.* **2010**, *11*, 276.
(190) Siegelman, M. H.; Stanescu, D.; Estess, P. The CD44-initiated pathway of T-cell extravasation uses VLA-4 but not LFA-1 for firm adhesion *J. Clin. Invest.* **2000**, *105*, 683.
(191) Williams, D. A.; Cancelas, J. A. Leukaemia - Niche retreats for stem cells *Nature* **2006**, *444*, 827.
(192) Yang, J.; Weinberg, R. A. Epithelial-mesenchymal transition: At the crossroads of development and tumor metastasis *Dev. Cell* **2008**, *14*, 818.
(193) Toole, B. P. Hyaluronan: From extracellular glue to pericellular cue *Nat. Rev. Cancer* **2004**, *4*, 528.
(194) Lobo, N. A.; Shimono, Y.; Qian, D.; Clarke, M. F. The biology of cancer stem cells *Annu. Rev. Cell Dev. Bi.* **2007**, *23*, 675.
(195) Tallman, M. S. New strategies for the treatment of acute myeloid leukemia including antibodies and other novel agents *Hematology Am Soc Hematol Educ Program* **2005**, 143.
(196) Wilson, A.; Trumpp, A. Bone-marrow haematopoietic-stem-cell niches *Nat. Rev. Immunol.* **2006**, *6*, 93.
(197) Lapidot, T.; Dar, A.; Kollet, O. How do stem cells find their way home? *Blood* **2005**, *106*, 1901.
(198) Ulyanova, T.; Blasioli, J.; Woodford-Thomas, T. A.; Thomas, M. L. The sialoadhesin CD33 is a myeloid-specific inhibitory receptor *Eur. J. Immunol.* **1999**, *29*, 3440.
(199) Taylor, V. C.; Buckley, C. D.; Douglas, M.; Cody, A. J.; Simmons, D. L.; Freeman, S. D. The myeloid-specific sialic acid-binding receptor, CD33,

associates with the protein-tyrosine phosphatases, SHP-1 and SHP-2 *J. Biol. Chem.* **1999**, *274*, 11505.
(200) Vitale, C.; Romagnani, C.; Puccetti, A.; Olive, D.; Costello, R.; Chiossone, L.; Pitto, A.; Bacigalupo, A.; Moretta, L.; Mingari, M. C. Surface expression and function of p75/AIRM-1 or CD33 in acute myeloid leukemias: Engagement of CD33 induces apoptosis of leukemic cells *Proc. Natl. Acad. Sci. USA.* **2001**, *98*, 5764.
(201) Schwemmlein, M.; Peipp, M.; Barbin, K.; Saul, D.; Stockmeyer, B.; Repp, R.; Birkmann, J.; Oduncu, F.; Emmerich, B.; Fey, G. H. A CD33-specific single-chain immunotoxin mediates potent apoptosis of cultured human myeloid leukaemia cells *Br J Haematol* **2006**, *133*, 141.
(202) Damle, N. K.; Frost, P. Antibody-targeted chemotherapy with immunoconjugates of calicheamicin *Curr Opin Pharmacol* **2003**, *3*, 386.
(203) Linenberger, M. L. CD33-directed therapy with gemtuzumab ozogamicin in acute myeloid leukemia: progress in understanding cytotoxicity and potential mechanisms of drug resistance *Leukemia* **2005**, *19*, 176.
(204) http://www.fda.gov/Safety/MedWatch/SafetyInformation/SafetyAlertsforHumanMedicalProducts/ucm216458.htm.
(205) Walter, R. B.; Appelbaum, F. R.; Estey, E. H.; Bernstein, I. D. Acute myeloid leukemia stem cells and CD33-targeted immunotherapy *Blood* **2012**.
(206) Furness, S. G. B.; McNagny, K. Beyond mere markers - Functions for CD34 family of sialomucins in hematopoiesis *Immunol. Res.* **2006**, *34*, 13.
(207) Civin, C. I.; Strauss, L. C.; Brovall, C.; Fackler, M. J.; Schwartz, J. F.; Shaper, J. H. Antigenic Analysis of Hematopoiesis .3. A Hematopoietic Progenitor-Cell Surface-Antigen Defined by a Monoclonal-Antibody Raised against Kg-1a Cells *J. Immunol.* **1984**, *133*, 157.
(208) Berenson, R. J.; Andrews, R. G.; Bensinger, W. I.; Kalamasz, D.; Knitter, G.; Buckner, C. D.; Bernstein, I. D. Antigen Cd34+ Marrow-Cells Engraft Lethally Irradiated Baboons *J. Clin. Invest.* **1988**, *81*, 951.
(209) Nielsen, J. S.; McNagny, K. M. Novel functions of the CD34 family *J. Cell Sci.* **2008**, *121*, 3683.
(210) Krause, D. S.; Ito, T.; Fackler, M. J.; Smith, O. M.; Collector, M. I.; Sharkis, S. J.; May, W. S. Characterization of Murine Cd34, a Marker for Hematopoietic Progenitor and Stem-Cells *Blood* **1994**, *84*, 691.
(211) Healy, L.; May, G.; Gale, K.; Grosveld, F.; Greaves, M.; Enver, T. The stem cell antigen CD34 functions as a regulator of hemopoietic cell adhesion *Proc. Natl. Acad. Sci. USA.* **1995**, *92*, 12240.
(212) Baumhueter, S.; Singer, M. S.; Henzel, W.; Hemmerich, S.; Renz, M.; Rosen, S. D.; Lasky, L. A. Binding of L-Selectin to the Vascular Sialomucin Cd34 *Science* **1993**, *262*, 436.
(213) Krause, D. S.; Fackler, M. J.; Civin, C. I.; May, W. S. CD34: Structure, biology, and clinical utility *Blood* **1996**, *87*, 1.

(214) Tan, P. C.; Furness, S. G. B.; Merkens, H.; Lin, S. J.; McCoy, M. L.; Roskelley, C. D.; Kast, J.; McNagny, K. M. Na+/H+ exchanger regulatory factor-1 is a hematopoietic ligand for a subset of the CD34 family of stem cell surface proteins *Stem Cells* **2006**, *24*, 1150.
(215) Fackler, M. J.; Krause, D. S.; Smith, O. M.; Civin, C. I.; May, W. S. Full-Length but Not Truncated Cd34 Inhibits Hematopoietic-Cell Differentiation of M1 Cells *Blood* **1995**, *85*, 3040.
(216) Gangenahalli, G. U.; Singh, V. K.; Verma, Y. K.; Gupta, P.; Sharma, R. K.; Chandra, R.; Luthra, P. M. Hematopoietic stem cell antigen CD34: Role in adhesion or homing *Stem Cells Dev.* **2006**, *15*, 305.
(217) Kawanobe, T.; Kogure, S.; Nakamura, S.; Sato, M.; Katayama, K.; Mitsuhashi, J.; Noguchi, K.; Sugimoto, Y. Expression of human ABCB5 confers resistance to taxanes and anthracyclines *Biochem. Bioph. Res. Co.* **2012**, *418*, 736.
(218) Frank, N. Y.; Margaryan, A.; Huang, Y.; Schatton, T.; Waaga-Gasser, A. M.; Gasser, M.; Sayegh, M. H.; Sadee, W.; Frank, M. H. ABCB5-mediated doxorubicin transport and chemoresistance in human malignant melanoma *Cancer Res.* **2005**, *65*, 4320.
(219) Wickstrom, M.; Larsson, R.; Nygren, P.; Gullbo, J. Aminopeptidase N (CD13) as a target for cancer chemotherapy *Cancer Sci.* **2011**, *102*, 501.
(220) Luan, Y. P.; Xu, W. F. The structure and main functions of aminopeptidase N *Curr. Med. Chem.* **2007**, *14*, 639.
(221) Umezawa, H.; Aoyagi, T.; Suda, H.; Hamada, M.; Takeuchi, T. Bestatin, an Inhibitor of Aminopeptidase-B, Produced by Actinomycetes *J. Antibiot.* **1976**, *29*, 97.
(222) Talmadge, J. E.; Lenz, B. F.; Pennington, R.; Long, C.; Phillips, H.; Schneider, M.; Tribble, H. Immunomodulatory and Therapeutic Properties of Bestatin in Mice *Cancer Res.* **1986**, *46*, 4505.
(223) Mathe, G. Bestatin, an Aminopeptidase Inhibitor with a Multi-Pharmacological Function *Biomed. Pharmacother.* **1991**, *45*, 49.
(224) Sekine, K.; Fujii, H.; Abe, F. Induction of apoptosis by bestatin (ubenimex) in human leukemic cell lines *Leukemia* **1999**, *13*, 729.
(225) Ezawa, K.; Minato, K.; Dobashi, K. Induction of apoptosis by ubenimex (Bestatin(R)) in human non-small-cell lung cancer cell lines *Biomed. Pharmacother.* **1996**, *50*, 283.
(226) Thunnissen, M. M. G. M.; Nordlund, P.; Haeggstrom, J. Z. Crystal structure of human leukotriene A(4) hydrolase, a bifunctional enzyme in inflammation *Nat. Struct. Biol.* **2001**, *8*, 131.
(227) Tholander, F.; Rudberg, P.; Thunnissen, M.; Haeggstrom, J. Z. Leukotriene A4 hydrolase, the gatekeeper of chemotactic leukotriene B4 biosynthesis *Prostag. Oth. Lipid M.* **2006**, *79*, 157.
(228) Fromm, J. R. Flow Cytometric Analysis of CD123 is Useful for Immunophenotyping Classical Hodgkin Lymphoma *Cytom. Part B-Clin. Cy.* **2011**, *80B*, 91.

(229) Lindberg, F. P.; Gresham, H. D.; Schwarz, E.; Brown, E. J. Molecular-Cloning of Integrin-Associated Protein - an Immunoglobulin Family Member with Multiple Membrane-Spanning Domains Implicated in Alpha-Nu-Beta-3-Dependent Ligand-Binding *J. Cell Biol.* **1993**, *123*, 485.
(230) Brown, E. J.; Frazier, W. A. Integrin-associated protein (CD47) and its ligands *Trends Cell Biol.* **2001**, *11*, 130.
(231) Hatherley, D.; Graham, S. C.; Turner, J.; Harlos, K.; Stuart, D. I.; Barclay, A. N. Paired receptor specificity explained by structures of signal regulatory proteins alone and complexed with CD47 *Mol. Cell* **2008**, *31*, 266.
(232) Majeti, R. Monoclonal antibody therapy directed against human acute myeloid leukemia stem cells *Oncogene* **2011**, *30*, 1009.
(233) Merfort, I. Perspectives on Sesquiterpene Lactones in Inflammation and Cancer *Curr. Drug Targets* **2011**, *12*, 1560.
(234) Neelakantan, S.; Nasim, S.; Guzman, M. L.; Jordan, C. T.; Crooks, P. A. Aminoparthenolides as novel anti-leukemic agents: Discovery of the NF-kappa B inhibitor, DMAPT (LC-1) *Bioorg. Med. Chem. Lett.* **2009**, *19*, 4346.
(235) Kwok, B. H. B.; Koh, B.; Ndubuisi, M. I.; Elofsson, M.; Crews, C. M. The anti-inflammatory natural product parthenolide from the medicinal herb Feverfew directly binds to and inhibits I kappa B kinase *Chem. Biol.* **2001**, *8*, 759.
(236) Picman, A. K. Biological activities of sesquiterpene lactones *Biochem. Syst. Ecol.* **1986**, *14*, 255.
(237) Ghantous, A.; Gali-Muhtasib, H.; Vuorela, H.; Saliba, N. A.; Darwiche, N. What made sesquiterpene lactones reach cancer clinical trials? *Drug Discov. Today* **2010**, *15*, 668.
(238) Knight, D. W. Feverfew: Chemistry and biological activity *Nat. Prod. Rep.* **1995**, *12*, 271.
(239) Soucek, M.; Herout, V.; Sorm, F. Terpenes. CXVIII. Constitution of parthenolide *Collect. Czech. Chem. Commun.* **1961**, *26*, 803.
(240) Han, C.; Barrios, F. J.; Riofski, M. V.; Colby, D. A. Semisynthetic Derivatives of Sesquiterpene Lactones by Palladium-Catalyzed Arylation of the α-Methylene-γ-lactone Substructure *J. Org. Chem.* **2009**, *74*, 7176.
(241) Anderson, K. N.; Bejcek, B. E. Parthenolide induces apoptosis in glioblastomas without affecting NF-kappa B *J. Pharmacol. Sci.* **2008**, *106*, 318.
(242) Nakshatri, H.; Rice, S. E.; Bhat-Nakshatri, P. Antitumor agent parthenolide reverses resistance of breast cancer cells to tumor necrosis factor-related apoptosis-inducing ligand through sustained activation of c-Jun N-terminal kinase *Oncogene* **2004**, *23*, 7330.
(243) Sweeney, C. J.; Mehrotra, S.; Sadaria, M. R.; Kumar, S.; Shortle, N. H.; Roman, Y.; Sheridan, C.; Campbell, R. A.; Murry, D. J.; Badve, S.; Nakshatri, H. The sesquiterpene lactone parthenolide in combination with docetaxel reduces metastasis and improves survival in a xenograft model of breast cancer *Mol. Cancer Ther.* **2005**, *4*, 1004.

(244) Steele, A. J.; Jones, D. T.; Ganeshaguru, K.; Duke, V. M.; Yogashangary, B. C.; North, J. M.; Lowdell, M. W.; Kottaridis, P. D.; Mehta, A. B.; Prentice, A. G.; Hoffbrand, A. V.; Wickremasinghe, R. G. The sesquiterpene lactone parthenolide induces selective apoptosis of B-chronic lymphocytic leukemia cells in vitro *Leukemia* **2006**, *20*, 1073.
(245) Hewamana, S.; Alghazal, S.; Lin, T. T.; Clement, M.; Jenkins, C.; Guzman, M. L.; Jordan, C. T.; Neelakantan, S.; Crooks, P. A.; Burnett, A. K.; Pratt, G.; Fegan, C.; Rowntree, C.; Brennan, P.; Pepper, C. The NF-κB subunit Rel A is associated with in vitro survival and clinical disease progression in chronic lymphocytic leukemia and represents a promising therapeutic target *Blood* **2008**, *111*, 4681.
(246) Guzman, M. L.; Rossi, R. M.; Karnischky, L.; Li, X.; Peterson, D. R.; Howard, D. S.; Jordan, C. T. The sesquiterpene lactone parthenolide induces apoptosis of human acute myelogenous leukemia stem and progenitor cells *Blood* **2005**, *105*, 4163.
(247) Ramachandran, P. V.; Pratihar, D.; Nair, H. N. G.; Walters, M.; Smith, S.; Yip-Schneider, M. T.; Wu, H. B.; Schmidt, C. M. Tailored alpha-methylene-gamma-butyrolactones and their effects on growth suppression in pancreatic carcinoma cells *Bioorg. Med. Chem. Lett.* **2010**, *20*, 6620.
(248) Sweeney, C.; Li, L.; Shanmugam, R.; Bhat-Nakshatri, P.; Jayaprakasan, V.; Baldridge, L. A.; Gardner, T.; Smith, M.; Nakshatri, H.; Cheng, L. Nuclear factor-kappa B is constitutively activated in prostate cancer in vitro and is overexpressed in prostatic intraepithelial neoplasia and adenocarcinoma of the prostate *Clin. Cancer Res.* **2004**, *10*, 5501.
(249) Shanmugam, R.; Jayaprakasan, V.; Gokmen-Polar, Y.; Kelich, S.; Miller, K. D.; Yip-Schneider, M.; Cheng, L.; Bhat-Nakshatri, P.; Sledge, G. W.; Nakshatri, H.; Zheng, Q. H.; Miller, M. A.; DeGrado, T.; Hutchins, G. D.; Sweeney, C. J. Restoring chemotherapy and hormone therapy sensitivity by parthenolide in a xenograft hormone refractory prostate cancer model *Prostate* **2006**, *66*, 1498.
(250) Fang, L.-J.; Shao, X.-T.; Wang, S.; Lu, G.-H.; Xu, T.; Zhou, J.-Y. Sesquiterpene lactone parthenolide markedly enhances sensitivity of human A549 cells to low-dose oxaliplatin via inhibition of NF-κB activation and induction of apoptosis *Planta Med.* **2010**, *76*, 258.
(251) Zhang, D.; Qiu, L.; Jin, X.; Guo, Z.; Guo, C. Nuclear Factor-κB Inhibition by Parthenolide Potentiates the Efficacy of Taxol in Non-Small Cell Lung Cancer In vitro and In vivo *Mol. Cancer Res.* **2009**, *7*, 1139.
(252) Jin, X.; Qiu, L.; Zhang, D.; Zhang, M.; Wang, Z.; Guo, Z.; Deng, C.; Guo, C. Chemosensitization in non-small cell lung cancer cells by IKK inhibitor occurs via NF-κB and mitochondrial cytochrome c cascade *J. Cell. Mol. Med.* **2009**, *13*, 4596.
(253) Suvannasankha, A.; Crean, C. D.; Shanmugam, R.; Farag, S. S.; Abonour, R.; Boswell, H. S.; Nakshatri, H. Antimyeloma effects of a sesquiterpene lactone parthenolide *Clin. Cancer Res.* **2008**, *14*, 1814.

(254) Lesiak, K.; Koprowska, K.; Zalesna, I.; Nejc, D.; Duchler, M.; Czyz, M. Parthenolide, a sesquiterpene lactone from the medical herb feverfew, shows anticancer activity against human melanoma cells in vitro *Melanoma Res.* **2010**, *20*, 21.
(255) Heon, S. K.; Ko, H.-M.; Kim, H.-A.; Choi, J.-H.; Jun, P. S.; Kim, K.-J.; Lee, H.-K.; Im, S.-Y. Platelet-activating factor induces up-regulation of antiapoptotic factors in a melanoma cell line through nuclear factor-kappaB activation *Cancer Res.* **2006**, *66*, 4681.
(256) Zhang, S.; Ong, C.-N.; Shen, H.-M. Critical roles of intracellular thiols and calcium in parthenolide-induced apoptosis in human colorectal cancer cells *Cancer Lett. (Amsterdam, Neth.)* **2004**, *208*, 143.
(257) Hehner, S. P.; Hofmann, T. G.; Droge, W.; Schmitz, M. L. The antiinflammatory sesquiterpene lactone parthenolide inhibits NF-kappa B by targeting the I kappa B kinase complex *J. Immunol.* **1999**, *163*, 5617.
(258) Garcia-Pineres, A. J.; Castro, V.; Mora, G.; Schmidt, T. J.; Strunck, E.; Pahl, H. L.; Merfort, I. Cysteine 38 in p65/NF-kappa B plays a crucial role in DNA binding inhibition by sesquiterpene lactones *J. Biol. Chem.* **2001**, *276*, 39713.
(259) Garcia-Pineres, A. J.; Lindenmeyer, M. T.; Merfort, I. Role of cysteine residues of p65/NF-kappa B on the inhibition by the sesquiterpene lactone parthenolide and-N-ethyl maleimide, and on its transactivating potential *Life Sci.* **2004**, *75*, 841.
(260) Guzman, M. L.; Neering, S. J.; Upchurch, D.; Grimes, B.; Howard, D. S.; Rizzieri, D. A.; Luger, S. M.; Jordan, C. T. Nuclear factor-kappa B is constitutively activated in primitive human acute myelogenous leukemia cells *Blood* **2001**, *98*, 2301.
(261) Curry, E. A.; Murry, D. J.; Yoder, C.; Fife, K.; Armstrong, V.; Nakshatri, H.; O'Connell, M.; Sweeney, C. J. Phase I dose escalation trial of feverfew with standardized doses of parthenolide in patients with cancer *Invest. New Drug* **2004**, *22*, 299.
(262) Lee, K. H.; Meck, R.; Piantado.C; Huang, E. S. Antitumor agents. 4. Cytotoxicity and in-vivo activity of helenalin esters and related derivatives *J. Med. Chem.* **1973**, *16*, 299.
(263) Schmidt, T.; Nour, A.; Khalid, S.; Kaiser, M.; Brun, R. Quantitative Structure – Antiprotozoal Activity Relationships of Sesquiterpene Lactones *Molecules* **2009**, *14*, 2062.
(264) Reddy, D. M.; Qazi, N. A.; Sawant, S. D.; Bandey, A. H.; Srinivas, J.; Shankar, M.; Singh, S. K.; Verma, M.; Chashoo, G.; Saxena, A.; Mondhe, D.; Saxena, A. K.; Sethi, V. K.; Taneja, S. C.; Qazi, G. N.; Sampath Kumar, H. M. Design and synthesis of spiro derivatives of parthenin as novel anti-cancer agents *Eur. J. Med. Chem.* **2011**, *46*, 3210.
(265) Kupchan, S. M.; Eakin, M. A.; Thomas, A. M. Tumor inhibitors. 69. Structure-cytotoxicity relations among the sesquiterpene lactones *J. Med. Chem.* **1971**, *14*, 1147.

(266) de Alvarenga, E. S.; Silva, S. A.; Barosa, L. C. A.; Demuner, A. J.; Parreira, A. G.; Ribeiro, R. I. M. A.; Marcussi, S.; Ferreira, J. M. S.; Resende, R. R.; Granjeiro, P. A.; Silva, J. A.; Soares, A. M.; Marangoni, S.; Da Silva, S. L. Synthesis and evaluation of sesquiterpene lactone inhibitors of phospholipase A2 from Bothrops jararacussu *Toxicon* **2011**, *57*, 100.
(267) Fernandes, M. B.; Scotti, M. T.; Ferreira, M. J. P.; Emerenciano, V. P. Use of self-organizing maps and molecular descriptors to predict the cytotoxic activity of sesquiterpene lactones *Eur. J. Med. Chem.* **2008**, *43*, 2197.
(268) Nasim, S.; Crooks, P. A. Antileukemic activity of aminoparthenolide analogs *Bioorg. Med. Chem. Lett.* **2008**, *18*, 3870.
(269) Guzman, M. L.; Rossi, R. M.; Neelakantan, S.; Li, X.; Corbett, C. A.; Hassane, D. C.; Becker, M. W.; Bennett, J. M.; Sullivan, E.; Lachowicz, J. L.; Vaughan, A.; Sweeney, C. J.; Matthews, W.; Carroll, M.; Liesveld, J. L.; Crooks, P. A.; Jordan, C. T. An orally bioavailable parthenolide analog selectively eradicates acute myelogenous leukemia stem and progenitor cells *Blood* **2007**, *110*, 4427.
(270) Lee, K.-H.; Huang, E.-S.; Piantadosi, C.; Pagano, J. S.; Geissman, T. A. Cytotoxicity of Sesquiterpene Lactones *Cancer Res.* **1971**, *31*, 1649.
(271) Hejchman, E.; Haugwitz, R. D.; Cushman, M. Synthesis and Cytotoxicity of Water-Soluble Ambrosin Prodrug Candidates *J. Med. Chem.* **1995**, *38*, 3407.
(272) Woods, J. R.; Mo, H.; Bieberich, A. A.; Alavanja, T.; Colby, D. A. Amino-derivatives of the sesquiterpene lactone class of natural products as prodrugs *MedChemComm* **2013**, *4*, 27.
(273) Srivastava, S. K.; Abraham, A.; Bhat, B.; Jaggi, M.; Singh, A. T.; Sanna, V. K.; Singh, G.; Agarwal, S. K.; Mukherjee, R.; Burman, A. C. Synthesis of 13-amino costunolide derivatives as anticancer agents *Bioorg. Med. Chem. Lett.* **2006**, *16*, 4195.
(274) Neukirch, H.; Kaneider, N. C.; Wiedermann, C. J.; Guerriero, A.; D'Ambrosio, M. Parthenolide and its photochemically synthesized 1(10)Z isomer: Chemical reactivity and structure-activity relationship studies in human leucocyte chemotaxis *Bioorg. Med. Chem.* **2003**, *11*, 1503.
(275) Hwang, D. R.; Chang, C. W.; Lien, T. W.; Chen, W. C.; Tan, U. K.; Hsu, J. T. A.; Hsieh, H. P. Synthesis and anti-viral activity of a series of sesquiterpene lactones and analogues in the subgenomic HCV replicon system *Bioorg. Med. Chem.* **2006**, *14*, 83.
(276) Dell'Agli, M.; Galli, G. V.; Bosisio, E.; D'Ambrosio, M. Inhibition of NF-kB and metalloproteinase-9 expression and secretion by parthenolide derivatives *Bioorg. Med. Chem. Lett.* **2009**, *19*, 1858.
(277) Macías, F. A.; Galindo, J. C. G.; Massanet, G. M. Potential allelopathic activity of several sesquiterpene lactone models *Phytochemistry* **1992**, *31*, 1969.
(278) Nasim, S.; Pei, S. S.; Hagen, F. K.; Jordan, C. T.; Crooks, P. A. Melampomagnolide B: A new antileukemic sesquiterpene *Bioorg. Med. Chem.* **2011**, *19*, 1515.

(279) Neukirch, H.; Guerriero, A.; D'Ambrosio, M. Transannular Cyclization in Cyclodecenes: The Case Study of Melampolides *Eur. J. Org. Chem.* **2003**, *2003*, 3969.
(280) Castanedaacosta, J.; Fischer, N. H.; Vargas, D. Biomimetic transformation of parthenolide *J. Nat. Prod.* **1993**, *56*, 90.
(281) Zhang, Q.; Lu, Y.; Ding, Y.; Zhai, J.; Ji, Q.; Ma, W.; Yang, M.; Fan, H.; Long, J.; Tong, Z.; Shi, Y.; Jia, Y.; Han, B.; Zhang, W.; Qiu, C.; Ma, X.; Li, Q.; Shi, Q.; Zhang, H.; Li, D.; Zhang, J.; Lin, J.; Li, L.-Y.; Gao, Y.; Chen, Y. Guaianolide Sesquiterpene Lactones, a Source To Discover Agents That Selectively Inhibit Acute Myelogenous Leukemia Stem and Progenitor Cells *J. Med. Chem.* **2012**, *55*, 8757.
(282) Govindachari, T. R.; Joshi, B. S.; Kamat, V. N. Structure of parthenolide *Tetrahedron* **1965**, *21*, 1509.
(283) Collu, F.; Bonsignore, L.; Casu, M.; Floris, C.; Gertsch, J.; Cottiglia, F. New cytotoxic saturated and unsaturated cyclohexanones from Anthemis maritima *Bioorg. Med. Chem. Lett.* **2008**, *18*, 1559.
(284) Zanotto-Filho, A.; Braganhol, E.; Schröder, R.; de Souza, L. H. T.; Dalmolin, R. J. S.; Pasquali, M. A. B.; Gelain, D. P.; Battastini, A. M. O.; Moreira, J. C. F. NFκB inhibitors induce cell death in glioblastomas *Biochem. Pharmacol.* **2011**, *81*, 412.
(285) Hsu, J.-L.; Pan, S.-L.; Ho, Y.-F.; Hwang, T.-L.; Kung, F.-L.; Guh, J.-H. Costunolide induces apoptosis through nuclear calcium2+ overload and DNA damage response in human prostate cancer *J Urol* **2011**, *185*, 1967.
(286) Kim, S. H.; Kang, S. N.; Kim, H. J.; Kim, T. S. Potentiation of 1,25-dihydroxyvitamin D3-induced differentiation of human promyelocytic leukemia cells into monocytes by costunolide, a germacranolide sesquiterpene lactone *Biochem. Pharmacol.* **2002**, *64*, 1233.
(287) Ogura, M.; Cordell, G. A.; Farnsworth, N. R. Anticancer sesquiterpene lactones of Michelia compressa (magnoliaceae) *Phytochemistry* **1978**, *17*, 957.
(288) Yip-Schneider, M. T.; Wu, H.; Njoku, V.; Ralstin, M.; Holcomb, B.; Crooks, P. A.; Neelakantan, S.; Sweeney, C. J.; Schmidt, C. M. Effect of Celecoxib and the Novel Anti-Cancer Agent, Dimethylamino-Parthenolide, in a Developmental Model of Pancreatic Cancer *Pancreas (Hagerstown, MD, U. S.)* **2008**, *37*, e45.
(289) Shanmugam, R.; Kusumanchi, P.; Appaiah, H.; Cheng, L.; Crooks, P.; Neelakantan, S.; Peat, T.; Klaunig, J.; Matthews, W.; Nakshatri, H.; Sweeney, C. J. A water soluble parthenolide analog suppresses in vivo tumor growth of two tobacco-associated cancers, lung and bladder cancer, by targeting NF-κB and generating reactive oxygen species *Int. J. Cancer* **2011**, *128*, 2481.
(290) Katz, E.; Willner, I. Integrated Nanoparticle–Biomolecule Hybrid Systems: Synthesis, Properties, and Applications *Angew. Chem. Int. Ed.* **2004**, *43*, 6042.
(291) Sperling, R. A.; Parak, W. J. Surface modification, functionalization and bioconjugation of colloidal inorganic nanoparticles *Philosophical Transactions*

of the Royal Society A: Mathematical, Physical and Engineering Sciences **2010**, *368*, 1333.
(292) Cai, W.; Gao, T.; Hong, H.; Sun, J. Applications of gold nanoparticles in cancer nanotechnology *Nanotechnol., Sci. Appl.* **2008**, *1*, 17.
(293) Gabizon, A. A. Stealth Liposomes and Tumor Targeting: One Step Further in the Quest for the Magic Bullet *Clin. Cancer Res.* **2001**, *7*, 223.
(294) Pang, Z.; Gao, H.; Yu, Y.; Chen, J.; Guo, L.; Ren, J.; Wen, Z.; Su, J.; Jiang, X. Brain delivery and cellular internalization mechanisms for transferrin conjugated biodegradable polymersomes *Int. J. Pharm.* **2011**, *415*, 284.
(295) Pissuwan, D.; Niidome, T.; Cortie, M. B. The forthcoming applications of gold nanoparticles in drug and gene delivery systems *J. Controlled Release* **2011**, *149*, 65.
(296) Sahoo, S. K.; Parveen, S.; Panda, J. J. The present and future of nanotechnology in human health care *Nanomedicine (N. Y., NY, U. S.)* **2007**, *3*, 20.
(297) Maeda, H.; Wu, J.; Sawa, T.; Matsumura, Y.; Hori, K. Tumor vascular permeability and the EPR effect in macromolecular therapeutics: a review *J. Control. Release* **2000**, *65*, 271.
(298) Chen, P. C.; Mwakwari, S. C.; Oyelere, A. K. Gold nanoparticles: from nanomedicine to nanosensing *Nanotechnol., Sci. Appl.* **2008**, *1*, 45.
(299) Verma, A.; Simard, J. M.; Worrall, J. W. E.; Rotello, V. M. Tunable Reactivation of Nanoparticle-Inhibited β-Galactosidase by Glutathione at Intracellular Concentrations *J. Am. Chem. Soc.* **2004**, *126*, 13987.
(300) Woodle, M. C.; Engbers, C. M.; Zalipsky, S. New Amphipatic Polymer-Lipid Conjugates Forming Long-Circulating Reticuloendothelial System-Evading Liposomes *Bioconjugate Chem.* **1994**, *5*, 493.
(301) Paciotti, G. F.; Kingston, D. G. I.; Tamarkin, L. Colloidal gold nanoparticles: a novel nanoparticle platform for developing multifunctional tumor-targeted drug delivery vectors *Drug Dev. Res.* **2006**, *67*, 47.
(302) Mishra, S.; Webster, P.; Davis, M. E. PEGylation significantly affects cellular uptake and intracellular trafficking of non-viral gene delivery particles *Eur. J. Cell. Biol.* **2004**, *83*, 97.
(303) Daniel, M.-C.; Astruc, D. Gold Nanoparticles: Assembly, Supramolecular Chemistry, Quantum-Size-Related Properties, and Applications toward Biology, Catalysis, and Nanotechnology *Chem. Rev.* **2004**, *104*, 293.
(304) Dykman, L.; Khlebtsov, N. Gold nanoparticles in biomedical applications: recent advances and perspectives *Chem. Soc. Rev.* **2012**, *41*, 2256.
(305) Alkilany, A. M.; Lohse, S. E.; Murphy, C. J. The Gold Standard: Gold Nanoparticle Libraries To Understand the Nano–Bio Interface *Acc. Chem. Res.* **2012**.
(306) Haiss, W.; Thanh, N. T. K.; Aveyard, J.; Fernig, D. G. Determination of Size and Concentration of Gold Nanoparticles from UV−Vis Spectra *Anal. Chem.* **2007**, *79*, 4215.

(307) Brust, M.; Fink, J.; Bethell, D.; Schiffrin, D. J.; Kiely, C. Synthesis and reactions of functionalized gold nanoparticles *J. Chem. Soc. Chem. Comm.* **1995**, 1655.
(308) Kennedy, L. C.; Bickford, L. R.; Lewinski, N. A.; Coughlin, A. J.; Hu, Y.; Day, E. S.; West, J. L.; Drezek, R. A. A New Era for Cancer Treatment: Gold-Nanoparticle-Mediated Thermal Therapies *Small* **2011**, *7*, 169.
(309) Turkevich, J.; Stevenson, P. C.; Hillier, J. A study of the nucleation and growth processes in the synthesis of colloidal gold *Farad. Discuss.* **1951**, *11*, 55.
(310) Weare, W. W.; Reed, S. M.; Warner, M. G.; Hutchison, J. E. Improved Synthesis of Small (dCORE ≈ 1.5 nm) Phosphine-Stabilized Gold Nanoparticles *J. Am. Chem. Soc.* **2000**, *122*, 12890.
(311) Gibson, J. D.; Khanal, B. P.; Zubarev, E. R. Paclitaxel-Functionalized Gold Nanoparticles *J. Am. Chem. Soc.* **2007**, *129*, 11653.
(312) Chen, Y.-H.; Tsai, C.-Y.; Huang, P.-Y.; Chang, M.-Y.; Cheng, P.-C.; Chou, C.-H.; Chen, D.-H.; Wang, C.-R.; Shiau, A.-L.; Wu, C.-L. Methotrexate Conjugated to Gold Nanoparticles Inhibits Tumor Growth in a Syngeneic Lung Tumor Model *Mol. Pharmaceutics* **2007**, *4*, 713.
(313) Li, J.; Wang, X.; Wang, C.; Chen, B.; Dai, Y.; Zhang, R.; Song, M.; Lv, G.; Fu, D. The enhancement effect of gold nanoparticles in drug delivery and as biomarkers of drug-resistant cancer cells *ChemMedChem* **2007**, *2*, 374.
(314) Patra, C. R.; Bhattacharya, R.; Wang, E.; Katarya, A.; Lau, J. S.; Dutta, S.; Muders, M.; Wang, S.; Buhrow, S. A.; Safgren, S. L.; Yaszemski, M. J.; Reid, J. M.; Ames, M. M.; Mukherjee, P.; Mukhopadhyay, D. Targeted Delivery of Gemcitabine to Pancreatic Adenocarcinoma Using Cetuximab as a Targeting Agent *Cancer Res.* **2008**, *68*, 1970.
(315) Agasti, S. S.; Chompoosor, A.; You, C.-C.; Ghosh, P.; Kim, C. K.; Rotello, V. M. Photoregulated Release of Caged Anticancer Drugs from Gold Nanoparticles *J. Am. Chem. Soc.* **2009**, *131*, 5728.
(316) Patra, C. R.; Bhattacharya, R.; Mukherjee, P. Fabrication and functional characterization of gold nanoconjugates for potential application in ovarian cancer *J. Mater. Chem.* **2010**, *20*, 547.
(317) Dreaden, E. C.; Mwakwari, S. C.; Sodji, Q. H.; Oyelere, A. K.; El-Sayed, M. A. Tamoxifen-Poly(ethylene glycol)-Thiol Gold Nanoparticle Conjugates: Enhanced Potency and Selective Delivery for Breast Cancer Treatment *Bioconjugate Chem.* **2009**, *20*, 2247.
(318) Eghtedari, M.; Liopo, A. V.; Copland, J. A.; Oraevsky, A. A.; Motamedi, M. Engineering of Hetero-Functional Gold Nanorods for the in vivo Molecular Targeting of Breast Cancer Cells *Nano Lett.* **2009**, *9*, 287.
(319) Asadishad, B.; Vossoughi, M.; Alemzadeh, I. Folate-Receptor-Targeted Delivery of Doxorubicin Using Polyethylene Glycol-Functionalized Gold Nanoparticles *Ind. Eng. Chem. Res.* **2010**, *49*, 1958.
(320) Hostetler, M. J.; Templeton, A. C.; Murray, R. W. Dynamics of Place-Exchange Reactions on Monolayer-Protected Gold Cluster Molecules *Langmuir* **1999**, *15*, 3782.

(321) Woehrle, G. H.; Brown, L. O.; Hutchison, J. E. Thiol-Functionalized, 1.5-nm Gold Nanoparticles through Ligand Exchange Reactions: Scope and Mechanism of Ligand Exchange *J. Am. Chem. Soc.* **2005**, *127*, 2172.
(322) Templeton, A. C.; Wuelfing, W. P.; Murray, R. W. Monolayer-Protected Cluster Molecules *Acc. Chem. Res.* **1999**, *33*, 27.

Appendix A: Crystal Structure of Parthenolide Analogue 4

checkCIF/PLATON report

No syntax errors found. CIF dictionary Interpreting this report

Datablock: 10067a

Bond precision: C-C = 0.0076 A Wavelength=0.71073

Cell: a=6.3639(19) b=7.595(2) c=28.621(8)
alpha=90 beta=90 gamma=90

Temperature: 123 K

	Calculated	Reported
Volume	1383.4(7)	1383.3(7)
Space group	P 21 21 21	P2(1)2(1)2(
Hall group	P 2ac 2ab	?
Moiety formula	C15 H22 O3	C15 H22 O3
Sum formula	C15 H22 O3	C15 H22 O3
Mr	250.33	250.33
Dx,g cm-3	1.202	1.202
Z	4	4
Mu (mm-1)	0.082	0.082
F000	544.0	544.0
F000'	544.27	
h,k,lmax	7,9,34	7,9,34
Nref	1464[2456]	1458
Tmin,Tmax	0.964,0.996	0.964,0.996
Tmin'	0.964	

Correction method= MULTI-SCAN

Data completeness= 1.00/0.59 Theta(max)= 25.070

R(reflections)= 0.0668(1195) wR2(reflections)= 0.1839(1458)

S = 1.195 Npar= 165

The following ALERTS were generated. Each ALERT has the format
test-name_ALERT_alert-type_alert-level.
Click on the hyperlinks for more details of the test.

Alert level B
PLAT213_ALERT_2_B Atom C13 has ADP max/min Ratio ..... 4.20 prola

Alert level C
STRVA01_ALERT_4_C Flack parameter is too small
From the CIF: _refine_ls_abs_structure_Flack -4.000

From the CIF: _refine_ls_abs_structure_Flack_su 4.000
PLAT213_ALERT_2_C Atom O3 has ADP max/min Ratio ..... 3.20 prola
PLAT241_ALERT_2_C Check High Ueq as Compared to Neighbors for O1
PLAT340_ALERT_3_C Low Bond Precision on C-C Bonds (x 1000) Ang .. 8
PLAT410_ALERT_2_C Short Intra H...H Contact H5A .. H10A .. 1.99 Ang.
PLAT032_ALERT_4_C Std. Uncertainty in Flack Parameter too High ... 4.00
PLAT033_ALERT_4_C Flack x Parameter Value Deviates from Zero ..... -4.00

Alert level G
REFLT03_ALERT_4_G Please check that the estimate of the number of Friedel pairs is
correct. If it is not, please give the correct count in the
_publ_section_exptl_refinement section of the submitted CIF.
From the CIF: _diffrn_reflns_theta_max 25.07
From the CIF: _reflns_number_total 1458
Count of symmetry unique reflns 1464
Completeness (_total/calc) 99.59%
TEST3: Check Friedels for noncentro structure
Estimate of Friedel pairs measured 0
Fraction of Friedel pairs measured 0.000
Are heavy atom types Z>Si present no
PLAT791_ALERT_4_G Note: The Model has Chirality at C4 (Verify) R
PLAT791_ALERT_4_G Note: The Model has Chirality at C5 (Verify) R
PLAT791_ALERT_4_G Note: The Model has Chirality at C6 (Verify) S
PLAT791_ALERT_4_G Note: The Model has Chirality at C7 (Verify) S
PLAT791_ALERT_4_G Note: The Model has Chirality at C10 (Verify) R

---

0 ALERT level A = In general: serious problem
1 ALERT level B = Potentially serious problem
7 ALERT level C = Check and explain
6 ALERT level G = General alerts; check

0 ALERT type 1 CIF construction/syntax error, inconsistent or missing data
4 ALERT type 2 Indicator that the structure model may be wrong or deficient
1 ALERT type 3 Indicator that the structure quality may be low
9 ALERT type 4 Improvement, methodology, query or suggestion
0 ALERT type 5 Informative message, check

Publication of your CIF in IUCr journals

A basic structural check has been run on your CIF. These basic checks will be run on all CIFs submitted for publication in IUCr journals (Acta Crystallographica **,** Journal of Applied Crystallography**,** Journal of Synchrotron Radiation **); however, if you intend to submit to** Acta Crystallographica Section C **or** E **, you should make sure that full publication checks are run on the final version of your CIF prior to submission.**

Publication of your CIF in other journals

Please refer to the Notes for Authors **of the relevant journal for any special instructions relating to CIF submission.**

PLATON version of 31/03/2010; check.def file version of 22/03/2010

Datablock 10067a - ellipsoid plot